



HAL
open science

Antibacterial surface based on new epoxy-amine networks from ionic liquid monomers

Sébastien Livi, Luanda Lins, Larissa Capeletti, Charline Chardin, Nour Halawani, Jérôme Baudoux, Mateus Cardoso

► To cite this version:

Sébastien Livi, Luanda Lins, Larissa Capeletti, Charline Chardin, Nour Halawani, et al.. Antibacterial surface based on new epoxy-amine networks from ionic liquid monomers. *European Polymer Journal*, 2019, 116, pp.56-64. 10.1016/j.eurpolymj.2019.04.008 . hal-02331812

HAL Id: hal-02331812

<https://normandie-univ.hal.science/hal-02331812>

Submitted on 22 Oct 2021

HAL is a multi-disciplinary open access archive for the deposit and dissemination of scientific research documents, whether they are published or not. The documents may come from teaching and research institutions in France or abroad, or from public or private research centers.

L'archive ouverte pluridisciplinaire **HAL**, est destinée au dépôt et à la diffusion de documents scientifiques de niveau recherche, publiés ou non, émanant des établissements d'enseignement et de recherche français ou étrangers, des laboratoires publics ou privés.



Distributed under a Creative Commons Attribution - NonCommercial 4.0 International License

Antibacterial Surface Based on New Epoxy- Amine Networks From Ionic Liquid Monomers

Sébastien Livi^{1,2,}, Luanda C. Lins⁴, Larissa. B. Capeletti², Charline Chardin³, Nour Halawani¹,
Jérôme Baudoux^{3*}, Mateus. B. Cardoso^{2,4}*

¹ Université de Lyon, CNRS, UMR 5223, Ingénierie des Matériaux Polymères, INSA Lyon, F-69621 Villeurbanne, France

² Laboratório Nacional de Nanotecnologia (LNNano) & Laboratório Nacional de Luz Sincrotron (LNLS), Centro Nacional de Pesquisa em Energia e Materiais (CNPEM), CEP 13083-970, Caixa Postal 6192, Campinas, SP, Brazil.

³ Laboratoire de Chimie Moléculaire et Thio-organique, ENSICAEN, Université de Normandie, CNRS, 6 boulevard du Maréchal Juin, 14050 Caen, France.

⁴ Instituto de Química (IQ), Universidade Estadual de Campinas (UNICAMP), CEP 13083-970, Caixa Postal 6154, Campinas, SP, Brazil.

ABSTRACT

The design of new highly effective polymer materials as active surfaces or coatings against microorganisms such as *Escherichia coli* (*E. coli*) is a major challenge for public health. In the present work, novel imidazolium ionic liquid monomers (ILMs) having a similar structure of conventional Bisphenol A diglycidyl ether epoxy prepolymer (DGEBA) have been designed without requiring to the use of toxic and carcinogenic compounds *i.e.* Bisphenol A and epichlorohydrin. Then, a facile and efficient polyaddition reaction-based polymerization via a one step process was used in order to prepare unprecedented antibacterial epoxy-amine networks. The ultimate role of the monomers architecture on the epoxy conversion as well as on the reactivity of the epoxy-functionalized imidazolium ionic liquid monomers with an aliphatic amine (D-230) was investigated while the average molecular weight between crosslinks (M_c) and the relaxation temperature of the resulting networks were determined. Thus, new epoxy thermosets with an excellent thermal stability, high hydrophobic behavior and good storage modulus at room temperature were produced. Finally, antimicrobial tests against *E. coli* were performed for the first time on these new cross-linked epoxy networks leading to a very strong inhibition of *E. coli* biofilm formation (- 95 %).

KEYWORDS. Ionic Liquids, Epoxy networks, Antibacterial activity, Thermo-mechanical properties, Epoxy conversion.

INTRODUCTION

It is well-known that the presence of pathogenic microorganisms such as *Escherichia coli* (*E. coli*), *Staphylococcus aureus* (*S. aureus*) and *Pseudomonas aeruginosa* (*P. aeruginosa*) are the origin of nosocomial infections causing real public health problems and generating high-

associated costs worldwide¹⁻³. In order to decrease the spread of these microorganisms, various polymers acting as active surfaces or coatings have been widely used and reported in the literature to protect metal surfaces, soils, clinics walls and hospitals as well as in the field of surgery equipment, dental restoration, textiles, water treatment and food packaging⁴⁻⁸. Thus, various strategies were developed to obtain antibacterial activities as i) the use of nanoparticles, especially silver (Ag)⁹⁻¹²; ii) the synthesis of polymer brushes or layers¹³⁻¹⁵, iii) the incorporation of leaching antibacterial additives into polymer matrices¹⁶⁻¹⁷ and iv) the synthesis of comonomers or polymers where the pendant groups act as antimicrobial agents¹⁸⁻²². Nevertheless, the majority of these different paths lead to other challenges to overcome such as the dispersion of the nanoparticles as well as their possible adverse effects on the human health, the complex polymer synthesis as well as a scale-up problem in the industry or the release of antibacterial groups in the nature thereby reducing their effect on the bacteria resistance²²⁻²³. Thus, the last approach seems the most promising to prepare surface-active antibacterial polymers.

Epoxy prepolymers are well-known to have good thermal, mechanical and adhesive properties as well as easy processing and low-cost production²⁴⁻²⁶. In recent years, various authors have developed bio- or epoxy networks with enhanced antibacterial properties²⁷⁻²⁹. For example, Liu *et al* have developed epoxy networks containing Tannic Acids that are well-known for their abundant terminal phenolic hydroxyl groups²⁷. In fact, they have demonstrated that the use of high amounts of these phenolic groups resulted in enhanced antibacterial properties. Other authors have shown that the use of high quantities of eugenol bio-based epoxy prepolymers (between 30 and 70 wt %) induced significant reduction in bacterial adhesion ranging from 59 to 92 %²⁸. According to the literature, quaternary ammonium salts are very effective agents against Gram-negative or Gram-positive bacteria and plays a key role on the antibacterial properties. In fact, the positive charge of the ammonium salts can generate a strong interaction with the

negative bacteria cell surface while the presence of a long alkyl chain can penetrate in the bacterial phospholipid membrane leading to a significant reduction of *E. coli*³⁰⁻³¹. For these reasons, several authors have investigated on the insertion of ammonium salts or ammonium polymerizable groups in epoxy-amine networks³²⁻³⁴. Ritter *et al* have processed epoxy networks by using bisphenol A diglycidyl ether (DGEBA) and diethylene triamine (DETA) as co-monomers with the presence of different amounts of synthesized amino-ammonium products³⁴. Thus, they have demonstrated that depending on the amount as well as the alkyl chain length of ammonium salts, epoxy-amine networks with good antibacterial properties could be developed. Alternatively, ionic liquids (ILs) are envisaged for distinct fields of research and applications³⁵⁻³⁷. It is mainly due to their unique properties such as chemical and thermal stabilities, low vapor pressure, antibacterial and antifungal properties and also versatility for tuning tailored combinations between cations and anions³⁸⁻⁴⁰. In particular, our research group has demonstrated that imidazolium and phosphonium ILs are useful platforms to design epoxy-IL networks with excellent thermomechanical properties, including thermal stability under nitrogen (> 300 °C), hydrophobic behavior and a glass transition temperature between 50 °C to 170 °C⁴¹⁻⁴⁴. Very recently, a new reaction mechanism has been put forward for an epoxy-amine network derived from one imidazolium ionic liquid monomer bearing two epoxide functions⁴⁵. Thus, the authors have shown that the use of an imidazolium ionic liquid monomer as co-monomer in the presence of a diamine could lead to the generation of quaternary ammonium species in addition to the three main reaction paths reported for the epoxy ring-opening reaction with a primary amine⁴⁶. In this work, novel epoxy-amine networks were designed from three imidazolium ionic liquid monomers (ILM) and the impact of ILM architectures on the final properties of these epoxy networks were investigated. Thus, the reactivity of the imidazolium ionic liquid monomers with an aliphatic amine, denoted Jeffamine D230, was firstly investigated. Then, the morphologies as

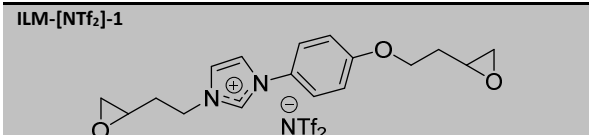
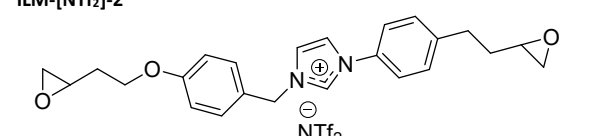
well as the thermo-mechanical behavior and the thermal stability properties were also studied. Finally, the potential of these unprecedented epoxy-amine networks containing 25 to 30 wt % of quaternary ammonium groups covalently linked was evaluated for the first time as new polymer materials with antibacterial properties.

EXPERIMENTAL

Materials

All reagents were purchased from Sigma Aldrich, Alfa Aesar or TCI and were used without further purification and used as received. Solvents were used in RPE grade without further purification. Anhydrous solvents were obtained from a PURESOLV SPS400 apparatus developed by Innovative Technology Inc. In this work, all structures and properties of the materials used are summarized in **Table 1**. Epoxy networks based on imidazolium ionic liquid monomers denoted ILM-[NTf₂]-1, ILM-[NTf₂]-2, ILM-[NTf₂]-3, liquid at room temperature, was synthesized according to the procedure described below. One commercial polyetheramine denoted Jeffamine D230 purchased by Huntsman was investigated as conventional hardener. The diamine was added in the stoichiometric ratio *i.e.* epoxy to amine hydrogen groups equal to 1, in pure mixture.

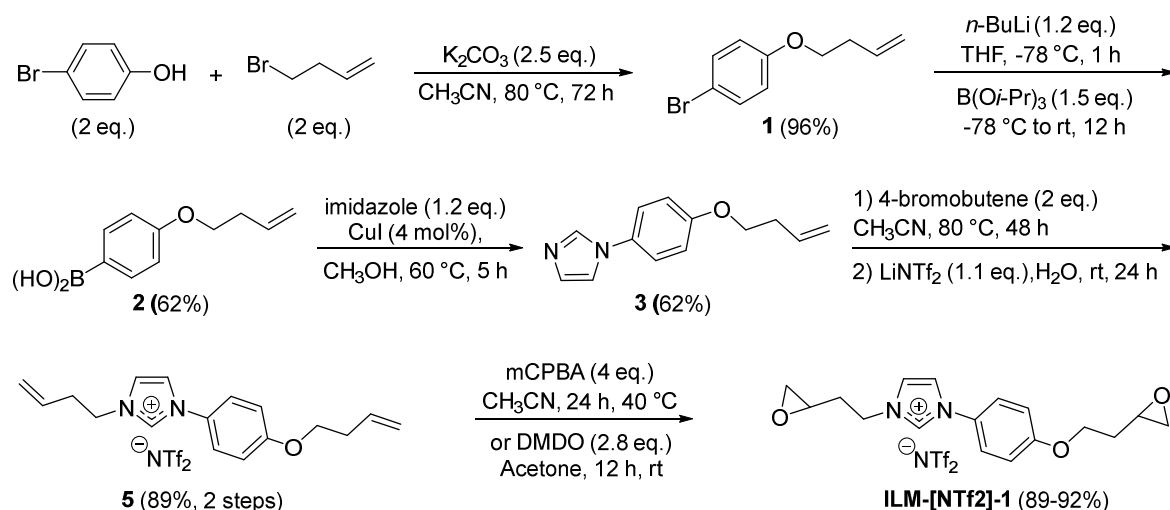
Table 1. Chemical structures, nomenclatures and properties of the materials used to design epoxy-amine networks

Chemical structure and name	Supplier	Properties
 <p>ILM-[NTf₂]-1</p>	« Homemade »	Epoxy equivalent (EEW): 290.75 g eq ⁻¹ T _g = -46 °C
 <p>ILM-[NTf₂]-2</p>	« Homemade »	Epoxy equivalent (EEW): 335.81 g eq ⁻¹ T _g = -26 °C

ILM-[NTf₂]-3 	« Homemade »	Epoxy equivalent (EEW): 282.75 g eq ⁻¹ T _g = -46 °C
Jeffamine D230 $x \approx 2.5$	Huntsmann	Amine hydrogen equivalent (AHEW): 60 g eq ⁻¹

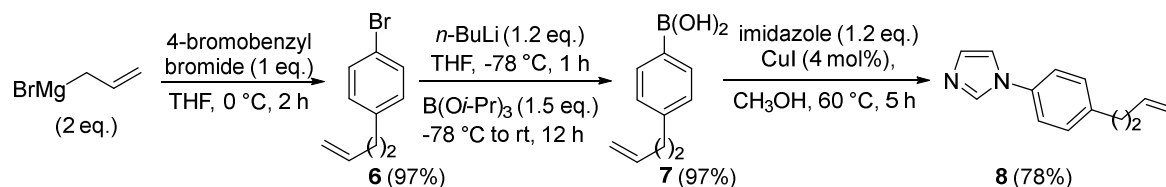
Synthesis of ionic liquid monomers (ILMs)

Here, three imidazolium salts denoted ILM-[NTf₂]-1, ILM-[NTf₂]-2 and ILM-[NTf₂]-3 were synthesized and analyzed by ¹H-, ¹³C-, ¹⁹F-NMR, infrared, and High-Resolution Mass Spectra. The first salt ILM-[NTf₂]-1 was prepared according to our previous work from 4-bromophenol, 4-bromobutene, bis(trifluoromethane)sulfonimide lithium salt and DMDO or mCPBA as main reagents⁴⁷. The six-step sequence to synthesize ILM-[NTf₂]-1 is fully illustrated below (**Scheme 1**) and the NMR assignments of resonance peaks are reported in the supporting information (see **Part II and V, Figure S1-S6**).



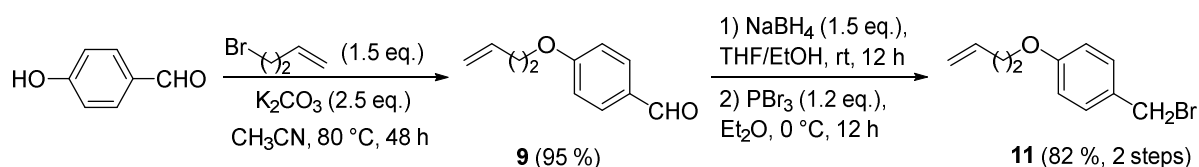
Scheme 1. Procedure synthesis of ILM-[NTf₂]-1

The preparation of monomers ILM-[NTf₂]-2 (**Part III** in the ESI) and ILM-[NTf₂]-3 (**Part IV** in the ESI) requires a three-step sequence to synthesize imidazole **8** (**Scheme 2**). In the first step, the reaction involves 4-bromobenzyl bromide (1 eq.) and allylmagnesium bromide (2 eq.) as Grignard reagent to form compound **6** in excellent yield. The aryl bromide **6** was then converted to boronic acid **7** to promote a copper-catalyzed Chan-Lam coupling with imidazole (1.2 eq.). The heterocycle **8** was prepared in 78% yield after 5 h at 60 °C. This reagent was synthesized on a several grams scale using a reproducible sequence (**Figure S7-S9** in the ESI) will allow efficient access to both salts (ILM-[NTf₂]-2 and ILM-[NTf₂]-3).



Scheme 2. Procedure synthesis of the compound **8**

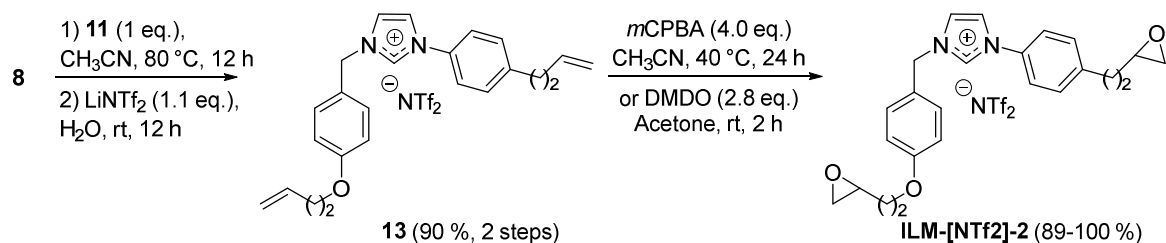
Thus, we optimized the synthesis of ILM-[NTf₂]-2 bearing two aromatic rings and terminal epoxides. For this purpose, the alcohol function of commercially available 4-hydroxybenzaldehyde was alkylated by 4-bromo-1-butene (1.5 eq.). In the presence of potassium carbonate, the ether **9** was isolated in 95% yield. The aldehyde function was reduced to alcohol **10** by sodium borohydride then subjected to bromination with phosphorus tribromide to give compound **11** in 82% yield overall yield (**Scheme 3** and **Figure S10-S12** in the ESI).



Scheme 3. Procedure synthesis of the compound **11**

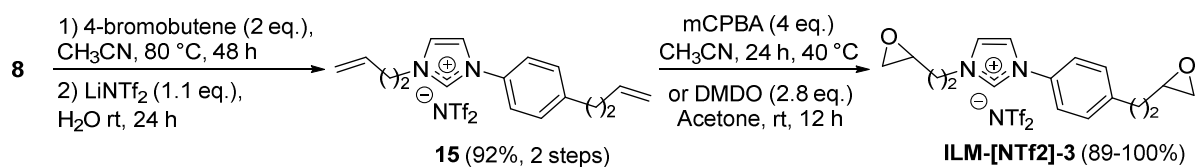
The synthesis of imidazolium NTf₂ **13** involves a nucleophilic substitution of benzyl bromide **11** with imidazole **8** and an anionic metathesis step with LiNTf₂. Finally, the oxidation of the alkenes

was carried out in presence of an excess of mCPBA (4 eq.) at 40°C or DMDO (2.8 eq.) at room temperature. The overall yield of this sequence is **90 %** to afford ILM-[NTf₂]-2 as clean oil (**Scheme 4** and **Figure S13-S15** in the ESI).



Scheme 4. Procedure synthesis of the ILM-[NTf₂]-2 from compounds **8** and **11**

In order to study the behavior and the efficacy of the previous salts, we prepared ILM-[NTf₂]-3 which was prepared from imidazole **8**. This salt was synthesized by quaternarization of the imidazole by 4-bromobutene (2 eq.) followed by the anion exchange with LiNTf₂ and oxidation under same conditions as previously. Once again, excellent yield was observed after this three-step sequence (**Scheme 5** and **Figure S13-S18** in the ESI).



Scheme 5. Procedure synthesis of the ILM-[NTf₂]-2 from compound **8**

Epoxy network processing

To prepare the network, ILM-[NTf₂]-1, ILM-[NTf₂]-2, ILM-[NTf₂]-3 and Jeffamine D230 were mixed with a suitable stoichiometric ratio under stirring at room temperature during 30-40 minutes. The mixture was then degassed in an ultrasonic bath during 15-20 minutes and was

poured into silicone molds. Finally, epoxy-amine networks named ILM-1, ILM-2 and ILM-3 were cured 2 h at 80 °C and 3h at 120 °C.

Characterization methods

Thermogravimetric Analyses (TGA) of ionic liquid monomers and the resulting epoxy networks were performed on a Q500 thermogravimetric analyzer (TA instruments). The samples were heated from 30 to 700 °C at a rate of 20 K min⁻¹ under nitrogen flow.

Differential Scanning Calorimetry measurements (DSC) of epoxy/IL blends and networks were performed on a Q20 (TA instruments) from 20 to 250 °C. The samples were kept for 3 min at 250 °C to erase the thermal history before being heated or cooled at a rate of 10 K min⁻¹ under nitrogen flow of 50 mL min⁻¹.

Surface energy of epoxy network was determined with the sessile drop method using a GBX goniometer. From contact angle measurements performed with water and diiodomethane as probe liquids on the samples, polar and dispersive components of surface energy were determined using Owens-Wendt theory⁴⁸.

Fourier Transform Infrared absorption spectra (FTIR) were recorded on a Thermo Scientific Nicolet iS10 Spectrometer with a transmission accessory from 4000 cm⁻¹ to 500 cm⁻¹ (32 scans, resolution 4 cm⁻¹). The IR absorptions were observed as strong bands and are given in cm⁻¹.

Dynamic mechanical analysis (DMA) was performed on rectangular samples with dimensions 15 mm and 5 mm and a thickness of 1 mm using an ARES-G2 rheometer with torsional fixture (TA Instruments). The material response was measured with a heating rate of 3 °C.min⁻¹. All tests were performed within the linear viscoelastic region of each material at a frequency of 1 Hz. Storage modulus E', Loss Modulus E'' and the loss factor tan δ were measured during temperature ramps from -80 °C up to 150 °C.

Transmission electron microscopy (TEM) was performed at the Technical Center of Microstructures (University of Lyon) using a Phillips CM 120 microscope operating at 80 kV to characterize the dispersion of thermoplastic phases in the epoxy networks. 60-nm-thick ultrathin sections of samples were obtained using an ultramicrotome equipped with a diamond knife and were then set on copper grids.

Liquid NMR ^1H -, ^{13}C -, and ^{19}F -NMR spectra were recorded on a Bruker Avance III 400 MHz, 500 MHz or AvanceNEO 600 MHz spectrometer. Samples were dissolved in an appropriate deuterated solvent (CDCl_3). The chemical shifts (δ) are expressed in ppm relative to internal tetramethylsilane for ^1H and ^{13}C nuclei, and coupling constants are indicated in Hz. Abbreviations for signal coupling are as follows: s=singlet; d=doublet; dd=doublet of doublets; t=triplet; q=quartet; quin=quintet; m=multiplet; br=broad signal. To assign the signals to the different proton and carbon atoms, as well as the relative stereochemistry of the cycloadducts, additional 2D NMR experiments (COSY, TOCSY, HSQC, HMBC) and NOESY experiments were performed.

Antibacterial activity was investigated by *Escherichia coli* (DH5 α) biofilm formation over the epoxy-amine polymers. A single bacteria colony was incubated overnight in Luria Bertani broth (LB, containing 10 g.L $^{-1}$ of peptone and NaCl, and 5 g.L $^{-1}$ of yeast extract) and then purified by washing with 1% NaCl twice and finally the pellet was suspended in phosphate buffered saline (PBS) solution. The optical density at 600nm (OD600) was determined and a solution of 0.1 OD was prepared in LB. The samples were cut into 4 mm squares, transferred to a 96-well plate containing 100 μL of the last bacteria solution and incubated at room temperature. After 24h, the squares were gently washed with PBS and incubated with 10% AlamarBlue at 37 $^\circ\text{C}$ for 2h. The fluorescence indicating microorganisms' viability was then measured in a Enspire Multimode Plate Reader (Perkin Elmer) with excitation at 570 nm and emission at 585 nm. Biofilm

inhibition was then calculated considering the reference polymer denoted DGEBA/D230 signal as 100% viability (zero inhibition). All the experiments were performed in octuplicate.

Scanning electronic microscopy (SEM) was performed with a high-resolution FEI Quanta 650 FEG operating at 5 kV using secondary electron detectors. The samples of the epoxy-amine networks were fixed with 4% glutaraldehyde overnight at room temperature and dehydrated with ascending ethanol concentration solutions (25%, 50%, 75% and 100%) for 1h each. After ethanol removal, samples were kept in a desiccator overnight. Finally the squares were then mounted in aluminum stubs and sputter-coated with carbon.

RESULTS AND DISCUSSIONS

Evaluation of the epoxy conversion (FTIR) and reactivity study (DSC) of epoxy-amine networks

The curing process as well as the determination of the conversion percentage of epoxide groups of all the systems was studied in the same conditions, *i.e.* 2h at 80 °C and 3h at 120 °C. Based on the literature, the evolution of the adsorption bands at 914 cm⁻¹ corresponding to epoxide groups () and at 1184 cm⁻¹ which corresponds to the ether linkage (C-O-C) was followed by FTIR spectroscopy^{42,44}. Taking this into account, the conversion of epoxide group was determined by using Equation (1):

$$X \% = \frac{A_0 - A_t}{A_t} \times 100\% \quad \text{Equation (1)}$$

where A_0 and A_t are the ratio between the area of two absorption peaks (914 cm⁻¹ and 1184 cm⁻¹) at $t=0$ as well as the reaction time t . Thus, the conversion of epoxy groups versus curing time of the three selected epoxy-amine systems, denoted ILM-1, ILM-2 and ILM-3, are summarized in

Figure 1. In addition, the FTIR spectra of ILM-1, ILM-2 and ILM-3 during curing process are presented in the Figure S19, S20, S21 on the supporting information

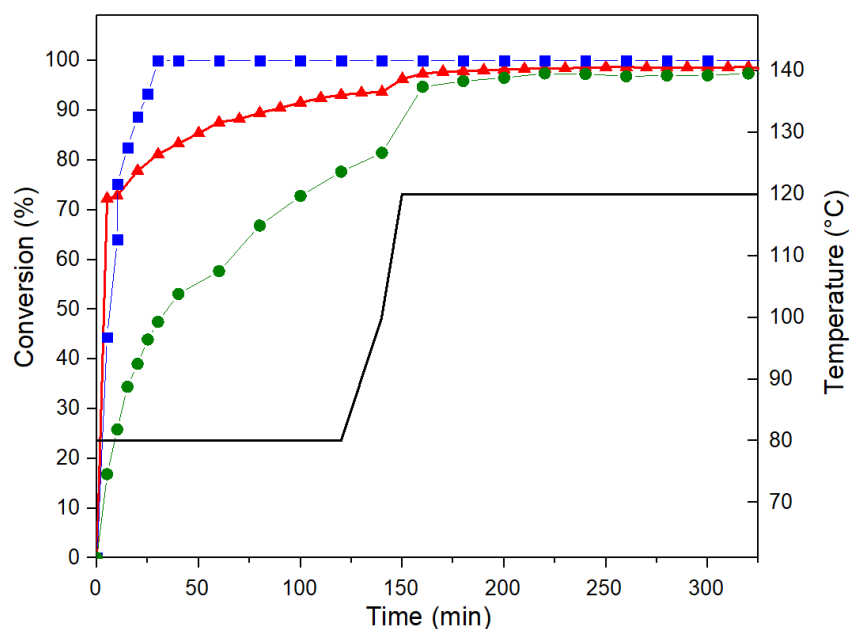


Figure 1. Epoxy group conversion as a function of curing time as determined by FTIR spectra for (●) ILM-1, (■) ILM-2, and (▲) ILM-3

An epoxy conversion higher than 96 % was observed for all epoxy-amine networks prepared with ILM-[NTf₂]-1,-2,-3 confirming the good reactivity between these salts and Jeffamine D230 used as curing agent. However, different behaviors were observed depending on the imidazolium ILM-[NTf₂] used. In fact, a very fast consumption of epoxy functions was observed for ILM-[NTf₂]-2 (>90 % after 25 minutes) whereas a progressive conversion of these functions was detected for ILM-[NTf₂]-1 and ILM-[NTf₂]-3. At 80 ° C, the ring opening reaction of ILM-[NTf₂]-3 requires 90 minutes to afford an epoxy conversion of about 90 % while ILM-[NTf₂]-1 gives 76% after 2 hours. The lower conversion detected with ILM-[NTf₂]-1 and ILM-[NTf₂]-3 could be related to the nature of the terminal epoxides. By comparison with ILM-[NTf₂]-2 which incorporates an aromatic ring between imidazolium and epoxides, ILM-[NTf₂]-1 and ILM-

[NTf₂]-3 have an epoxide directly linked to the imidazolium. In such cases, the short aliphatic chain could slow down the ring opening reaction. Finally, the presence of an ether group between the aromatic ring and the epoxyde is able to slightly modify the chemical kinetics too. Thus, the reaction between ILM-[NTf₂]-2 and Jeffamine D230 during 35 minutes at 80 °C led to a full conversion of the epoxy functions opening some perspectives in the development of fast cure epoxy-amine systems. These results are in agreement with DSC curves highlighting the influence of the ILM-[NTf₂] chemical nature on the epoxy prepolymer reactivity with the amine. For both ILM-1 and ILM-3, DSC thermograms showed the presence of two exothermic peaks indicating a two-step mechanism (See Figure S22 and S24 in the ESI). This phenomenon was already observed by Maka *et al* by using imidazolium ILs as hardeners of DGEBA prepolymer^{43,49}. They have attributed this bimodal character to the adduct formation and chain addition polymerization⁴². Like conventional epoxy-amine networks, especially DGEBA cured with Jeffamine D230, a single exothermic peak was observed at 120 °C for ILM-2 (See Figure 20 in the ESI) confirming its high reactivity as demonstrated by FTIR spectroscopy. In terms of enthalpies, the exothermicity generated during the polymerization between the ILM-[NTf₂] and the amine is significantly lower compared to a conventional epoxy-amine reaction. Indeed, enthalpy values of 150 and 230 J.g⁻¹ were calculated for ILM-2, ILM-1 and ILM-3 compared to 550-600 J.g⁻¹ for DGEBA/D230 networks⁵⁰⁻⁵¹.

In conclusion, epoxy-amine networks prepared from these three ILM-[NTf₂] have shown similar reactivity's compared to DGEBA/D230 network combined with a full epoxy conversion.

Determination of the relaxation temperature (T_α) and approximation of the average molecular weight between crosslinks (M_c) by dynamical mechanical analysis (DMA)

The effect of the ILM architecture on the thermomechanical properties of the epoxy-amine networks was studied by DMA (**Figure 2**). The dynamical mechanical curves of the epoxy networks display the storage moduli G' and the main relaxation peak ($T\alpha$).

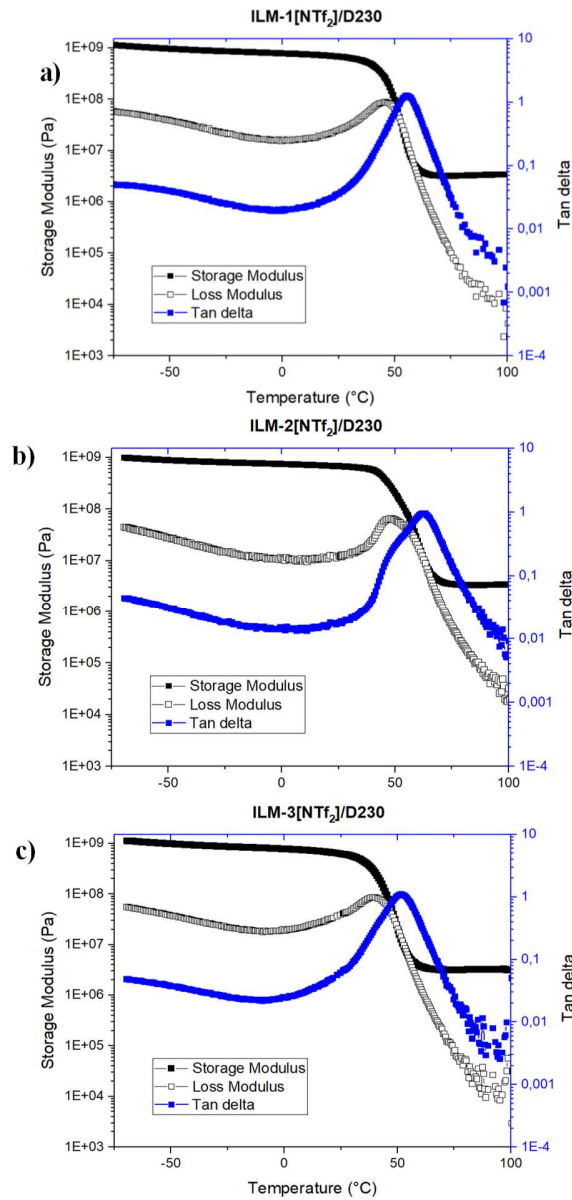


Figure 2. Evolution of storage modulus (G') and loss factor ($\tan\delta$) as a function of temperature for (a) ILM-1, (b) ILM-2, and (c) ILM-3

As it can be seen in **Figure 2**, the use of **ILM-[NTf₂]** as epoxy prepolymer led to homogeneous epoxy networks characterized by the presence of only one single and well-defined relaxation peak ($T\alpha$). Thus, DMA curves highlighted that ILM-1 and ILM-3 exhibited glass transition temperatures at 55 and 53 °C, respectively while ILM-2, presented one glass transition at 62 °C. These Tg differences can be attributed to the presence of a second phenyl group bringing more rigidity to the chemical structure. In all cases, the glass transition temperatures determined by DMA are slightly lower compared to conventional epoxy-amine networks processed from diglycidyl prepolymer (DGEBA EPON 828 or DGEBA DER 332) and Jeffamine D230⁵⁰⁻⁵². However, these new networks represent a new sustainable alternative to the DGEBA prepolymer commonly used in the epoxy resin market.

Then, the crosslinking density (M_c) of the resulting epoxy-amine networks was determined by using the rubbery elasticity theory Equation (2).

$$M_c = \rho_0 RT / G' \quad \text{Equation (2)}$$

Where G' (MPa) represent the equilibrium rubber moduli determined at $T = T\alpha + 30$ °C, R is the gas constant (8.314 J.K⁻¹.mol⁻¹). All DMA values and M_c are summarized in **Table 2**.

Table 2. DMA data of epoxy-amine networks issue from DGEBA and ILM-1, -2, -3.

Sample	$T\alpha$ (°C)	M_c (g.mol ⁻¹)	G' (MPa)
ILM-1	55	890	3.1
ILM-2	62	650	4.3
ILM-3	53	822	3.3
DGEBA/D230	90	590-630	-

The use of ILM-1 and ILM-3 led to similar values of average molecular weight between crosslinks with M_c values of $890 \text{ g}\cdot\text{mol}^{-1}$ and $820 \text{ g}\cdot\text{mol}^{-1}$, respectively while ILM-2 induced a M_c value close to the conventional epoxy-amine network (DGEBA/D230)⁵²⁻⁵³. These results are likely correlated to the evolution of the glass transition temperature and clearly highlight the formation of homogeneous networks. Moreover, these results also demonstrate that the ILM-[NTf₂] act as a conventional diglycidyl co-monomers⁵²⁻⁵³.

In conclusion, epoxy-amine networks from imidazolium ILM-[NTf₂] have shown good thermomechanical properties at room temperature as well as considerable ductility due to their lower glass transition temperatures.

Thermal behavior of the resulting networks

The thermal behavior of the resulting epoxy-amine networks denoted ILM-1, ILM-2 and ILM-3 was investigated by thermogravimetric analysis (TGA) in order to show the impact of the ILM-[NTf₂] architecture on the degradation mechanism. The evolution of the weight loss as a function of the temperature was presented in **Figure 3**.

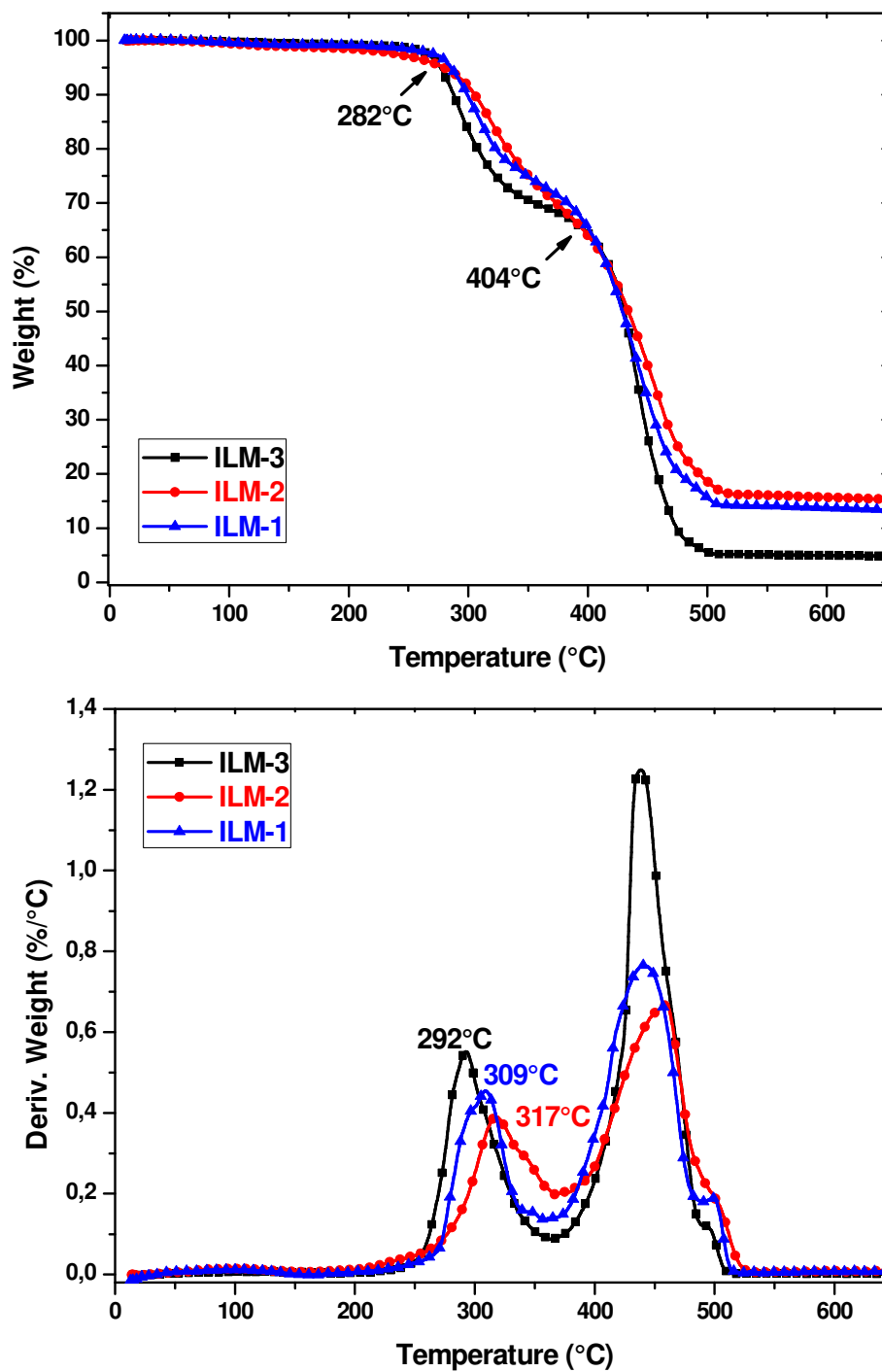


Figure 3. Evolution of the weight loss as a function of temperature (TGA, DTG) of (■) ILM-1, (●) ILM-2, and (▲) ILM-3. The heating ramp was performed at 20 K.min⁻¹ under N₂ atmosphere.

In all cases, the use of imidazolium ILM-[NTf₂] as epoxy prepolymers induced the formation of epoxy networks with thermally stable behavior (up to 300 °C). In addition, two degradation peaks were clearly observed corresponding to *i*) the decomposition of the covalently linked quaternary ammonium which was generated during the polymerization of the epoxy prepolymer at around 300 °C⁴⁵ and *ii*) the degradation of the epoxy networks at 440 °C⁴⁴. Moreover, a slight difference in thermal stability can be observed depending of ILM-[NTf₂] architecture used. For ILM-[NTf₂]-1 and ILM-[NTf₂]-3 having a similar chemical structure, *i.e.* with only one aromatic ring, the similar thermal behaviors were obtained. Contrarily, a better thermal stability for the first and second degradation peaks (+ 30 °C) was demonstrated for ILM-[NTf₂]-2 which can be explained by the presence of a second aromatic ring.

These results are in agreement with the literature reported on epoxy systems where imidazolium and phosphonium ionic liquids were used as co-monomers or initiators of the epoxy polymerization⁴²⁻⁴⁴. Thus, they have shown a significant increase of the degradation temperatures (+ 50-60 °C) in presence of ILs. Very recently, our research group has investigated for the first time the reaction mechanism between ionic monoepoxide based on imidazolium core and various amines used as model substrates in order to bring a clear understanding about the polymerization mechanism that can take place between one ILM-[NTf₂] and one aliphatic diamine⁴⁵. We have highlighted that the use of ILM-[NTf₂] as epoxy prepolymer led to the formation of quaternary ammonium confined and covalently attached in the network⁴⁵. Thus, 25 to 30 wt % of the quaternary ammonium is contained in the epoxy networks as can be seen in **Figure 3**. These results are promising in the design of antibacterial polymers where many authors have investigated the use of quaternary ammonium as additives incorporated or not by electrostatic attraction^{54-55, 34}. The major drawback of this strategy is the possibility of ammonium salts leaching which induces a decrease in their effect over time.

In conclusion, the use of I ILM-[NTf₂] as epoxy prepolymer induced thermally stable networks containing imidazolium and ammonium ionic species, which are well-known to have antibacterial properties. In addition, thermally stable epoxy networks were obtained opening new perspectives for various applications requiring high processing temperatures.

Surface energy of epoxy networks

The sessile drop method was performed from the contact angles with water and methylene diode by using Owens-Wendt method (**Table 3**) in order to determine the surface energies of the epoxy networks.

Table 3. Contact angles and surface energies of epoxy-amine networks measured by sessile drop method.

Sample	θ water (°C)	θ (CH ₂ I ₂) (°C)	$\gamma_{\text{dispersive}}$ (mJ.m ⁻²)	$\gamma_{\text{nondispersive}}$ (mJ.m ⁻²)	γ_{total} (mJ.m ⁻²)
ILM-1	101.7	51.7	33.3	0.1	33.4
ILM-2	107	40	40	0.3	40.3
ILM-3	91	61.9	27.5	2.5	30
DGEBA/D230[60]	72	50	27.5	9.2	37

Surface energies between 38-42 mJ.m⁻² have been commonly seen for conventional epoxy-amine networks based on bisphenol A diglycidyl ether (DGEBA) cured with aliphatic or aromatic amines⁵⁶⁻⁵⁷. In all cases, the substitution of the diglycidyl prepolymer by ILM-[NTf₂]-1, -2 and -3 induced a significant decrease of the polar component which results in an increase of the water contact angle (from 72 ° to 107 °). These results highlight hydrophobic behavior due to the hydrophobic nature of the ILs combined with fluorinated counter anion [NTf₂] and having surface energies around 29-30 mJ.m⁻²⁵⁸⁻⁵⁹. However, some differences were observed depending on the chemical nature of the imidazolium monomers. In fact, ILM-2 and DGEBA/D230 have

similar surface energies which can be attributed to the presence of both aromatic rings. Contrarily, ILM-1 and ILM-3 present similar chemical structures and surface energies close to polyolefins.

In summary, epoxy-amine networks containing imidazolium and ammonium ionic species combined with hydrophobic behavior were designed. This strategy should lead to polymer materials with the ability to attract bacteria by the positive charge of imidazolium and ammonium compounds and inhibit their proliferation by penetrating the bacterial phospholipid membrane³⁴.

Antibacterial activity of epoxy-amine networks

The influence of the ILM on the antibacterial activity of the corresponding crosslinked epoxy networks against *E. coli* was investigated and the results concerning the biofilm inhibition potential are presented in **Figure 4**. SEM images (**Figure 5**) were also obtained to highlight the decrease of *E. coli* adhesion. Moreover, the results obtained were compared with the conventional epoxy-amine network (DGEBA/D230) which was considered as the reference polymer.

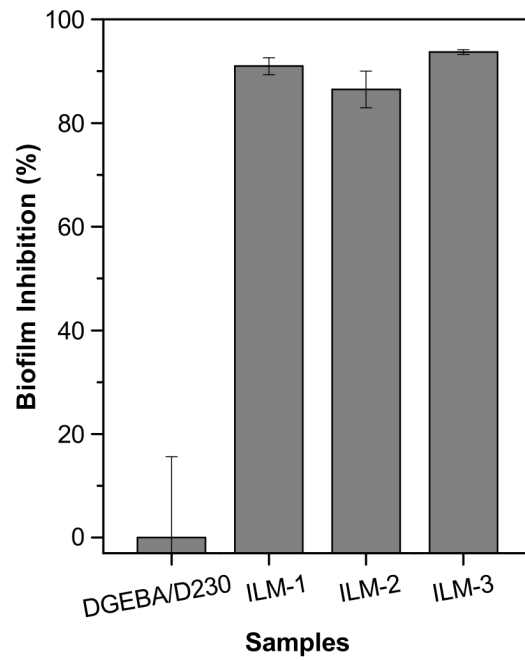


Figure 4. Biofilm inhibition potential of ILM-1, ILM-2 and ILM-3

If compared with the reference epoxy-amine network, the use of the three imidazolium ILMs led to a significant increase in biofilm inhibition (between 87 and 92 %). These results were further confirmed by the SEM micrographs which clearly showed the decrease of the amount of bacteria on the surface of the epoxy networks.

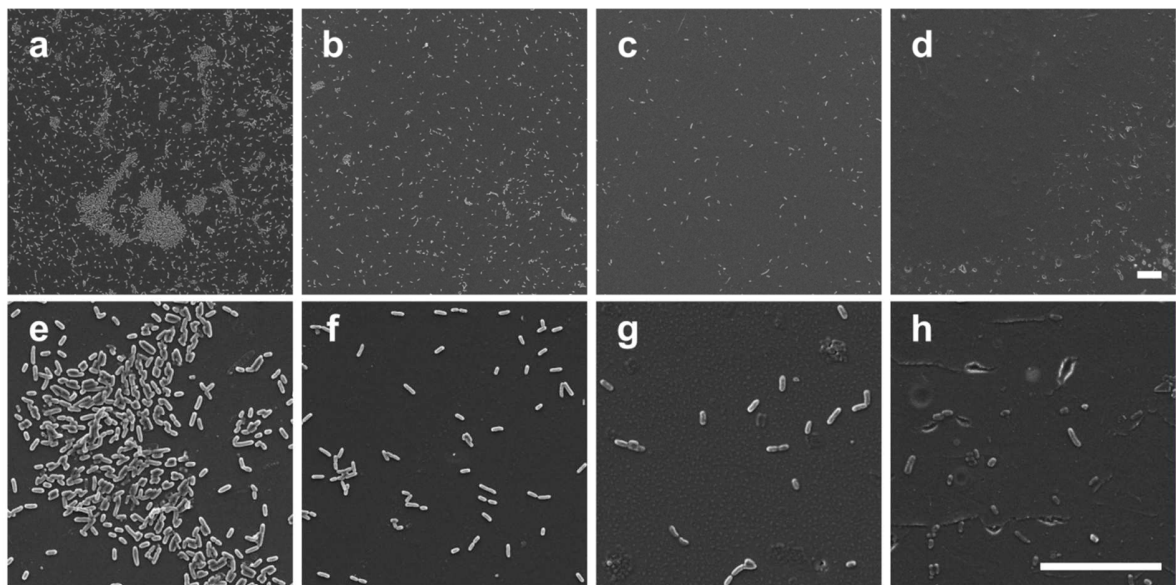


Figure 5. SEM micrographs of the active surface of DGEBA/D230 (a,e) ILM-1 (b, f), ILM-2 (c, g) and ILM-3 (d, h)

As can be seen in **Figure 5**, the most significant decreases were obtained for ILM-1 and ILM-3 where the presence of damaged bacteria was also observed. These results can be explained by the formation of quaternary ammonium salts well-known for their antibacterial activities⁶⁰⁻⁶². For example, Druvari *et al* have synthesized two series of copolymers via free radical copolymerization by incorporating covalently 4-vinyl-benzyl-dimethylhexadecylammonium chloride or by electrostatically bounded cetyltrimethylammonium 4-styrene sulfonate (SSAmC₁₆)⁵⁵. Thus, they demonstrated a strong antimicrobial activity against *S. aureus* and *P. aeruginosa* in function of the concentration of SSAmC₁₆⁵⁵. Indeed, for their best composition, they highlighted a log reduction of 5.3, 5.4 compared to 5 for the homopolymer PSSAmC₁₆⁵⁵. Other authors like Ritter *et al* have showed a significant decrease of *E. coli* when they have used 16 mol % of aminoammonium salts functionalized only with long alkyl chain (C₁₂) into an epoxy-amine network³⁴. In addition, it is also widely reported in the literature that imidazolium ionic liquids have excellent antibacterial properties⁶³⁻⁶⁴. Recently, Zhang *et al* have demonstrated that the incorporation of polyether block imidazolium into polysiloxane generated good antibacterial activity against *E. coli* and *S. aureus*⁶³. Other authors have shown that the use of imidazolium ILs functionalized by long alkyl chains (> C₁₂) has a significant influence on the growth, adhesion and biofilm formation^{38,64}. Thus, various authors have demonstrated that an increase in the hydrophobic character of the ionic liquid led to better antibacterial efficiency⁶⁴. These results are in agreement with the previously obtained surface energies (see **Table 3**) where the most hydrophobic networks, *i.e* ILM-1 and ILM-3 induced better antibacterial activities against *E. coli*.

In summary, these new epoxy-amine networks combining the antibacterial activity of imidazolium and ammonium ionic liquids led to polymeric materials with excellent anti-biofilm properties for bacteria. Moreover, their easy processing opens new perspectives in the development of high performance polymer coatings.

CONCLUSION

In this work, three new thermally stable epoxy-amine networks with good thermomechanical properties, hydrophobic behavior and with glass transition similar to the conventional diglycidyl ether epoxy prepolymer (DGEBA) were prepared for the first time from imidazolium ionic liquid monomers not requiring the use of toxic and carcinogenic compounds. First, the influence of the ILM monomers was studied on the reactivity with an aliphatic amine (D-230) leading to a total conversion of the epoxy functions, especially for ILM-[NTf₂]-2 (35 min at 80 °C). Then, we have highlighted that the chemical nature of the ILM-[NTf₂] plays a key role on the hydrophobic behavior of the networks and as a consequence on the antibacterial properties. In fact, these new networks showed enhanced antibacterial activity against *E. coli* where the antibacterial efficiency is mainly dependent of the hydrophobic behavior of the surface polymeric networks. These promising results open new perspectives in the development of antibacterial active surface epoxy coatings. Nevertheless, future works are required to develop high-performance epoxy materials for specific applications.

ACKNOWLEDGEMENTS

The authors gratefully acknowledge FAPESP (Grant numbers: 2015/25406-5, 2017/11060-5, 2017/01167-7, 17/26471-0) and from Groupement de Recherches Liquides Ioniques et PolymèreS (GDR LIPS-CNRS #5223).

REFERENCES AND NOTES

- (1) Yepez, E.S.; Bovera, M.M.; Rosenthal, V.D.; González Flores, H.A.; Pazmiño, L.; Valencia, F.; Alquina, N.; Ramirez, V.; Jara, E.; Lascano, M.; Delgado, V.; Cevallos, C.; Santacruz, G.; Pelaéz, C.; Zaruma, C.; Pinto, D.B.; Device-associated infection rates, mortality, length of stay and bacterial resistance in intensive care units in Ecuador: International Nosocomial Infection Control Consortium's findings, *World J Biol Chem.* **2017**, 8(1), 95-101, DOI: 10.4331/wjbc.v8.i1.95.
- (2) Goldmann, D.A.; Huskins, W.C.; Control of Nosocomial Antimicrobial-Resistant Bacteria: A Strategic Priority for Hospitals Worldwide, *Clinical Infectious Diseases*, **1997**, 24, S139-S145, DOI: 10.1093/clinids/24.Supplement_1.S139.
- (3) Richards, M.J., Edwards, J.R.; Culver, D.H.; Gaynes, R.P.; Nosocomial infections in medical intensive care units in the United States, *Critical Care Medicine*, **1999**, 27 (5), 887-892.
- (4) Li, F.; Weir, M.D.; Fouad, A.F.; Xu, H.H.K.; Effect of salivary pellicle on antibacterial activity of novel antibacterial dental adhesives using a dental plaque microcosm biofilm model, *Dental Materials*, **2014**, 30 (2), 182-191, DOI: 10.1016/j.dental.2013.11.004.
- (5) He, J.; Söderling, E.; Lassila, L.V.J.; Vallittu, P.K.; Preparation of antibacterial and radio-opaque dental resin with new polymerizable quaternary ammonium monomer, *Dental Materials*, **2015**, 31 (5), 575-582, DOI: 10.1016/j.dental.2015.02.007.
- (6) Díez-Pascual, A.M.; Díez-Vicente, A.L.; Antimicrobial and sustainable food packaging based on poly (butylene adipate-co-terephthalate) and electrospun chitosan nanofibers, *RSC Adv.*, **2015**, 5, 93095-93107, DOI: 10.1039/C5RA14359D.

- (7) Goli, K.K, Rojas, O.J, Genzer, J., Formation and Antifouling Properties of Amphiphilic Coatings on Polypropylene Fibers, *Biomacromolecules*, **2012**, 13 (11), 3769-3779, DOI: 10.1021/bm301223b.
- (8) Wang, B-L.; Ren, K-F.; Chang, H.; Wang, J-L.; Ji, J.; Construction of Degradable Multilayer Films for Enhanced Antibacterial Properties, *ACS Appl. Mater. Interfaces*, **2013**, 5 (10), 4136-4143, DOI: 10.1021/am4000547.
- (9) Ballesteros, C.A.S.; Bernardi, J.C.; Corrêa, D.S.; Zucolotto, V.; Controlled release of silver nanoparticles contained in photo-responsive nanogels, *ACS Appl. Bio Mater.*, **2019**, DOI: 10.1021/acsabm.8b00366.
- (10) Somayajula, D.; Agarwal, A.; Sharma, A.; Pall, A.; Datta, S.; Ghosh, G.; In Situ Synthesis of Silver Nanoparticles within Hydrogel-conjugated Membrane for Enhanced Anti-Bacterial Properties, *ACS Appl. Bio Mater.*, **2019**, DOI: 10.1021/acsabm.8b00471.
- (11) Lee, J.; Yoo, J.; Kim, J.; Jang, Y.; Shin, K.; Ha, E.; Ryu, S.; Kim, B-G.; Wooh, S.; Char, K.; Development of Multimodal Antibacterial Surfaces Using Porous Amine-Reactive Films Incorporating Lubricant and Silver Nanoparticles, *ACS Appl. Mater. Interfaces*, **2019**, DOI: 10.1021/acsami.8b20092.
- (12) Shao, W.; Liu, Y.; Min, H.; Dong, G.; Feng, Q.; Zuo, S.; Preparation, characterization, and antibacterial activity of silver nanoparticle-decorated graphene oxide nanocomposite, *ACS Appl. Mater. Interfaces*, **2015**, 7 (12), 6966-6973, DOI: 10.1021/acsami.5b00937.
- (13) Lowe, A.B.; Thiol-ene “click” reactions and recent applications in polymer and materials synthesis, *Polym. Chem.*, **2010**, 1, 17-36, DOI: 10.1039/B9PY00216B.
- (14) Wang, B.; Xu, Q.; Ye, Z.; Liu, H.; Lin, Q.; Nan, K.; Li, Y.; Wang, Y.; Qi, L.; Chen, H.; Copolymer brushes with temperature-triggered, reversibly switchable bactericidal and antifouling

properties for biomaterial surfaces, *ACS Appl. Mater. Interfaces*, **2016**, 8 (40), 27207-27217, DOI: 10.1021/acsami.6b08893.

(15) Yu, K.; Lo, J.C.Y.; Mei, Y.; Haney, E.F.; Siren, E.; Kalathottukaren, M.T.; Hancock, R.E.W.; Lange, D.; Kizhakkedathu, J.N.; Toward infection-resistant surfaces: achieving high antimicrobial peptide potency by modulating the functionality of polymer brush and peptide, *ACS Appl. Mater. Interfaces*, **2015**, 7 (51), 28591- 28605, DOI: 10.1021/acsami.5b10074.

(16) Aumsuwan, N.; Heinhorst, S.; Urban, M.W.; Antibacterial Surfaces on Expanded Polytetrafluoroethylene; Penicillin Attachment, *Biomacromolecules*, **2007**, 8 (2), 713-718, DOI: 10.1021/bm061050k.

(17) Murata, H.; Koepsel, R.R.; Matyjaszewski, K.; Russell, A.J.; Permanent, non-leaching antibacterial surfaces—2: How high density cationic surfaces kill bacterial cells, *Biomaterials*, **2007**, 28 (32), 4870-4879, DOI: 10.1016/j.biomaterials.2007.06.012.

(18) Zheng, Z.; Xu, Q.; Guo, J.; Qin, J.; Mao, H.; Wang, B.; Yan, F.; Structure–Antibacterial Activity Relationships of Imidazolium-Type Ionic Liquid Monomers, Poly(ionic liquids) and Poly(ionic liquid) Membranes: Effect of Alkyl Chain Length and Cations, *ACS Appl. Mater. Interfaces*, **2016**, 8 (20), 12684-12692, DOI: 10.1021/acsami.6b03391.

(19) Makvandi, P.; Ghaemy, M.; Mohsenib, M.; Synthesis and characterization of photo-curable bis-quaternary ammonium dimethacrylate with antimicrobial activity for dental restoration materials, *Eur. Polym. J.*, **2016**, 74, 81-90, DOI: 10.1016/j.eurpolymj.2015.11.011.

(20) Richards, S-J.; Jones, M.W.; Hunaban, M.; Haddleton, D.M.; Gibson, M.I.; Probing Bacterial-Toxin Inhibition with Synthetic Glycopolymers Prepared by Tandem Post-Polymerization Modification: Role of Linker Length and Carbohydrate Density, *Angew. Chem.*, **2012**, 51(31), DOI:10.1002/anie.201202945.

(21) Koromilas, N.D.; Lainioti, G.; Vasilopoulos, G., Vantarakis, A. ; Kallitsis, J.K. ; Synthesis of antimicrobial block copolymers bearing immobilized bacteriostatic groups, *Polym. Chem.* **2016**, 7, 3562-3575, DOI: 10.1039/C6PY00553E.

(22) Guan, J.; Wang, Y.; Wu, S.; Li, Y.; and Li, J.; Durable Anti-Superbug Polymers: Covalent Bonding of Ionic Liquid onto the Polymer Chains, *Biomacromolecules*, **2017**, 18 (12), pp 4364-4372, DOI: 10.1021/acs.biomac.7b01416.

(23) Grillet, A.C.; Galy, J.; Gérard, J-F.; Pascault, J-P.; Mechanical and viscoelastic properties of epoxy networks cured with aromatic diamines, *Polymer*, **1991**, 32 (10), 1885-1891, DOI: 10.1016/0032-3861(91)90380-2.

(24) Bonnet, A.; Pascault, J-P.; Sautereau, H.; Taha, M.; Epoxy–Diamine Thermoset/Thermoplastic Blends. 1. Rates of Reactions before and after Phase Separation, *Macromolecules*, **1999**, 32 (25), 8517-8523, DOI: 10.1021/ma981754p.

(25) Chen, D.; Pascault, J-P.; Sage, D.; Surface properties of epoxy systems, 1. Influence of the chemical structure on surface energy of monomers, comonomers and additives, *Makromol. Chem* **1991**, 192 (4), 867-882, DOI: 10.1002/macp.1991.021920412.

(26) Auvergne, R.; Caillol, S.; David, G.; Boutevin, B.; Pascault, J-P. ; Biobased thermosetting epoxy: present and future, *Chem. Rev.*, **2014**, 114 (2), 1082-1115, DOI: 10.1021/cr3001274.

(27) Glaive, A-S.; Modjinou, T.; Versace, D-L.; Andaloussi, S.A.; Dubot, P.; Langlois, V.; Renard , E.; Design of antibacterial and sustainable antioxidant networks based on plant phenolic derivatives used as delivery system of carvacrol or tannic acid, *ACS Sustainable Chem. Eng.*, **2017**, 5 (3), 2320-2329, DOI: 10.1021/acssuschemeng.6b02655.

(28) Modjinou, T.; Versace, D-L.; Andaloussi, S.A.; Langlois, V.; Renard , E.; Antibacterial and antioxidant photoinitiated epoxy co-networks of resorcinol and eugenol derivatives, *Mat. Today Comm*, **2017**, 12, 19-28, DOI: 10.1016/j.mtcomm.2017.03.005.

- (29) Fei, X.; Wei, W.; Zhao, F.; Zhu, Y., Luo, J.; Chen, M.; Liu, X.; Efficient toughening of epoxy–anhydride thermosets with a biobased tannic acid derivative, *ACS Sustainable Chem. Eng.*, **2017**, 5 (1), 596-603, DOI: 10.1021/acssuschemeng.6b01967.
- (30) Tiller, J.C.; Lia, C-J. ; Lewis, K.; Klibanov, A.M.; Designing surfaces that kill bacteria on contact, *PNAS*, **2001**, 98 (11), 5981-5985, DOI: 10.1073/pnas.111143098.
- (31) Vasilev, K.; Cook, J.; Griesser, H.J.; Antibacterial surfaces for biomedical devices, *Expert Review of Medical Devices*, **2009**, 6 (5), DOI: 10.1586/erd.09.36.
- (32) Klee, J.; Hörhold, H.H.; Kremer, F.; Unvernetzte Epoxid-Amin-Additionspolymere, 31. Polykationen auf Basis von Epoxid-Amin-Additionspolymeren. Herstellung und Eigenschaften, *Die Makromolekulare Chemie*, **1989**, 190 (12), 3055-3060, DOI: 10.1002/macp.1989.021901202.
- (33) Ikeda, T.; Tazuke, S.; Suzuki, Y.; Biologically active polycations, 4. Synthesis and antimicrobial activity of poly (trialkylvinylbenzylammonium chloride) s, *Die Makromolekulare Chemie*, **1984**, 185 (5), 869-876, DOI: 10.1002/macp.1984.021850503.
- (34) Mondrzyk, A.; Fischer, J.; Ritter, H.; Antibacterial materials: structure–bioactivity relationship of epoxy–amine resins containing quaternary ammonium compounds covalently attached, *Polymer International*, **2014**, 63 (7), 1192-1196, DOI: 10.1002/pi.4690.
- (35) Zhou, Y.; Qu, J.; Ionic liquids as lubricant additives: a review, *ACS Appl. Mater. Interfaces*, **2017**, 9 (4), 3209-3222, DOI: 10.1021/acsam.6b12489.
- (36) Aparicio, S.; Atilhan, M.; Karadas, F.; Thermophysical properties of pure ionic liquids: review of present situation, *Ind. Eng. Chem. Res.*, **2010**, 49 (20), 9580-9595, DOI: 10.1021/ie101441s.
- (37) Welton, T.; Room-temperature ionic liquids. Solvents for synthesis and catalysis, *Chem. Rev.*, **1999**, 99 (8), 2071-2084, DOI: 10.1021/cr980032t.

- (38) Garcia, M.T.; Ribosa, I.; Perez, L.; Manresa, A.; Comelles, F.; Micellization and Antimicrobial Properties of Surface-Active Ionic Liquids Containing Cleavable Carbonate Linkages, *Langmuir*, **2017**, 33 (26), 6511-6520, DOI: 10.1021/acs.langmuir.7b00505.
- (39) Egorova, K.S.; Gordeev, E.G.; Ananikov, V.P.; Biological activity of ionic liquids and their application in pharmaceutics and medicine, *Chem. Rev.*, **2017**, 117 (10), 7132-7189, DOI: 10.1021/acs.chemrev.6b00562.
- (40) Qin, J.; Guo, J.; Xu, Q.; Zheng, Z.; Mao, Z.; Yan, F.; Synthesis of pyrrolidinium-type poly(ionic liquid) membranes for antibacterial applications, *ACS Appl. Mater. Interfaces*, **2017**, 9 (12), 10504-10511, DOI: 10.1021/acsami.7b00387.
- (41) Livi, S.; Silva, A. A.; Thimont, Y.; Nguyen, T. K. L.; Soares, B. G.; Gérard, J.-F.; Duchet-Rumeau, J. Nanostructured thermosets from ionic liquid building block–epoxy prepolymer mixtures, *RSC Adv.* **2014**, 4, 28099-28106, DOI 10.1039/C4RA03643C.
- (42) Nguyen, T. K. L.; Livi, S.; Soares, B. G.; Pruvost, S.; Duchet-Rumeau, J.; Gérard, J.-F. Ionic liquids: A new route for the design of epoxy networks. *ACS Sustainable Chem. Eng.* **2016**, 4, 481-490, DOI 10.1021/acssuschemeng.5b00953.
- (43) Maka, H.; Spychaj, T.; Pilawka, R. Epoxy resin/ionic liquid systems: the influence of imidazolium cation size and anion type on reactivity and thermomechanical properties. *Ind. Eng. Chem. Res.*, **2012**, 51, 5197-5206, DOI 10.1021/ie202321j.
- (44) Nguyen, T. K. L.; Livi, S.; Pruvost, S.; Soares, B. G.; Duchet-Rumeau, J. Ionic liquids as reactive additives for the preparation and modification of epoxy networks. *J. Polym. Sci.; Part A: Polym. Chem.* **2014**, 52, 3463-3471, DOI 10.1002/pola.27420.
- (45) Livi, S.; Chardin, C.; Lins, L.C.; Halawani, N.; Pruvost, S.; Duchet-Rumeau, J.; Gerard, J.-F.; Baudoux, J.; From Ionic Liquid Epoxy Monomer to Tunable Epoxy-Amine Network: Reaction

Mechanism and final properties, *ACS Sustainable Chem. Eng.*, **2019**, DOI: 10.1021/acssuschemeng.8b06271.

(46) Pascault, J.-P.; Williams, R. J. J. *Epoxy Polymers: New Materials and Innovations*, Eds.; Wiley-VCH Verlag GmbH & Co. KGaA: Weinheim, **2010**, ISBN: 978-3-527-62871-1.

(47) Chardin, C.; Rouden, J.; Livi, S.; Baudoux, J. Dimethyldioxirane (DMDO) as a valuable oxidant for the synthesis of polyfunctional aromatic imidazolium monomers bearing epoxides, *Green Chem.* **2017**, 19, 5054-5059, DOI 10.1039/C7GC02372C.

(48) Owens, D. K.; Wendt, R. C. Estimation of the Surface Free Energy of Polymers. *J. Appl. Polym. Sci.* **1969**, 13, 1741-1747, DOI 10.1002/app.1969.070130815.

(49) Maka, H.; Spychaj, T.; Zenker, M. High performance epoxy composites cured with ionic liquids, *J. Ind. Eng. Chem.* **2015**, 31, 192-198, DOI 10.1016/j.jiec.2015.06.023.

(50) Cai, H.; Li, P.; Sui, G.; Yu, Y.; Li, G.; Yang, X.; Ryu, S. Curing kinetics study of epoxy resin/flexible amine toughness systems by dynamic and isothermal DSC. *Thermochim. Acta.* **2008**, 473, 101-105, DOI 10.1016/j.tca.2008.04.012.

(51) Yang, G.; Fu, S.-Y.; Yang, J.-P. Preparation and mechanical properties of modified epoxy resins with flexible diamines. *Polymer*, **2007**, 48, 302-310, DOI 10.1016/j.polymer.2006.11.031.

(52) De Nograro, F. F.; Guerrero, P.; Corcuera, M. A.; Mondragon, I. Effects of chemical structure of hardener on curing evolution and on the dynamic mechanical behavior of epoxy resins. *J. Appl. Polym. Sci.* **1995**, 56, 177-192, DOI 10.1002/app.1995.070560208.

(53) McAninch, I. M.; Palmese, G. R.; Lenhart, J. L.; La Scala, J. J. Characterization of epoxies cured with bimodal blends of polyetheramines. *J. Appl. Polym. Sci.* **2013**, 130, 1621-1631, DOI 10.1002/app.39322.

(54) Druvari, D.; Koromilas, N.; Bekiari, V.; Bokias, G.; Kallitsis, J.; Polymeric Antimicrobial Coatings Based on Quaternary Ammonium Compounds, *Coatings*, **2018**, 8(1), 8; DOI:10.3390/coatings8010008.

(55) Druvari, D.; Koromilas, N.; Lainioti, G. Ch.; Bokias, G.; Vasilopoulos, G.; Vantarakis, A.; Baras, I.; Dourala, N.; Kallitsis, J.K.; Polymeric quaternary ammonium-containing coatings with potential dual contact-based and release-based antimicrobial activity, *ACS Appl. Mater. Interfaces*, **2016**, 8 (51), 35593-35605, DOI: 10.1021/acsami.6b14463.

(56) Van de Grampel, R.D.; Ming, W.; Van Gennip, W.J.H.; van der Velden, F.; Laven, J.; Niemantsverdriet, J.W.; van der Linde, R.; Thermally cured low surface-tension epoxy films, *Polymer*, **2015**, 46 (23), 10531-10537, DOI: 10.1016/j.polymer.2005.08.024.

(57) Miccio, L.A.; Fasce, D.P.; Schreiner, W.H.; Montemartini, P.E.; Oyanguren, P.A.; Influence of fluorinated acids bonding on surface properties of crosslinked epoxy-based polymers, *Eur. Polym. J.*, **2010**, 46 (4), 744-753, DOI: 10.1016/j.eurpolymj.2010.01.001.

(58) Almeida, H. F. D.; Lopes-da-Silva, J. A.; Freire, M. G.; Coutinho, J. A. P. Surface tension and refractive index of pure and water-saturated tetradecyltriethylphosphonium-based ionic liquids. *J. Chem. Thermodyn.* **2013**, 57, 372-379, DOI 10.1016/j.jct.2012.09.004.

(59) Carvalho, P. J.; Neves, C. M. S. S.; Coutinho, J. A. P. Surface tensions of bis (trifluoromethyl-sulfonyl)imide anion-based ionic liquids. *J. Chem. Eng. Data*, **2010**, 55, 3807-3812, DOI: 10.1021/je100253m.

(60) Lu, G.; Wu, D.; Fu, R.; Studies on the synthesis and antibacterial activities of polymeric quaternary ammonium salts from dimethylaminoethyl methacrylate, *Reactive and Functional Polymers*, **2007**, 67 (4), 355-366, DOI:10.1016/j.reactfunctpolym.2007.01.008.

(61) Shelton, R.S.; van Campen, M.G.; Tilford, C.H.; Lang, H.C.; Nisonger, L.; Bandelin, F.J.; Rubenkoenig, H.L.; Quaternary Ammonium Salts as Germicides. I. Non-acylated Quaternary

Ammonium Salts Derived from Aliphatic Amines, *J. Am. Chem. Soc.*, **1946**, 68 (5), 753-755,

DOI: 10.1021/ja01209a012.

(62) Tischer, M.; Pradel, G.; Ohlsen, K.; Holzgrabe, U.; Quaternary ammonium salts and their antimicrobial potential: targets or nonspecific interactions?, *ChemMedChem*, **2012**, 7 (1), 22-31,

DOI: 10.1002/cmdc.201100404.

(63) Zhang, G.; Jiang, S.; Gao, Y.; Sun, F.; Initiating the Photopolymerization Behaviors of Water-Soluble Polymerizable Polysiloxane–Polyether Block Imidazolium Ionic Liquids with Antibacterial Capability, *Macromol. Chem. Phys.*, **2017**, 218 (19), DOI:

170022210.1002/macp.201700222.

(64) Kiran, G.; Reddy, K.; Nancharaiah, Y.V.; Venugopalan, V.P.; Long alkyl-chain imidazolium ionic liquids: Antibiofilm activity against phototrophic biofilms, *Colloids and Surfaces B: Biointerfaces*, **2017**, 155, 487-496. DOI: 10.1016/j.colsurfb.2017.04.040.

Supporting Information

Antibacterial Surface Based on New Epoxy-Amine Networks From Ionic Liquid Monomers

Sebastien Livi^{1,2,*}, Luanda C. Lins⁴, Larissa B. Capeletti², Charline Chardin³, Nour Halawani¹, Jérôme Baudoux^{3*}, Mateus B. Cardoso^{2,4}

¹ Université de Lyon, CNRS, UMR 5223, Ingénierie des Matériaux Polymères, INSA Lyon, F-69621 Villeurbanne, France

² Laboratório Nacional de Nanotecnologia (LNNano) & Laboratório Nacional de Luz Síncrotron (LNLS), Centro Nacional de Pesquisa em Energia e Materiais (CNPEM), CEP 13083-970, Caixa Postal 6192, Campinas, SP, Brazil.

⁴ Laboratoire de Chimie Moléculaire et Thio-organique, ENSICAEN, Université de Normandie, CNRS, 6 boulevard du Maréchal Juin, 14050 Caen, France.

⁵ Instituto de Química (IQ), Universidade Estadual de Campinas (UNICAMP), CEP 13083-970, Caixa Postal 6154, Campinas, SP, Brazil.

Number of pages: 33

Number of Figures: 24

I.	General experimental and analytical data	(S-2)
II.	Procedure for the synthesis of ILM-[NTf ₂]-1	(S-3)
III.	Procedure for the synthesis of ILM-[NTf ₂]-2	(S-5)
IV.	Procedure for the synthesis of ILM-[NTf ₂]-3	(S-8)
V.	NMR spectra	(S-9)
VI.	FTIR spectra	(S-31)
VII.	DSC analysis	(S-32)

I. General experimental and analytical data

All reagents were purchased from Sigma Aldrich, Alfa Aesar or TCI and were used without further purification and used as received. Solvents were used in RPE grade without further purification. Anhydrous solvents were obtained from a PURESOLV SPS400 apparatus developed by Innovative Technology Inc. ^1H , ^{13}C and ^{19}F NMR spectra were recorded on a Bruker AvanceIII 400 MHz spectrometer. Samples were dissolved in an appropriate deuterated solvent (CDCl_3). The chemical shifts (δ) are expressed in ppm relative to internal tetramethylsilane for ^1H and ^{13}C nuclei, and coupling constants are indicated in Hz. Abbreviations for signal coupling are as follows: s=singlet; d=doublet; dd=doublet of doublets; t=triplet; q=quartet; quin=quintet; m=multiplet; br=broad signal. To assign the signals to the different proton and carbon atoms, as well as the relative stereochemistry of the cycloadducts, additional 2D NMR experiments (COSY, HSQC, HMBC) and NOESY experiments were performed. Mass spectra were obtained on a GC/MS Saturn 2000 spectrometer. High-resolution mass spectra (HRMS) were performed on Q-TOF Micro WATERS by electrospray ionization (ESI) or atmospheric solids analysis probe (ASAP). Infrared (IR) spectra were recorded with a Perkin Elmer 16 PC FTIR ATR spectrometer, using the pure product (oil or solid). Thin Layer Chromatography (TLC) was run on pre-coated aluminum plates of silica gel 60 F-254 (Merck). Flash chromatography was performed on silica gel column (Merck silica gel, 40-63 mm) using air pressure.

Preparation of Dimethyldioxirane. This reagent was prepared according to the procedure described by D. F. Taber.¹ Titration of different solutions prepared by this procedure afforded a DMDO concentration between 0.04 mol/L and 0.09 mol/L.²

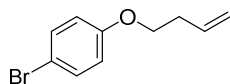
In a 1 mL volumetric test tube, a 0.7 M (C_{sol}) solution of thioanisole in acetone- d_6 is prepared, to a total volume of 1 mL (0.08 mL of thioanisole + 0.92 mL of acetone- d_6). A 0.6 mL portion of this solution is transferred to a tube and chilled to ca. 10 °C in a dry ice/water bath. Upon reaching 10 °C, 3.0 mL of the obtained DMDO solution is added to the thioanisole solution. The resulting solution is stirred for 10 min and then a portion of the solution is added directly to an NMR tube.

¹ Taber, D. F.; DeMatteo, P. W.; Hassan, R. A. Simplified Preparation of Dimethyldioxirane (DMDO). *Org. Synth.* **2013**, *90*, 350-357. DOI: 10.15227/orgsyn.090.0350.

² Mikula, H.; Svatunek, D.; Lumpi, D.; Glöcklhofer, F.; Hametner, C.; Fröhlich, J. Practical and Efficient Large-Scale Preparation of Dimethyldioxirane. *Org. Process Res. Dev.* **2013**, *17*, 313-316. DOI: 10.1021/op300338q.

II. Procedure for the synthesis of ILM-[NTf₂]-1

1-Bromo-4-(3-buten-1-yloxy)benzene (1)

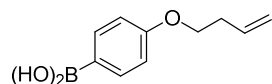


The title compound was prepared with 4-bromophenol (5.00 g, 28.90 mmol, 1.0 eq.), K₂CO₃ (9.99 g, 72.25 mmol, 2.5 eq.) and 4-bromobutene (11.64 mL, 57.80 mmol, 2.0 eq.) in CH₃CN (140 mL). The mixture was stirred and refluxed for 72 h.

The product **1** was obtained as a yellow oil (6.28 g, 96 %).

¹H NMR (400 MHz, CDCl₃) δ 7.37 (d, *J* = 9.0 Hz, 2H), 6.78 (d, *J* = 9.0 Hz, 2H), 5.90 (ddt, *J* = 17.1, 10.3, 6.7 Hz, 1H), 5.11-5.20 (m, 2H), 3.98 (t, *J* = 6.7 Hz, 2H), 2.54 (q, *J* = 6.7 Hz, 2H). ¹³C NMR (100 MHz, CDCl₃) δ 158.1, 134.3, 132.4, 117.3, 116.5, 112.9, 67.6, 33.7. IR (neat) cm⁻¹ 3078, 2926, 1591, 1488, 1470, 1285, 1239, 1171, 1033, 1002. HRMS *m/z* (ASAP): calcd. for C₁₀H₁₁BrO [M]⁺: 225.9993, found: 225.9992.

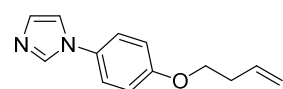
4-(3-Buten-1-yloxy)phenyl boronic acid (2)



In a dry round-bottom flask purged with N₂, compound **1** (5.87 g, 25.86 mmol, 1.0 eq.) was dissolved in dry THF (39 mL) and cooled to -78 °C. *n*-BuLi 2.5 M in hexane (12.41 mL, 31.03 mmol, 1.2 eq.) was added dropwise and the reaction mixture was stirred for 1 h. Triisopropyl borate (7.83 mL, 38.79 mmol, 1.5 eq.) was added dropwise and the reaction mixture was allowed to slowly warm up to room temperature overnight. Water (13 mL) was slowly added followed by acidification with 1 M HCl (39 mL) and the reaction mixture was stirred for 1 h. The reaction mixture was extracted with diethyl ether and the combined organic layers were dried over MgSO₄. Evaporation of volatile compounds under reduced pressure afforded the product **2** as a white solid (3.08 g, 62 %) which was used without purification.

¹H NMR (400 MHz, CDCl₃) δ 8.15 (d, *J* = 9.0 Hz, 2H), 7.01 (d, *J* = 9.0 Hz, 2H), 5.86-6.00 (m, 1H), 5.12-5.23 (m, 2H), 4.11 (t, *J* = 6.7 Hz, 2H), 2.59 (q, *J* = 6.7 Hz, 2H). ¹³C NMR (100 MHz, CDCl₃) δ 162.7, 137.6, 135.4, 134.5, 117.3, 114.2, 67.2, 33.8. IR (neat) cm⁻¹ 1603, 1353, 1245, 1172, 1028, 919, 835, 746, 688, 570. Mp: 118.5 °C. HRMS *m/z* (ESI): calcd. for C₁₀H₁₂BO₃ [M-H]⁻: 191.0879, found: 191.0876.

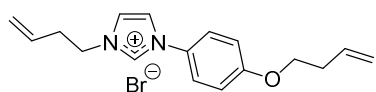
1-[4-(3-buten-1-yloxy)phenyl]-1*H*-imidazole (3)



Boronic acid **2** (1.26 g, 6.57 mmol, 1.0 eq.), imidazole (537 mg, 7.89 mmol, 1.2 eq.) and copper iodide (50 mg, 0.26 mmol, 0.04 eq.) were solubilized in methanol (40 mL). The mixture solution was refluxing 5 h at 60 °C with pumping air continuously. Then, the solvent was evaporated under reduced pressure and diethyl ether was added. The organic phase was filtered through celite and concentrated *in vacuo*. The crude was purified by flash chromatography on silica gel with 100 % ethyl acetate. The product **3** was obtained as a pale yellow solid (868 mg, 62 %).

¹H NMR (400 MHz, CDCl₃) δ 7.76 (s, 1H), 7.29 (d, *J* = 9.0 Hz, 2H), 7.18-7.20 (m, 2H), 6.98 (d, *J* = 9.0 Hz, 2H), 5.91 (ddt, *J* = 17.1, 10.2, 6.8 Hz, 1H), 5.12-5.21 (m, 2H), 4.05 (t, *J* = 6.7 Hz, 2H), 2.57 (q, *J* = 6.7 Hz, 2H). ¹³C NMR (100 MHz, CDCl₃) δ 158.4, 136.0, 134.3, 130.9, 130.2, 123.3, 118.9, 117.4, 115.7, 67.8, 33.7. IR (neat) cm⁻¹ 3100, 2925, 1517, 1302, 1260, 1242, 1177, 1058, 913, 832. Mp: 50.8 °C. HRMS *m/z* (ESI): calcd. for C₁₃H₁₅N₂O [M+H]⁺: 215.1184, found: 215.1190.

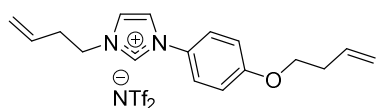
3-(3-Buten-1-yl)-1-[4-(3-buten-1-yloxy)phenyl]imidazolium bromide (4)



To a solution of compound **3** (4.78 g, 22.32 mmol, 1.0 eq.) in CH₃CN (100 mL) was added 4-bromobutene (4.5 mL, 44.63 mmol, 2.0 eq.). The mixture was refluxed at 80 °C for 48 h and was cooled to room temperature. The volatile compounds were removed under reduced pressure to afford the product **4** (7.64 g, 98 %) as a yellow oil which was directly engaged for the next step.

¹H NMR (400 MHz, CDCl₃) δ 10.79 (s, 1H), 7.63-7.69 (m, 4H), 7.00 (d, *J* = 9.0 Hz, 2H), 5.81-5.91 (m, 2H), 5.06-5.18 (m, 4H), 4.67 (t, *J* = 6.7 Hz, 2H), 4.01 (t, *J* = 6.7 Hz, 2H), 2.73 (q, *J* = 6.7 Hz, 2H), 2.53 (q, *J* = 6.7 Hz, 2H). ¹³C NMR (100 MHz, CDCl₃) δ 160.2, 135.9, 134.0, 132.7, 127.5, 123.4, 123.1, 120.7, 119.7, 117.6, 116.2, 67.9, 49.6, 34.6, 33.5. IR (neat) cm⁻¹ 3072, 2980, 1552, 1512, 1250, 1185, 1073, 995, 918, 832. HRMS *m/z* (ESI): calcd. for C₁₇H₂₁N₂O [M]⁺: 269.1654, found: 269.1653.

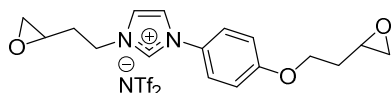
3-(3-Buten-1-yl)-1-[4-(3-buten-1-yloxy)phenyl]imidazolium 1,1,1-trifluoro-*N*-[(trifluoromethyl)sulfonyl]methanesulfonamide (5)



To a solution of compound **4** (7.64 g, 21.89 mmol, 1.0 eq.) in H₂O (350 mL) was added lithium bis(trifluoromethanesulfonyl)imide (6.91 g, 24.08 mmol, 1.1 eq.). The solution was stirred at room temperature for 24 h and then extracted with dichloromethane. The organic layer was washed several times with water, dried over MgSO₄ and concentrated under reduced pressure. The product **5** was obtained as a yellow oil (11.0 g, 91 %) and was pure enough to be used for the next step.

¹H NMR (400 MHz, CDCl₃) δ 8.97 (s, 1H), 7.44-7.52 (m, 4H), 7.04 (d, *J* = 9.0 Hz, 2H), 5.74-5.94 (m, 2H), 5.08-5.21 (m, 4H), 4.39 (t, *J* = 6.7 Hz, 2H), 4.06 (t, *J* = 6.7 Hz, 2H), 2.67 (q, *J* = 6.7 Hz, 2H), 2.57 (q, *J* = 6.7 Hz, 2H). ¹³C NMR (100 MHz, CDCl₃) δ 160.7, 134.3, 134.0, 132.2, 127.3, 123.8, 123.1, 121.9, 120.1, 120.0 (q, *J*_{CF} = 322.4 Hz), 117.6, 116.3, 68.0, 49.9, 34.3, 33.5. ¹⁹F NMR (376 MHz, CDCl₃) δ -78.9. IR (neat) cm⁻¹ 3146, 2930, 1554, 1513, 1348, 1178, 1133, 1052, 925, 832. HRMS *m/z* (ESI): calcd. for C₁₇H₂₁N₂O [M]⁺: 269.1654, found: 269.1656.

3-[2-(Oxiran-2-yl)ethyl]-1-[4-[(2-oxiran-2-yl)ethoxy]phenyl]imidazolium 1,1,1-trifluoro-*N*-[(trifluoromethyl)sulfonyl]methanesulfonamide (ILM-[NTf₂]-1)



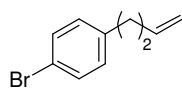
Procedure I. To a solution of compound **5** (3.51 g, 6.39 mmol, 1.0 eq.) in CH₃CN (80 mL), was added *m*CPBA (5.73 g, 25.55 mmol, 4.0 eq.) and the reaction mixture was stirred at 40 °C for 24 h. The reaction mixture was concentrated under reduced pressure and the crude product was washed with diethyl ether to extract the excess of *m*CPBA and 3-chlorobenzoic acid. The product was obtained as yellow oil (3.32 g, 89 %).

Procedure II. To a solution of compound **5** (100 mg, 0.18 mmol, 1.0 eq.) in acetone (1.0 mL) was added freshly prepared DMDO (0.087 mol/L) (5.86 mL, 0.510 mmol, 2.8 eq.). The reaction mixture was stirred at room temperature for 12 h. Two drops of DMS was added to quench the reaction mixture and neutralized the excess of DMDO. The crude was concentrated under reduced pressure to afford the product as a yellow oil (98 mg, 92 %).

¹H NMR (400 MHz, CDCl₃) δ 9.02 (s, 1H), 7.45-7.57 (m, 4H), 7.05 (d, *J* = 9.0 Hz, 2H), 4.50 (t, *J* = 6.7 Hz, 2H), 4.13-4.20 (m, 2H), 3.04-3.17 (m, 2H), 2.77-2.85 (m, 2H), 2.43-2.60 (m, 3H), 2.12-2.21 (m, 1H), 1.84-1.96 (m, 2H). ¹³C NMR (100 MHz, CDCl₃) δ 160.5, 134.6, 127.5, 124.0, 123.6, 122.0, 120.0 (q, *J*_{CF} = 322.4 Hz), 116.2, 65.5, 49.6, 49.4, 48.1, 47.2, 46.5, 32.6, 32.4. ¹⁹F NMR (376 MHz, CDCl₃) δ -78.9. IR (neat) cm⁻¹ 3147, 2933, 1556, 1514, 1348, 1330, 1178, 1132, 1052, 831. HRMS *m/z* (ESI): calcd. for C₁₇H₂₁N₂O₃ [M]⁺: 301.1552, found: 301.1554.

III. Procedure for the synthesis of (ILM-[NTf₂]-2)

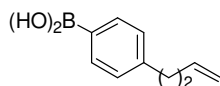
1-Bromo-4-(3-buten-1-yl)benzene (6)



Under inert atmosphere, allylmagnesium bromide 1.0 M in diethyl ether (16 mL, 16.00 mmol, 2 eq.) was added dropwise to a solution of 4-bromobenzyl bromide (2.0 g, 8.0 mmol, 1.0 eq.) in dry THF (38 mL) cooled at 0 °C. The reaction was stirred for 2 h at 0 °C. A saturated aqueous NH₄Cl (60 mL) was added and the aqueous layer was extracted 3 times with CH₂Cl₂. The combined organic layers were dried over MgSO₄ and concentrated under reduced pressure. The product **6** was obtained as clear yellow oil (1.64 g, 97 %).

¹H NMR (400 MHz, CDCl₃) δ 7.40 (d, *J* = 8.3 Hz, 2H), 7.06 (d, *J* = 8.3 Hz, 2H), 5.80 (ddt, *J* = 17.2, 10.3, 6.6 Hz, 1H), 4.95-5.06 (m, 2H), 2.66 (t, *J* = 7.3 Hz, 2H), 2.35 (q, *J* = 7.3 Hz, 2H). ¹³C NMR (100 MHz, CDCl₃) δ 140.9, 137.7, 131.5, 130.4, 119.7, 115.4, 35.4, 34.9. IR (neat) cm⁻¹ 3078, 2929, 2857, 1641, 1488, 1403, 1072, 1011, 911, 801. HRMS *m/z* (ASAP): calcd. for C₁₀H₁₁Br [M]⁺: 210.0044, found: 210.0042.

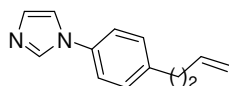
4-(3-Buten-1-yl)phenyl boronic acid (7)



In a dry round-bottom flask purged with N₂, compound **6** (1.56 g, 7.39 mmol, 1.0 eq.) was dissolved in dry THF (13 mL) and cooled to -78 °C. *n*-BuLi (3.55 mL, 8.87 mmol, 1.2 eq.) was added dropwise and the reaction mixture was stirred for 1 h. Triisopropyl borate (2.56 mL, 11.09 mmol, 1.5 eq.) was added dropwise and the reaction mixture was allowed to slowly warm up to room temperature overnight. Water (5 mL) was slowly added followed by acidification with 1 M HCl (12.65 mL) and the reaction mixture was stirred for 1 h. The reaction mixture was extracted with diethyl ether and the combined organic layers were dried over MgSO₄. Evaporation of volatile compounds under reduced pressure afforded the product **7** as a white solid (1.26 g, 97 %) which was used without purification.

¹H NMR (400 MHz, CDCl₃) δ 8.16 (d, *J* = 8.3 Hz, 2H), 7.33 (d, *J* = 8.3 Hz, 2H), 5.99 (ddt, *J* = 17.1, 10.1, 6.7 Hz, 1H), 5.11-4.98 (m, 2H), 2.81 (t, *J* = 7.3 Hz, 2H), 2.44 (q, *J* = 7.3 Hz, 2H). ¹³C NMR (100 MHz, CDCl₃) δ 147.0, 138.0, 135.9, 133.7, 128.3, 115.3, 35.9, 35.4. IR (neat) cm⁻¹ 3078, 2926, 2857, 1609, 1407, 1337, 1305, 1181, 1020, 910. Mp: 69.5 °C. HRMS *m/z* (ESI): calcd. for C₁₀H₁₂BO₂ [M-H]⁻: 175.0930, found: 175.0928.

1-[4-(3-Buten-1-yl)phenyl]-1*H*-imidazole (8)

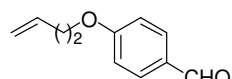


Boronic acid **7** (1.19 g, 6.76 mmol, 1.0 eq.), imidazole (552 mg, 8.11 mmol, 1.2 eq.) and copper iodide (51.50 mg, 0.270 mmol, 0.04 eq.) were mixed in methanol (36 mL). The mixture solution was refluxing 5 h with pumping air continuously. Then, the solvent was evaporated under reduced pressure and diethyl ether was added. The organic phase was filtered through celite and concentrated under reduced pressure. The crude was purified by flash chromatography on silica gel with 100 % ethyl acetate. The product **8** was obtained as a clear yellow oil (1.05 g, 78 %).

¹H NMR (400 MHz, CDCl₃) δ 7.80 (s, 1H), 7.14-7.29 (m, 6H), 5.81 (ddt, *J* = 17.0, 10.4, 6.6 Hz, 1H), 4.94-5.06 (m, 2H), 2.69-2.76 (t, *J* = 7.3 Hz, 2H), 2.32-2.40 (q, *J* = 7.3 Hz, 2H). ¹³C NMR (100 MHz, CDCl₃) δ 141.6, 137.6, 135.8, 135.5, 130.4, 130.0, 121.7, 118.5, 115.6, 35.4, 34.9. IR (neat) cm⁻¹ 3116, 2925, 1640, 1521,

1488, 1303, 1245, 1056, 904, 810. HRMS m/z (ESI): calcd. for $C_{13}H_{15}N_2$ $[M+H]^+$: 199.1235, found: 199.1237.

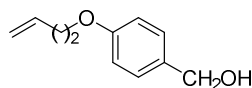
4-(But-3-enyloxy)benzaldehyde (**9**)³



To a solution of 4-hydroxybenzaldehyde (10.0 g, 81.9 mmol, 1.0 eq.) and K_2CO_3 (28.3 g, 204.7 mmol, 2.5 eq.) in CH_3CN (300 mL), 4-bromobutene (12.37 mL, 122.8 mmol, 1.5 eq.) was added. The mixture was refluxed at 80 °C for 48 h (the reaction advancement was monitored by TLC or NMR). After cooling to room temperature, the solvent was removed under reduced pressure. The residue was partitioned between CH_2Cl_2 and water and the aqueous layer was extracted with CH_2Cl_2 (2×10 mL). The combined organic extracts were washed with water, dried, and concentrated to afford the product **9** as a pale yellow oil (13.77 g, 95 %).

1H NMR (400 MHz, $CDCl_3$) δ 9.88 (s, 1H), 7.83 (d, $J = 8.7$ Hz, 2H), 7.00 (d, $J = 8.7$ Hz, 2H), 5.90 (ddt, $J = 17.1, 10.3, 6.7$ Hz, 1H), 5.12–5.21 (m, 2H), 4.10 (t, $J = 6.7$ Hz, 2H), 2.58 (q, $J = 6.7$ Hz, 2H). ^{13}C -NMR (100 MHz, $CDCl_3$) δ 191.0, 164.1, 134.0, 132.1, 130.1, 117.6, 114.9, 67.7, 33.5. IR (neat) cm^{-1} 3078, 2938, 2739, 1686, 1598, 1576, 1508, 1250, 1157, 1024. HRMS m/z (ESI): calcd. for $C_{11}H_{13}O_2$ $[M + H]^+$: 177.0916, found: 177.0917.

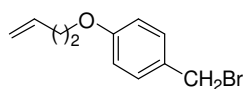
4-(3-buten-1-yloxy)benzenemethanol (**10**)



At 0 °C, compound **9** (5.0 g, 28.37 mmol, 1.0 eq.) in a THF/EtOH mixture (1:1 volume ratio, 40 mL) was added dropwise to a stirred solution of $NaBH_4$ (1.61 g, 42.56 mmol, 1.5 eq.) in a THF/EtOH mixture (1:1 volume ratio, 40 mL). The mixture was stirred at room temperature for 12 h then cooled to 0 °C and quenched with aqueous NH_4Cl solution. The volatiles were evaporated and the residue was extracted with EtOAc (2×20 mL). The combined organic extracts were washed with water (2×10 mL), dried over $MgSO_4$, and concentrated under reduced pressure. The product **10** was obtained as a pale yellow oil (4.62 g, 91 %).

1H NMR (400 MHz, $CDCl_3$) δ 7.28 (d, $J = 8.7$ Hz, 2H), 6.89 (d, $J = 8.7$ Hz, 2H), 5.91 (ddt, $J = 17.1, 10.3, 6.7$ Hz, 1H), 5.10–5.19 (m, 2H), 4.61 (s, 2H), 4.02 (t, $J = 6.7$ Hz, 2H), 2.55 (q, $J = 6.7$ Hz, 2H). ^{13}C -NMR (100 MHz, $CDCl_3$) δ 158.7, 134.5, 133.3, 128.8, 117.2, 114.8, 67.4, 65.2, 33.8. IR (neat) cm^{-1} 3078, 2926, 2872, 1612, 1511, 1241, 1172, 1033, 994, 917. HRMS m/z (ASAP): calcd. for $C_{11}H_{14}O_2$ $[M]^+$: 178.0994, found: 178.0993.

1-(Bromomethyl)-4-(but-3-enyloxy)benzene (**11**)



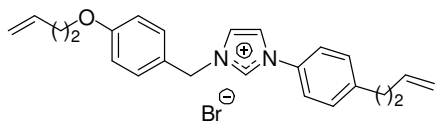
To a stirred solution of compound **10** (4.0 g, 22.44 mmol, 1.0 eq.) in Et_2O (40 mL) at 0 °C was added slowly a solution of PBr_3 (2.56 mL, 26.93 mmol, 1.2 eq.) in Et_2O (20 mL). The mixture was stirred for 6 h at 0 °C and was stirred at room temperature for another 6 h. The reaction mixture was placed in an acetone ice bath, water was added, and the solution was extracted with diethyl ether. The organic extracts were washed with aqueous $NaHCO_3$ solution, water then dried over $MgSO_4$. The solvent was removed under reduced pressure. The product **11** was obtained as a pale yellow liquid (4.94 g, 91 %).

1H NMR (400 MHz, $CDCl_3$) δ 7.31 (d, $J = 8.7$ Hz, 2H), 6.88 (d, $J = 8.7$ Hz, 2H), 5.90 (ddt, $J = 17.1, 10.3, 6.7$ Hz, 1H), 5.10–5.20 (m, 2H), 4.50 (s, 2H), 4.01 (t, $J = 6.7$ Hz, 2H), 2.54 (q, $J = 6.7$ Hz, 2H). ^{13}C -NMR (100

³ Lipshutz, B. H.; Ghorai, S.; Leong, W. W. Y. Deprotection of Homoallyl (¹³C-Allyl) Derivatives of Phenols, Alcohols, Acids, and Amines. *J. Org. Chem.* **2009**, *74*, 2854–2857. DOI: 10.1021/jo900012z.

MHz, CDCl₃) δ 159.1, 134.4, 130.6, 130.1, 117.3, 115.0, 67.4, 34.2, 33.7. IR (neat) cm⁻¹ 3077, 2924, 2870, 1610, 1509, 1246, 1174, 1033, 988, 916. HRMS *m/z* (ASAP): calcd. for C₁₁H₁₄OBr [M + H]⁺: 241.0228, found: 241.0229.

1-[4-(3-Buten-1-yl)phenyl]-3-[4-(3-buten-1-yloxy)benzyl]imidazolium bromide (**12**)

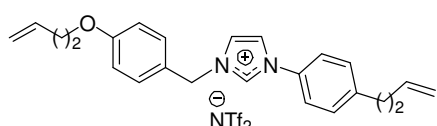


To a solution of compound **8** (2.0 g, 10.1 mmol, 1.0 eq.) in CH₃CN (20 mL) was added a solution of compound **11** (2.43 g, 10.1 mmol, 1.0 eq.) in CH₃CN (20 mL), and the mixture was stirred at 80 °C for 12 h. It was then cooled to 22 °C and the solvent was removed under reduced pressure. The product was obtained as a white solid (4.4 g, 99 %).

¹H NMR (400 MHz, CDCl₃) δ 11.17 (s, 1H), 7.64 (d, *J* = 8.3 Hz, 2H), 7.55 (d, *J* = 8.3 Hz, 2H), 7.45-7.49 (m, 1H), 7.37-7.40 (m, 1H), 7.35 (d, *J* = 8.3 Hz, 2H), 6.90 (d, *J* = 8.3 Hz, 2H), 5.76-5.95 (m, 2H), 5.75 (s, 2H), 4.96-5.21 (m, 4H), 3.99 (t, *J* = 6.7 Hz, 2H), 2.76 (t, *J* = 7.3 Hz, 2H), 2.53 (q, *J* = 6.7 Hz, 2H), 2.37 (q, *J* = 7.3 Hz, 2H). ¹³C NMR (100 MHz, CDCl₃) δ 160.0, 144.8, 137.2, 136.2, 134.3, 132.5, 131.2, 130.7, 125.0, 122.2, 121.9, 120.3, 117.4, 115.9, 115.5, 67.5, 53.5, 35.1, 34.9, 33.6. IR (neat) cm⁻¹ 3034, 2940, 1612, 1554, 1515, 1247, 1230, 1181, 1031, 917. Mp: 163.1 °C. HRMS *m/z* (ESI): calcd. for C₂₄H₂₇N₂O [M]⁺: 359.2123, found: 359.2125.

1-[4-(3-Buten-1-yl)phenyl]-3-[4-(3-buten-1-yloxy)benzyl]imidazolium [(trifluoromethyl)sulfonyl]methanesulfonamide (**13**)

1,1,1-trifluoro-*N*-

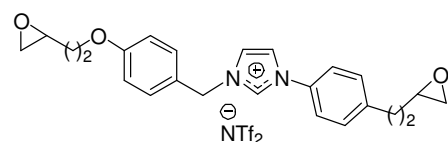


To a solution of compound **12** (4.37 g, 9.94 mmol, 1.0 eq.) in H₂O (35 mL) and CH₃CN (15 mL) was added LiNTf₂ (3.14 g, 10.94 mmol, 1.1 eq.). The solution was stirred at room temperature for 24 h and then extracted with dichloromethane. The organic layer was washed several times with water, dried over MgSO₄ and concentrated under reduced pressure. The product **13** was obtained as a yellow oil (5.82 g, 91 %).

¹H NMR (400 MHz, CDCl₃) δ 9.08 (s, 1H), 7.32-7.53 (m, 8H), 6.93 (d, *J* = 8.3 Hz, 2H), 5.74-5.95 (m, 2H), 5.39 (s, 2H), 4.96-5.22 (m, 4H), 4.00 (t, *J* = 6.7 Hz, 2H), 2.77 (t, *J* = 7.3 Hz, 2H), 2.54 (q, *J* = 6.7 Hz, 2H), 2.37 (q, *J* = 7.3 Hz, 2H). ¹³C NMR (100 MHz, CDCl₃) δ 160.3, 145.3, 137.1, 134.3, 134.0, 132.3, 131.0, 130.7, 124.0, 122.9, 122.3, 121.7, 120.0 (q, *J*_{CF} = 322.4 Hz), 117.4, 115.9, 115.7, 67.5, 53.8, 35.1, 34.9, 33.6. ¹⁹F NMR (376 MHz, CDCl₃) δ -78.8. IR (neat) cm⁻¹ 3143, 2933, 1552, 1514, 1348, 1329, 1177, 1133, 1053, 917. HRMS *m/z* (ESI): calcd. for C₂₄H₂₇N₂O [M]⁺: 359.2123, found: 359.2131.

1-[4-[2-(Oxiran-2-yl)ethyl]phenyl]-3-[4-[2-(oxiran-2-yl)ethoxy]benzyl]imidazolium [(trifluoromethyl)sulfonyl]methanesulfonamide (ILM-[NTf₂]-2)

1,1,1-trifluoro-*N*-



Procedure I. To a solution of compound **13** (5.757 g, 9.00 mmol, 1.0 eq.) in CH₃CN (75 mL), was added *m*CPBA (8.06 g, 36.00 mmol, 4.0 eq.). The reaction mixture was stirred at 40 °C for 24 h. The reaction mixture was concentrated under reduced pressure and the crude product was washed with diethyl ether

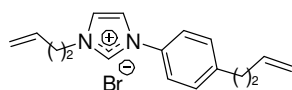
to extract the excess of *m*CPBA and 3-chlorobenzoic acid. The product was obtained as a yellow oil (5.40 g, 89 %).

Procedure II. To a solution of **13** (50 mg, 0.078 mmol, 1.0 eq.) in acetone (1.0 mL) was added freshly prepared DMDO (0.045 mol/L) (4.86 mL, 0.219 mmol, 2.8 eq.) and the mixture was stirred for 2 h. Two drops of DMS was added to quench the reaction mixture and neutralized the excess of DMDO. The crude was concentrated under reduced pressure. The product was obtained as a yellow oil (52 mg, 100 %).

^1H NMR (400 MHz, CDCl_3) δ 9.03 (s, 1H), 7.34-7.58 (m, 8H), 6.95 (d, $J = 8.3$ Hz, 2H), 5.39 (s, 2H), 4.05-4.17 (m, 2H), 3.10-3.17 (m, 1H), 2.73-2.97 (m, 5H), 2.54-2.60 (m, 1H), 2.46-2.51 (m, 1H), 2.08-2.19 (m, 1H), 1.84-2.00 (m, 2H), 1.71-1.83 (m, 1H). ^{13}C NMR (100 MHz, CDCl_3) δ 160.1, 144.8, 134.1, 132.5, 131.1, 130.7, 124.1, 122.9, 122.5, 121.8, 120.0 (q, $J_{\text{CF}} = 322.4$ Hz), 115.7, 65.0, 53.9, 51.6, 49.7, 47.3, 34.0, 32.5, 32.0. ^{19}F NMR (376 MHz, CDCl_3) δ -78.8. IR (neat) cm^{-1} 3142, 2930, 1553, 1515, 1348, 1329, 1177, 1132, 1052, 831. HRMS m/z (ESI): calcd. for $\text{C}_{24}\text{H}_{27}\text{N}_2\text{O}_3$ $[\text{M}]^+$: 391.2022, found: 391.2022.

IV. Procedure for the synthesis of the salt (ILM-[NTf₂]-3)

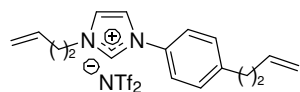
1-[4-(3-Buten-1-yl)phenyl]-3-(3-buten-1-yl)imidazolium bromide (14)



To a solution of compound **8** (1.05 g, 5.27 mmol, 1.0 eq.) in CH_3CN (35 mL) was added 4-bromobutene (1.06 mL, 10.54 mmol, 2.0 eq.). The mixture was refluxed at 80 °C for 48 h and the reaction mixture was cooled to room temperature. Evaporation of volatile compounds under reduced pressure afforded the product **14** as a yellow oil (1.75 g, 100 %) which was directly engaged for the next step.

^1H NMR (400 MHz, CDCl_3) δ 10.94 (s, 1H), 7.63-7.72 (m, 4H), 7.34 (d, $J = 8.3$ Hz, 2H), 5.72-5.94 (m, 2H), 4.95-5.12 (m, 4H), 4.71 (t, $J = 6.7$ Hz, 2H), 2.73-2.77 (m, 4H), 2.35 (q, $J = 7.3$ Hz, 2H). ^{13}C NMR (100 MHz, CDCl_3) δ 144.7, 137.1, 136.1, 132.7, 132.5, 130.7, 123.2, 121.8, 120.4, 119.7, 115.8, 49.6, 35.1, 34.9, 34.7. IR (neat) cm^{-1} 3049, 2855, 1640, 1566, 1550, 1515, 1438, 1198, 1071, 914. HRMS m/z (ESI): calcd. for $\text{C}_{17}\text{H}_{21}\text{N}_2$ $[\text{M}]^+$: 253.1705, found: 253.1704.

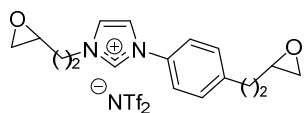
1-[4-(3-Buten-1-yl)phenyl]-3-(3-buten-1-yl)imidazolium 1,1,1-trifluoro-*N*-[(trifluoromethyl) sulfonyl]methanesulfonamide (15)



To a solution of compound **14** (3.21 g, 9.64 mmol, 1.0 eq.) in H_2O (80 mL) was added lithium bis(trifluoromethanesulfonyl)imide (3.04 g, 10.60 mmol, 1.1 eq.). The solution was stirred at room temperature for 24 h and then extracted with dichloromethane. The organic layer was washed several times with water, dried over MgSO_4 and concentrated under reduced pressure. The product **15** was obtained as a yellow oil (4.73 g, 92 %) and was pure enough to be used for the next step.

^1H NMR (400 MHz, CDCl_3) δ 9.09 (s, 1H), 7.36-7.60 (m, 6H), 5.74-5.88 (m, 2H), 4.97-5.20 (m, 4H), 4.43 (t, $J = 6.7$ Hz, 2H), 2.79 (t, $J = 7.3$ Hz, 2H), 2.68 (q, $J = 6.7$ Hz, 2H), 2.39 (q, $J = 7.3$ Hz, 2H). ^{13}C NMR (100 MHz, CDCl_3) δ 145.3, 137.1, 134.5, 132.3, 132.2, 130.8, 123.3, 122.2, 121.6, 120.1, 120.0 (q, $J_{\text{CF}} = 322.4$ Hz), 115.9, 49.9, 35.1, 35.0, 34.3. ^{19}F NMR (376 MHz, CDCl_3) δ -78.9. IR (neat) cm^{-1} 3145, 2931, 1553, 1348, 1329, 1179, 1133, 1053, 918, 838. HRMS m/z (ESI): calcd. for $\text{C}_{17}\text{H}_{21}\text{N}_2$ $[\text{M}]^+$: 253.1705, found: 253.1704.

3-[2-(Oxiran-2-yl)ethyl]-1-[4-[2-(oxiran-2-yl)ethyl]phenyl]imidazolium 1,1,1-trifluoro-*N*-[(trifluoromethyl)sulfonyl]methanesulfonamide (ILM-[NTf₂]-3)



Procedure I. To a solution of compound **15** (1.35 g, 2.54 mmol, 1.0 eq.) in CH_3CN (32 mL), was added *m*CPBA (2.27 g, 10.14 mmol, 4.0 eq.) and the reaction mixture was stirred at 40 °C for 24 h. The reaction mixture was concentrated under reduced pressure and the crude product was washed with diethyl ether to extract the excess of *m*CPBA and 3-chlorobenzoic acid. The product was obtained as a yellow oil (1.27 g, 89 %).

Procedure II. To a solution of compound **15** (100 mg, 0.187 mmol, 1.0 eq.) in acetone (1.0 mL) was added freshly prepared DMDO (0.046 mol/L) (11.41 mL, 0.525 mmol, 2.8 eq.). The reaction mixture was stirred at room temperature for 12 h. Two drops of DMS was added to quench the reaction mixture and neutralized the excess of DMDO. The crude was concentrated under reduced pressure to afford the product as a yellow oil (106 mg, 100 %).

^1H NMR (400 MHz, CDCl_3) δ 9.03 (s, 1H), 7.58-7.64 (m, 2H), 7.36-7.50 (m, 4H), 4.49 (t, $J = 6.7$ Hz, 2H), 3.00-3.08 (m, 1H), 2.71-2.96 (m, 5H), 2.37-2.53 (m, 3H), 1.72-1.96 (m, 3H). ^{13}C NMR (100 MHz, CDCl_3) δ 144.6, 134.4, 132.5, 130.6, 123.8, 122.3, 121.7, 120.0 (q, $J_{\text{CF}} = 322.4$ Hz), 51.6, 49.3, 48.0, 47.2, 46.4, 33.9, 32.6, 31.9. ^{19}F NMR (376 MHz, CDCl_3) δ -78.9. IR (neat) cm^{-1} 3146, 2932, 1555, 1459, 1348, 1329, 1178, 1133, 1052, 915. HRMS m/z (ESI): calcd. for $\text{C}_{17}\text{H}_{21}\text{N}_2\text{O}_2$ $[\text{M}]^+$: 285.1603, found: 285.1602.

V. NMR spectra

Compound 1:

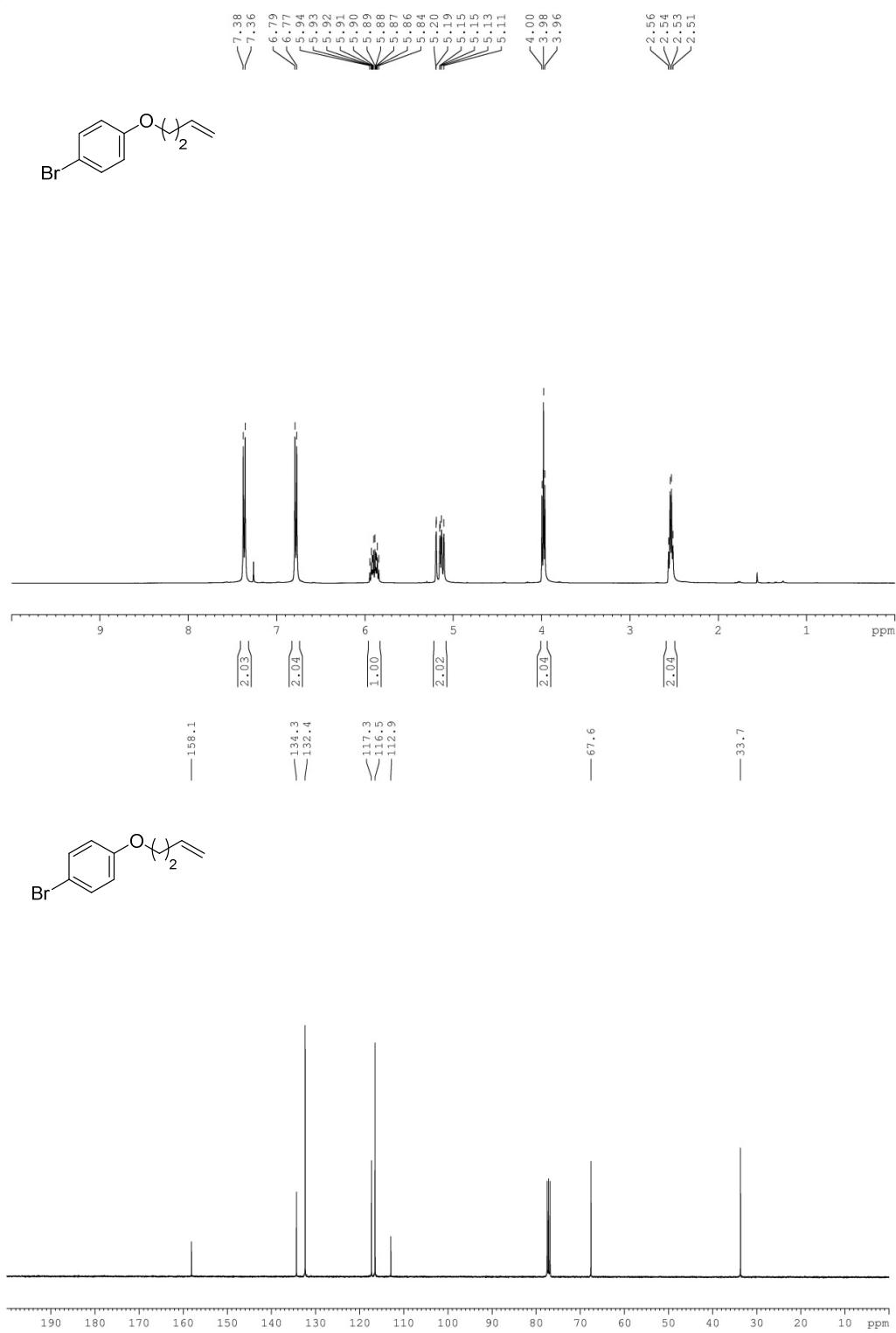


Figure S1: Analysis report for compound 1

Compound 2:

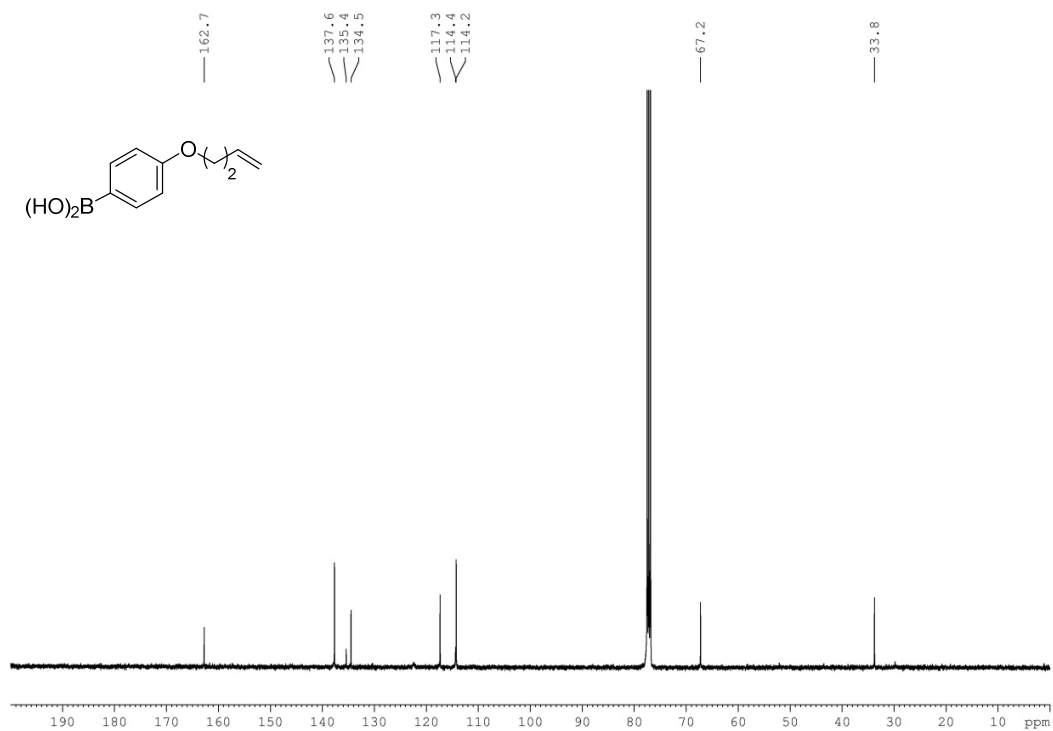
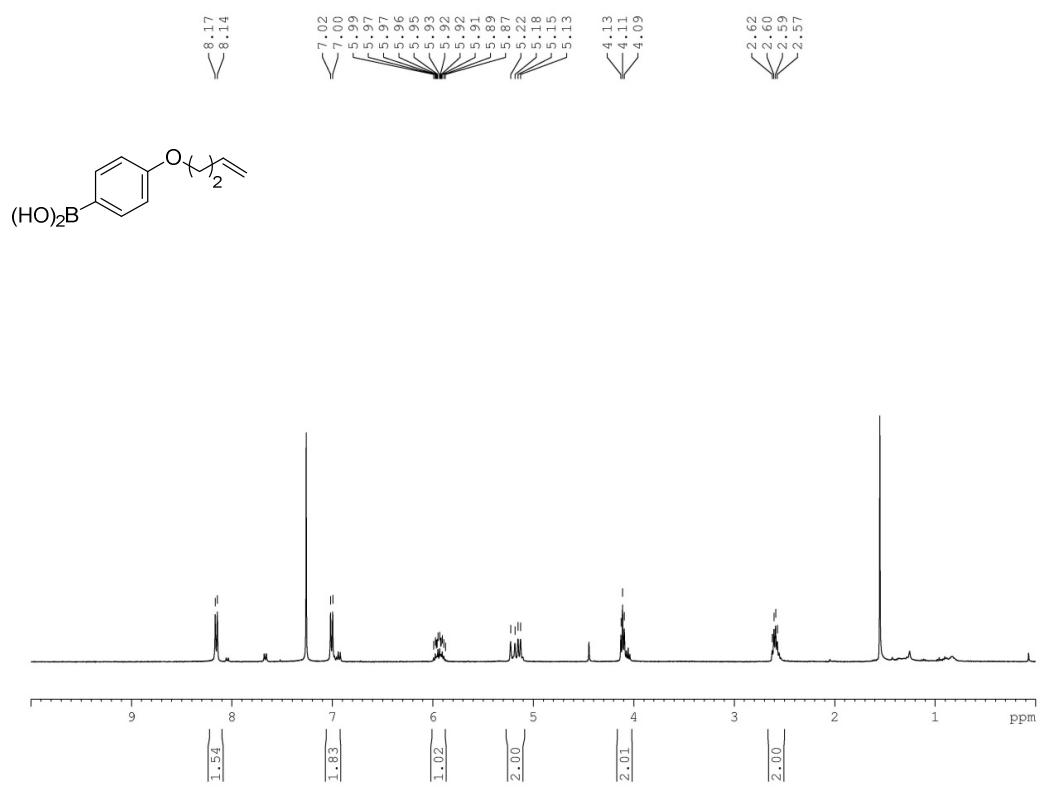


Figure S2: Analysis report for compound 2

Compound 3:

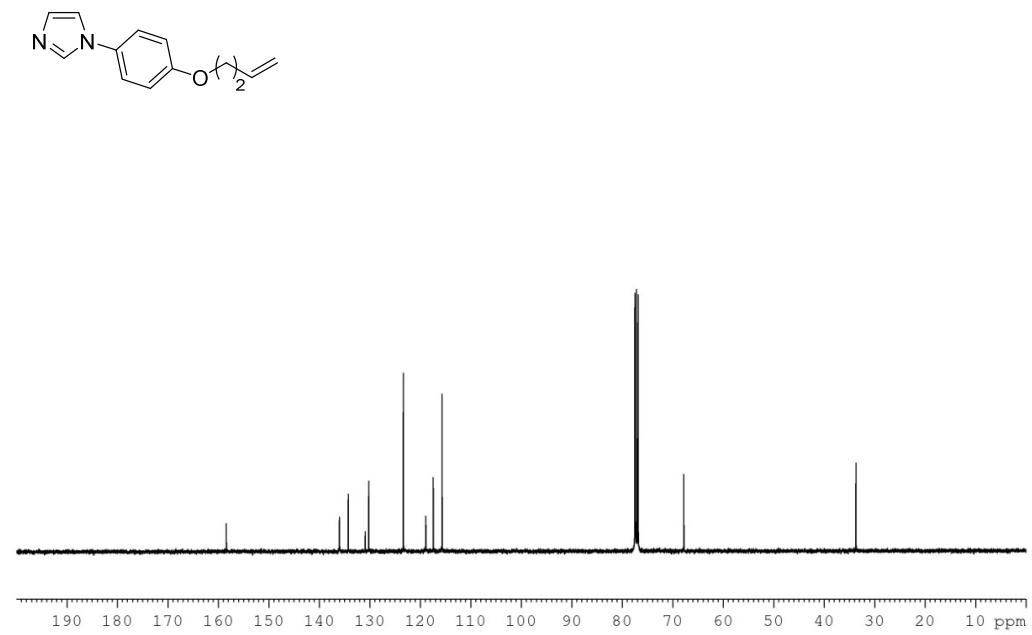
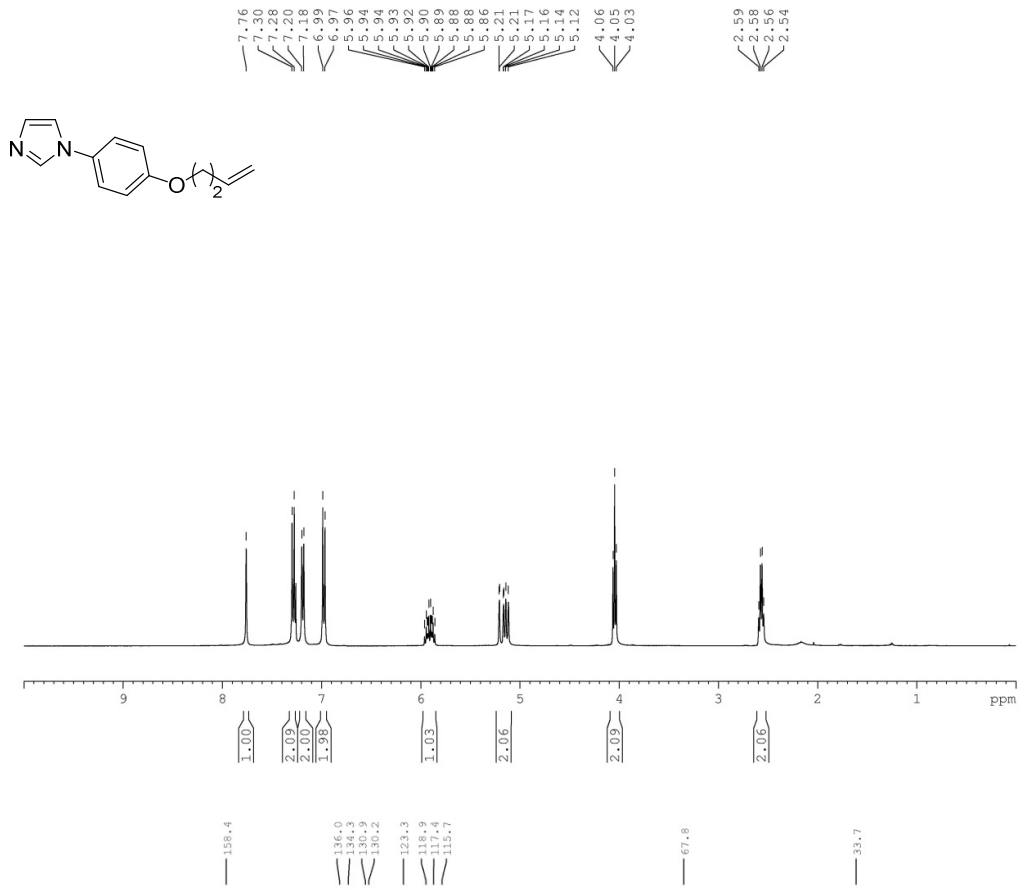


Figure S3: Analysis report for compound 3

Compound 4:

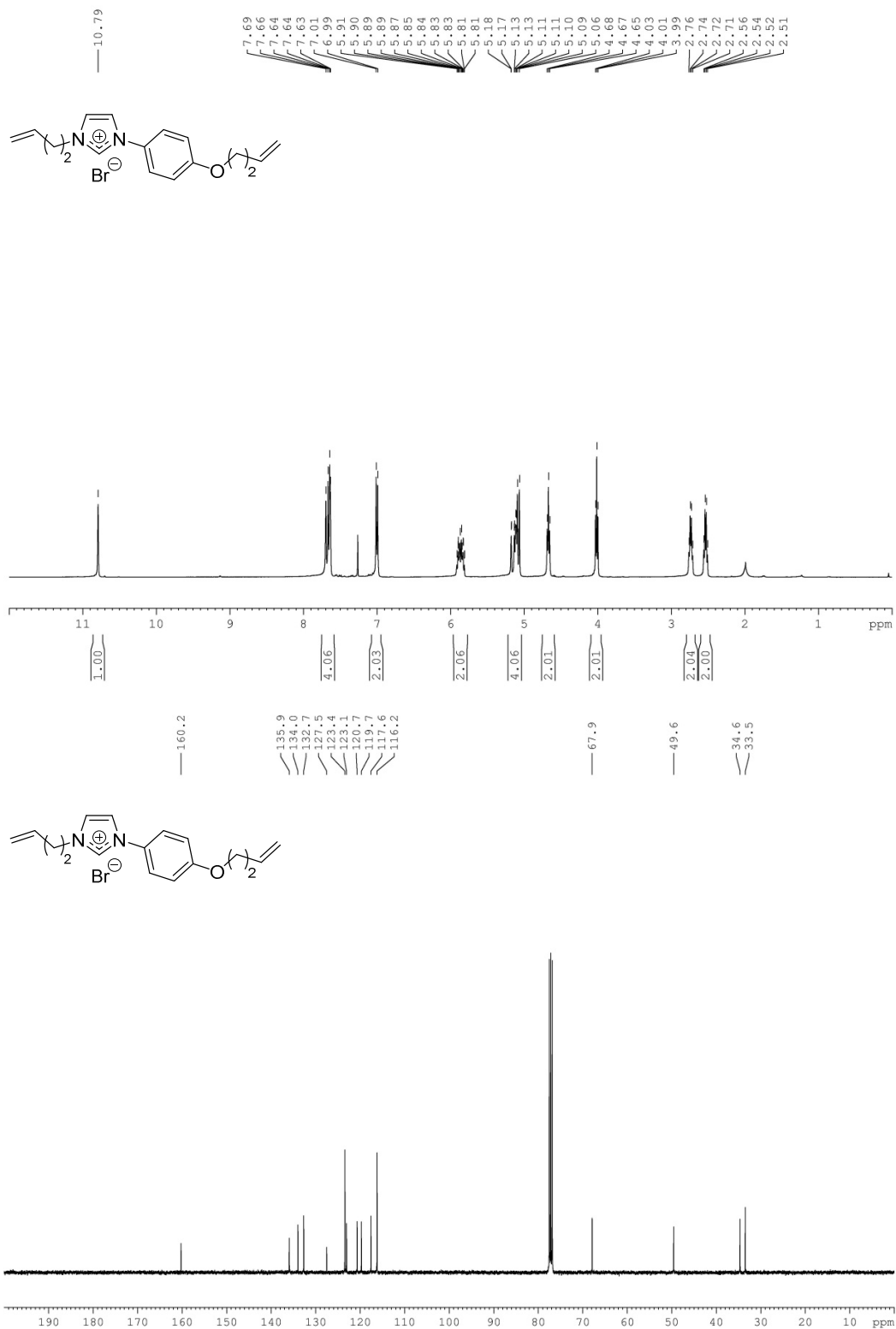
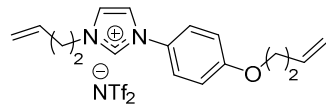
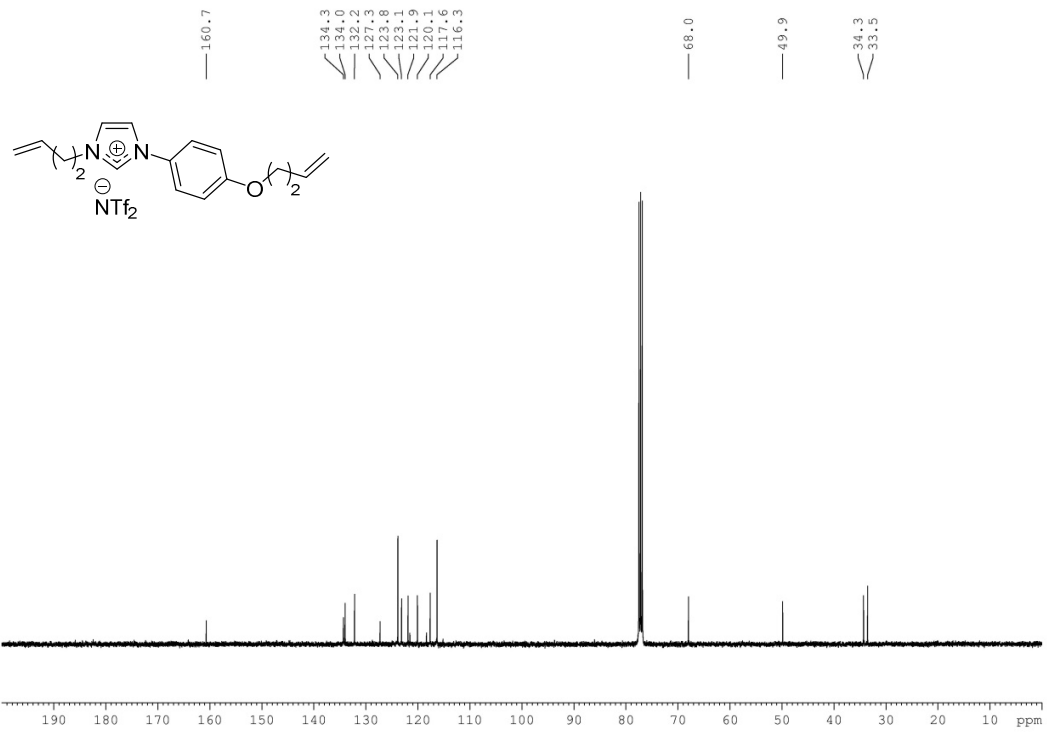
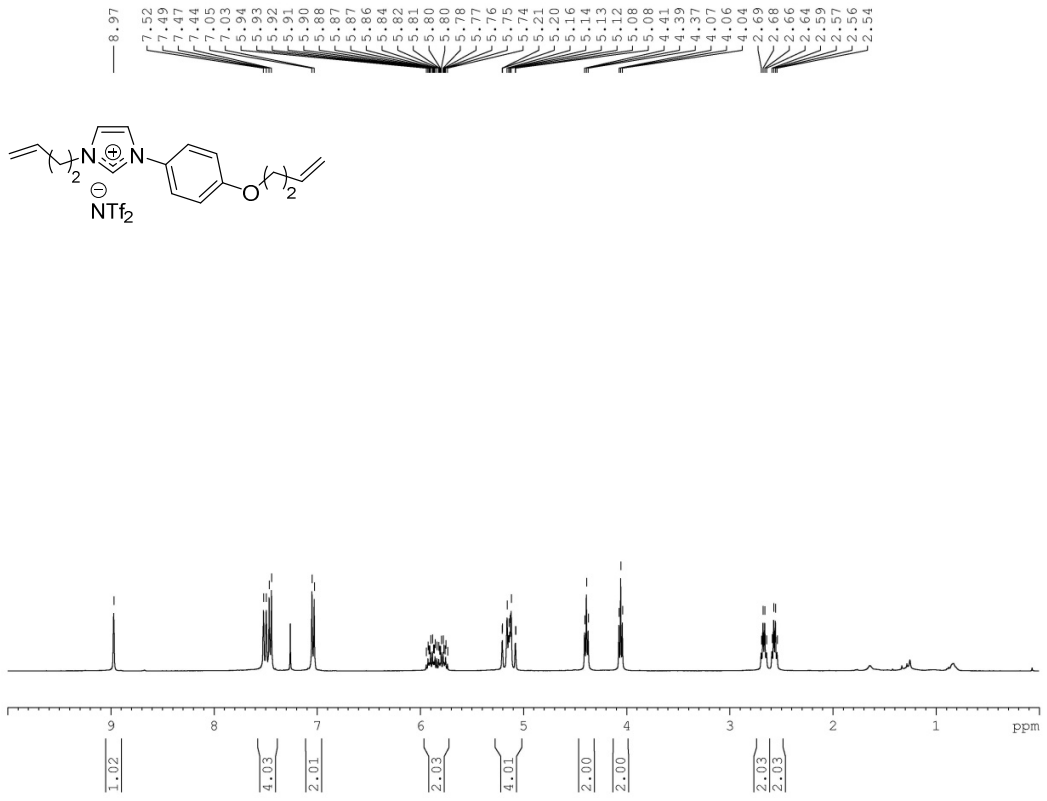


Figure S4: Analysis report for compound 4

Compound 5:



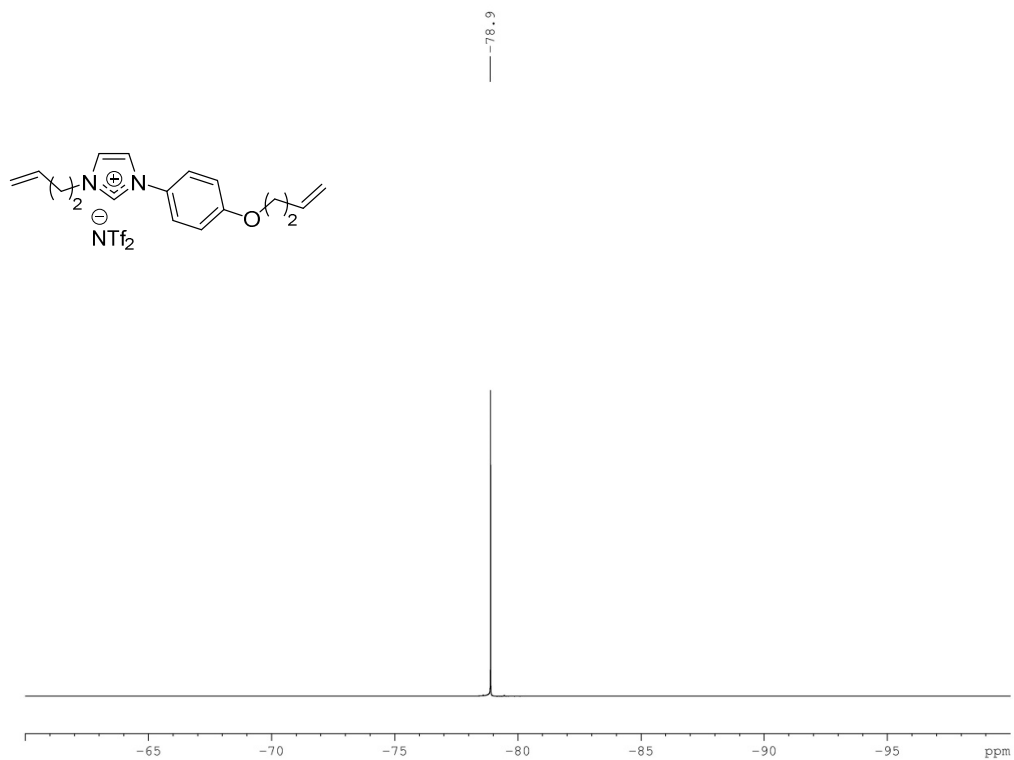
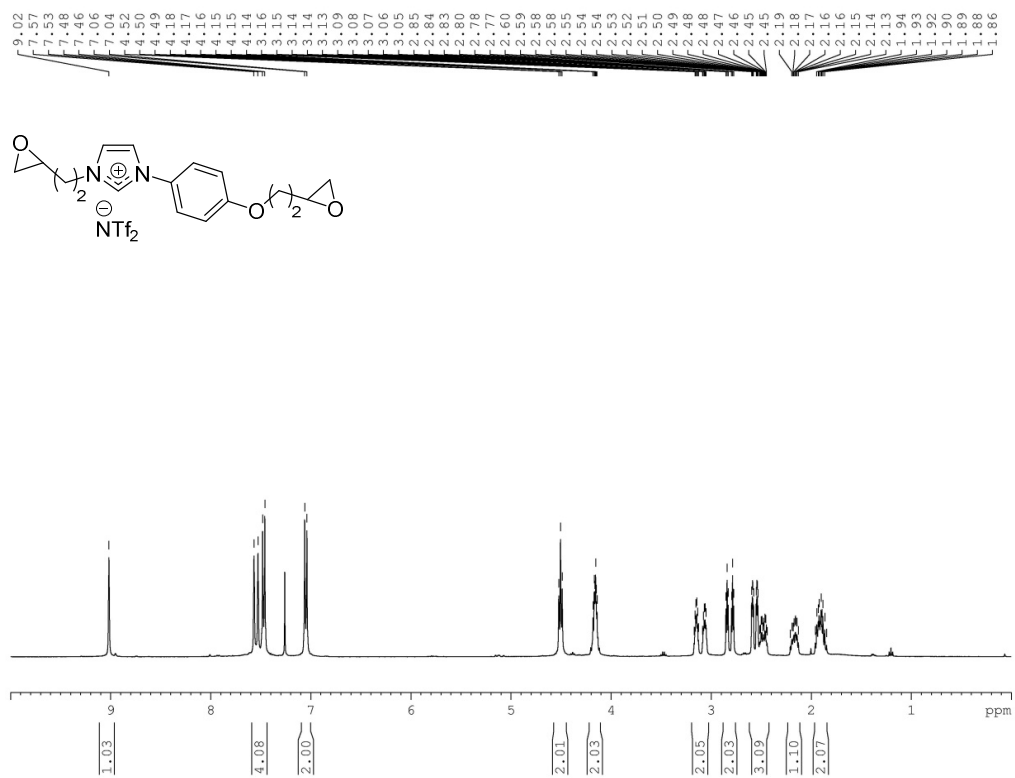


Figure S5: Analysis report for compound 5

Compound ILM-[NTf₂]-1:



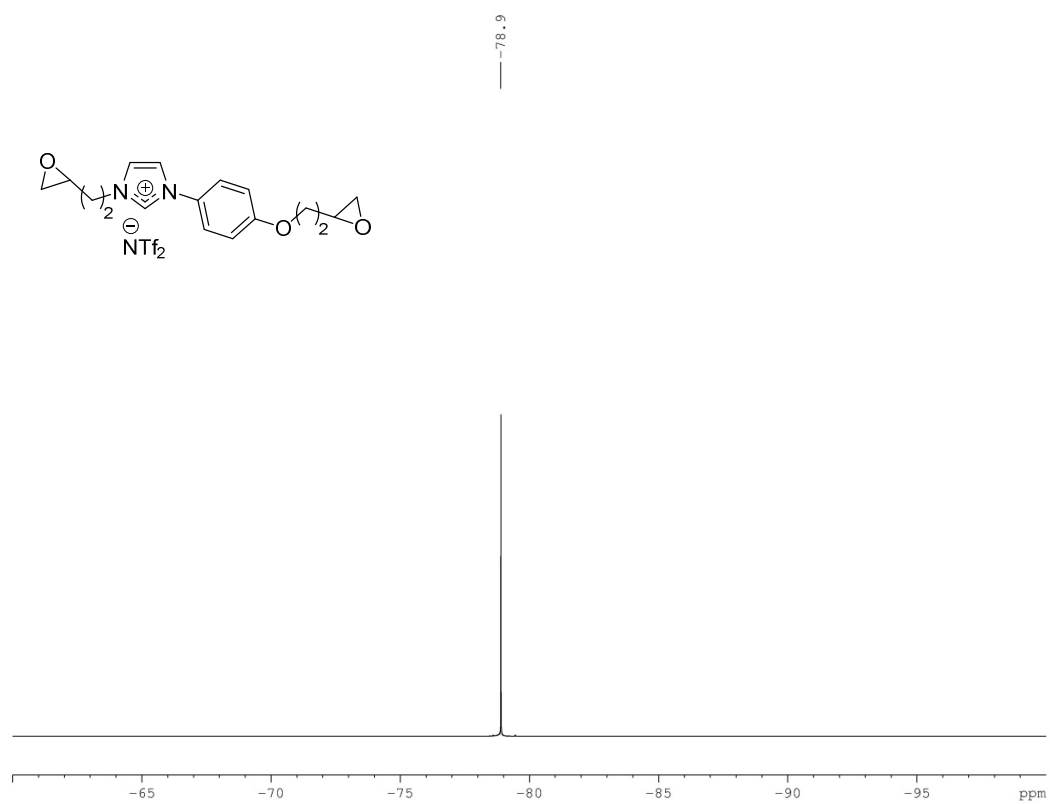
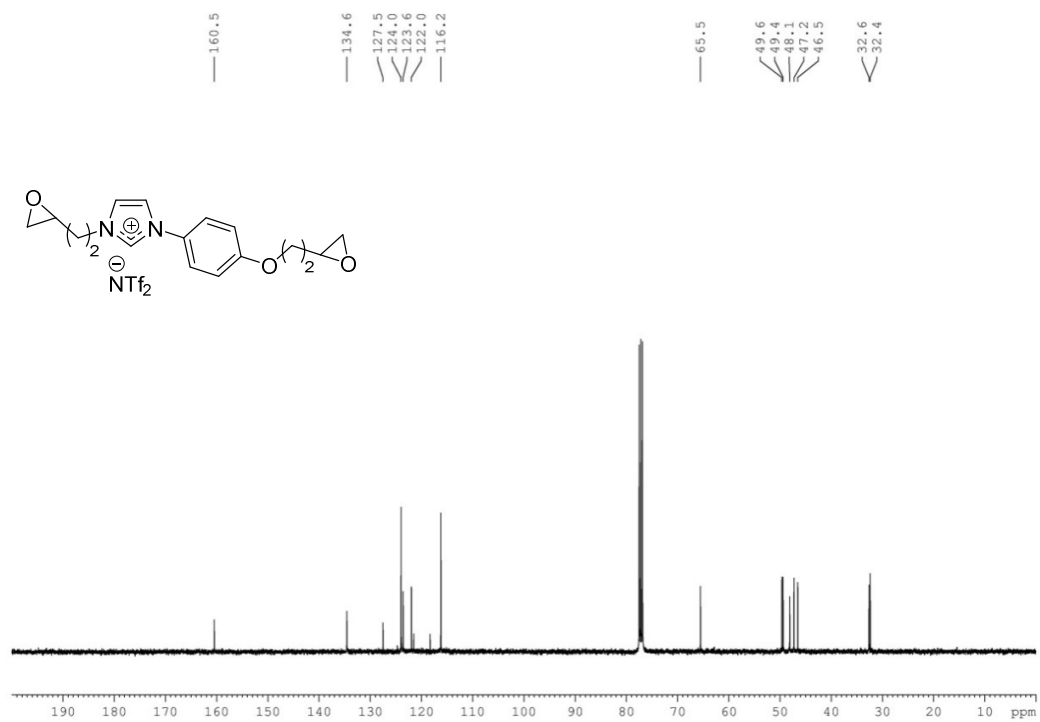


Figure S6: Analysis report for compound ILM-[NTf₂]-1

Compound 6:

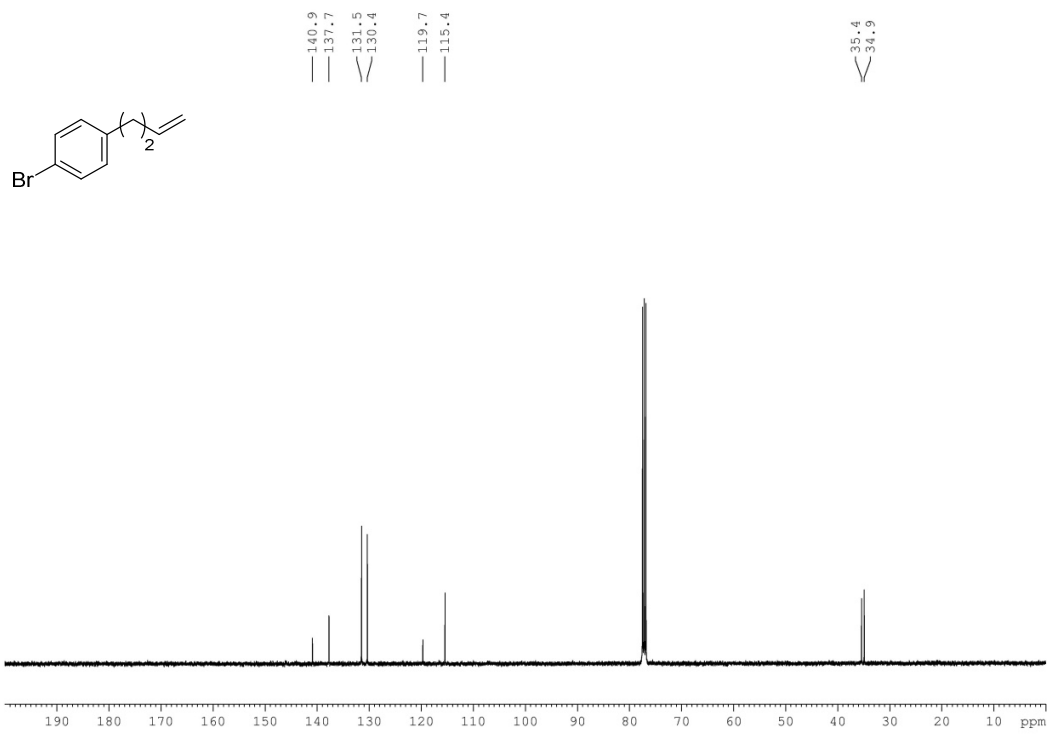
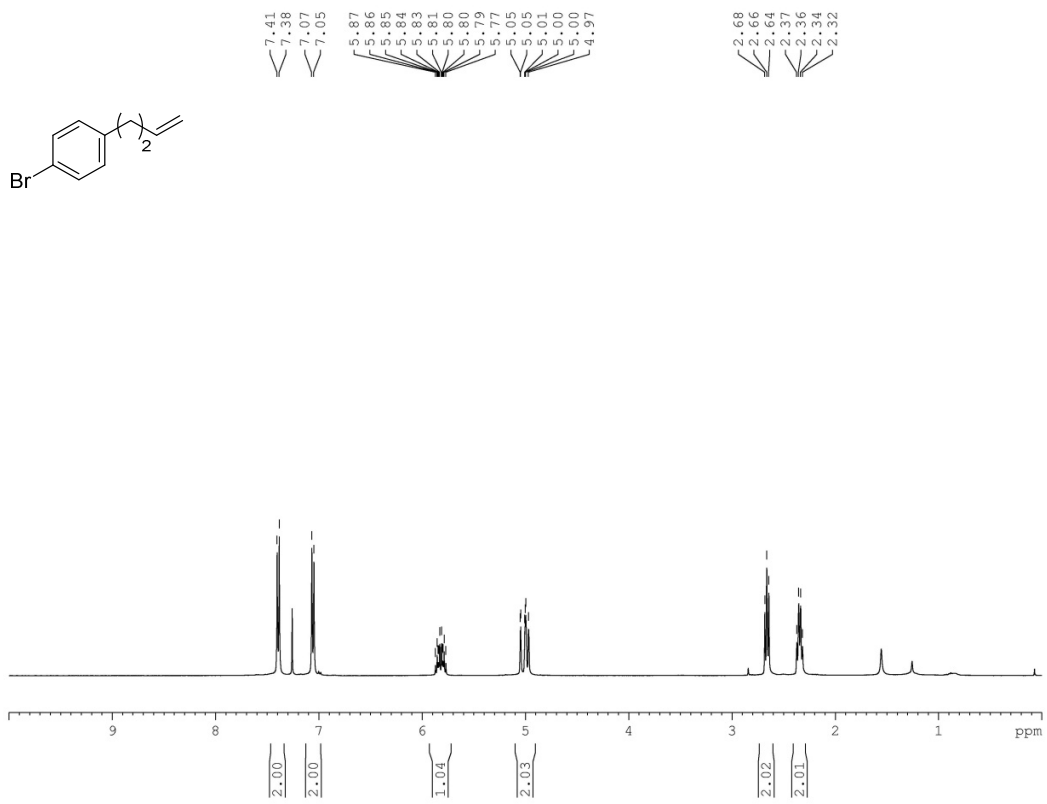


Figure S7: Analysis report for compound 6

Compound 7:

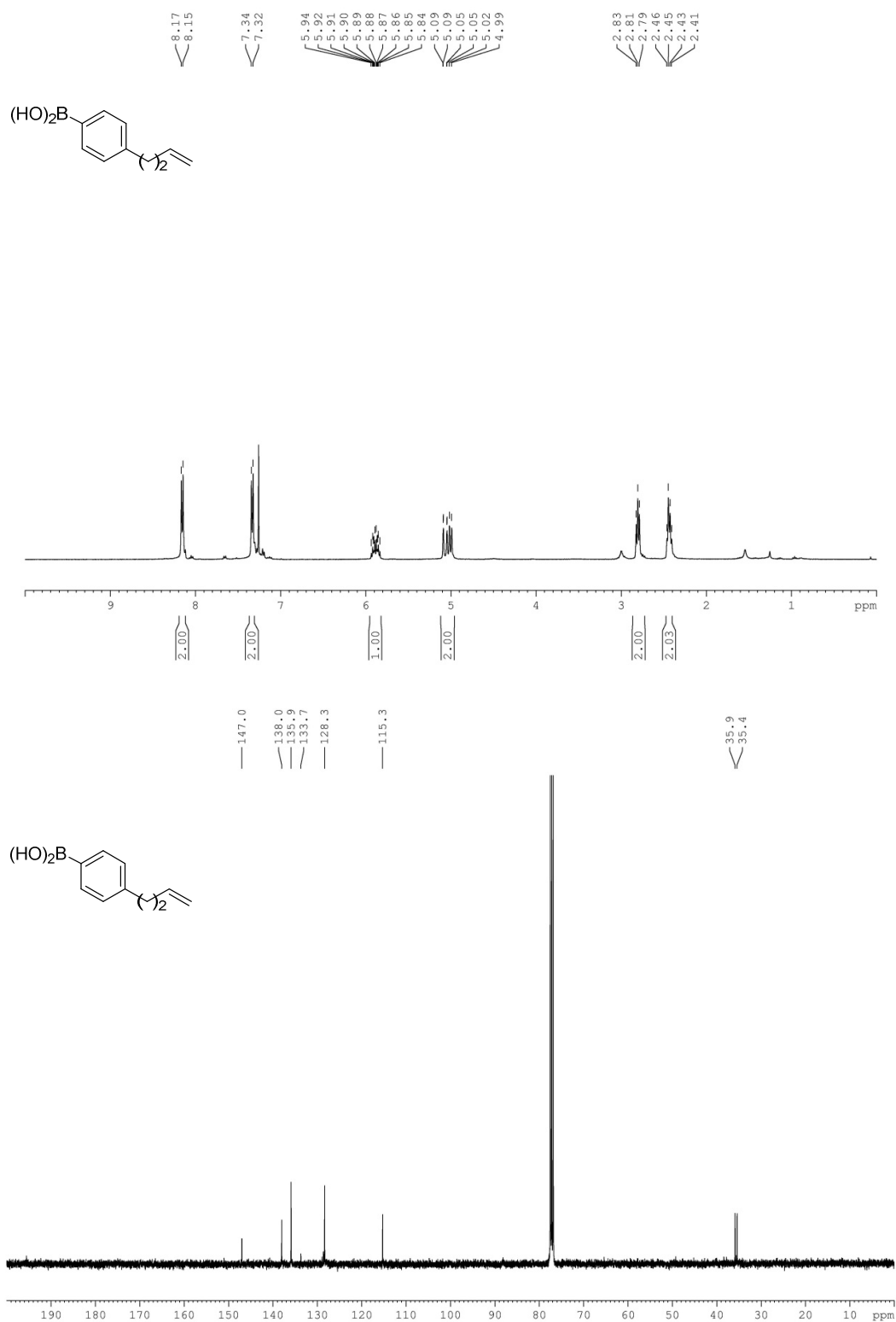


Figure S8: Analysis report for compound 7

Compound 8:

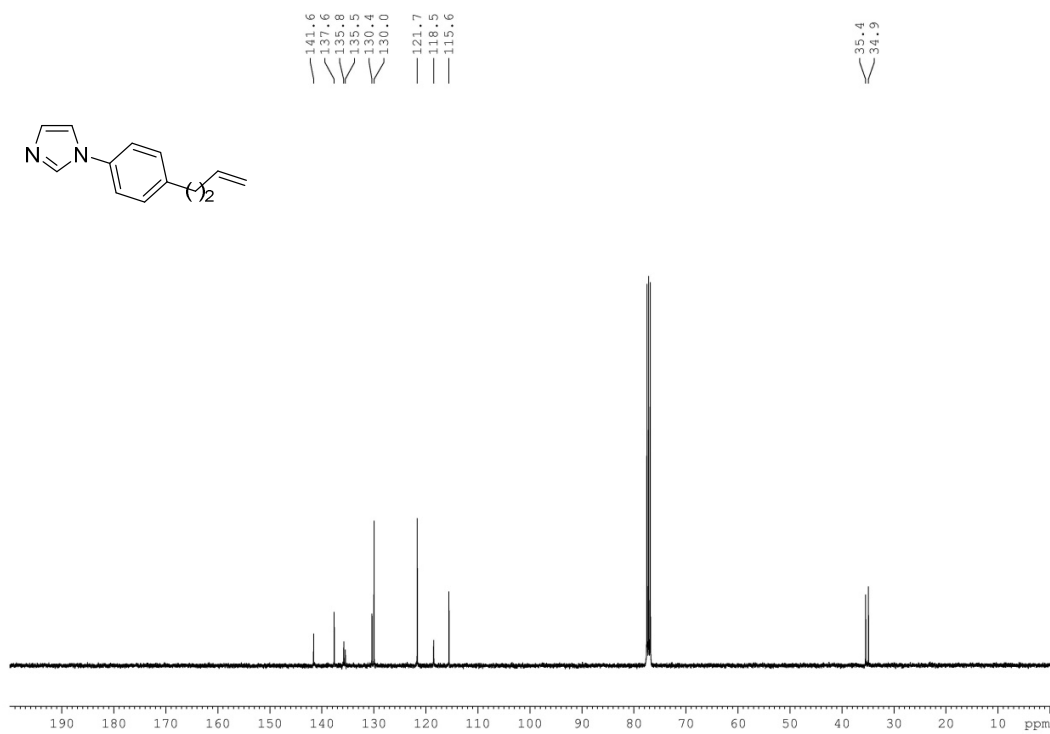
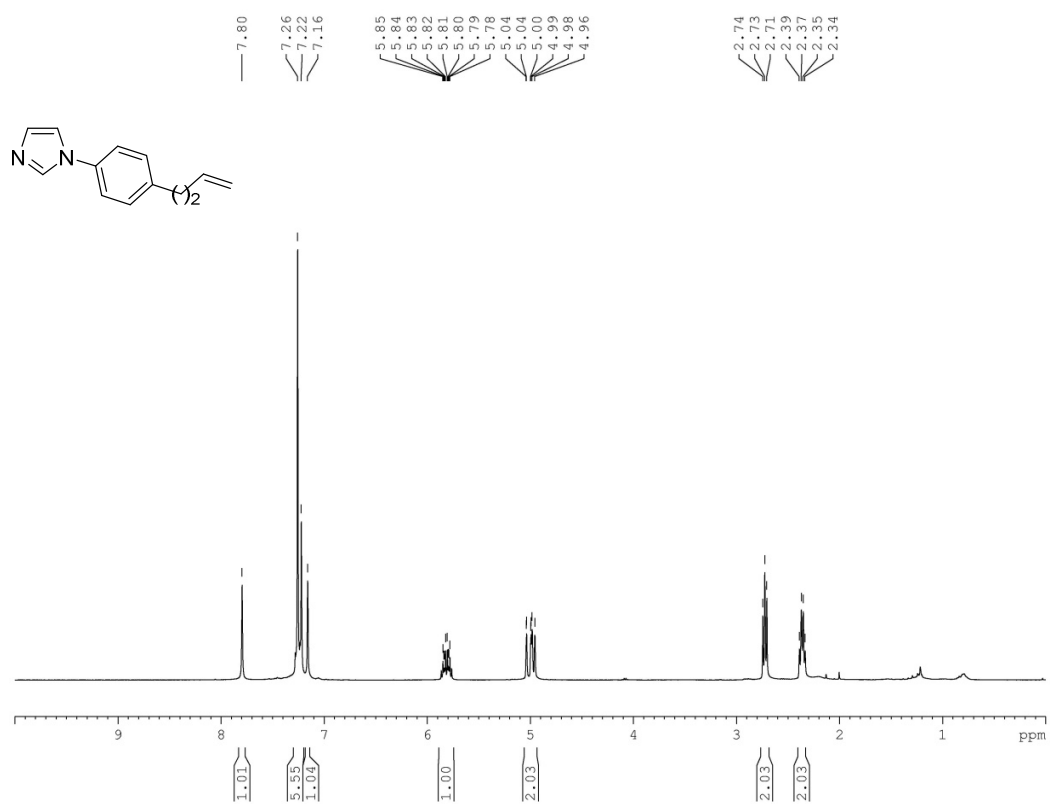


Figure S9: Analysis report for compound 8

Compound 9:

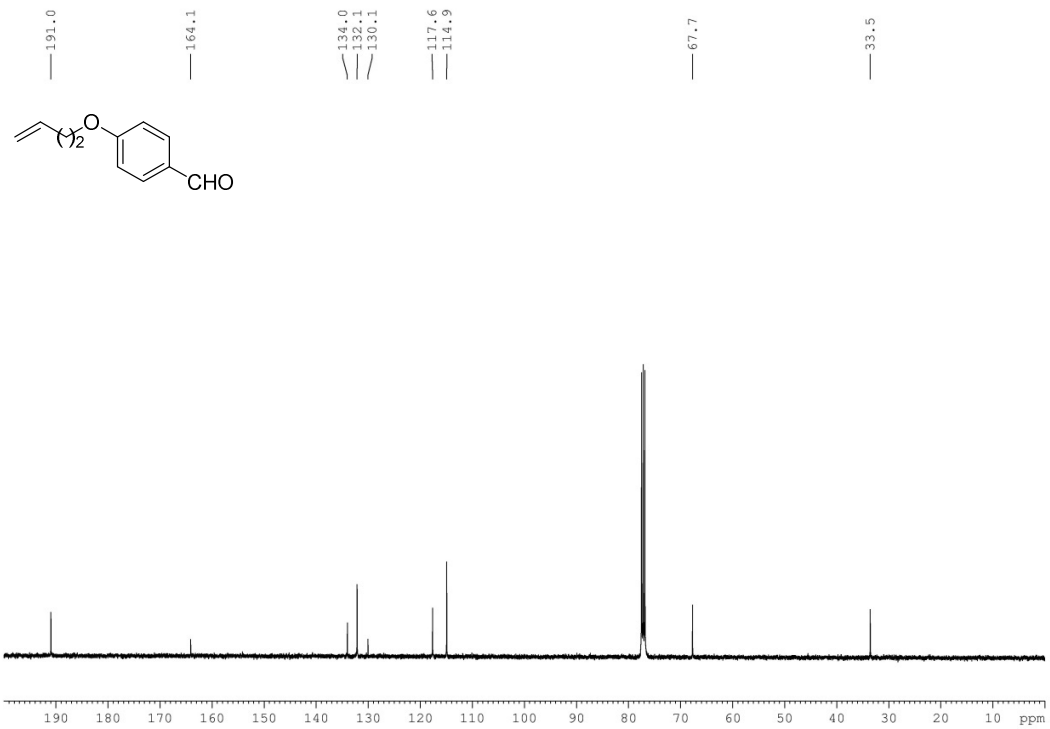
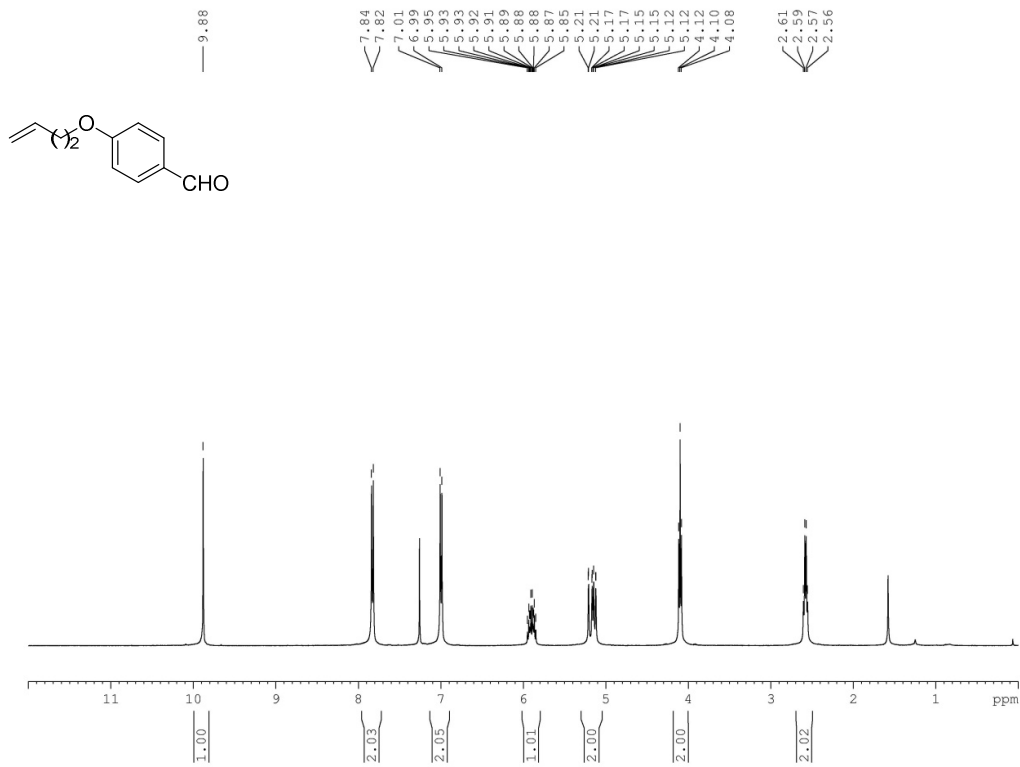


Figure S10: Analysis report for compound 9

Compound 10:

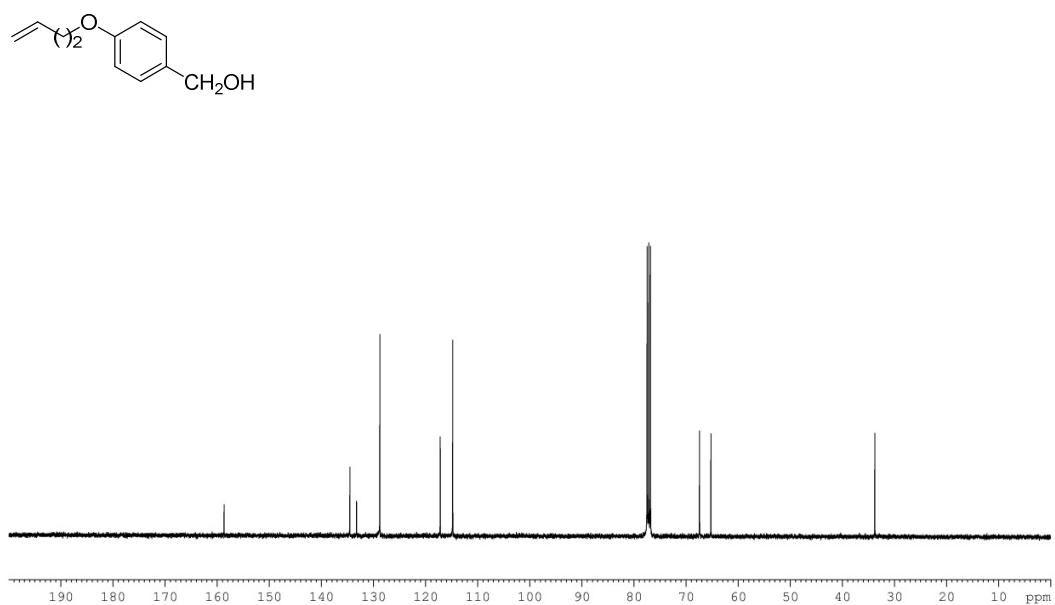
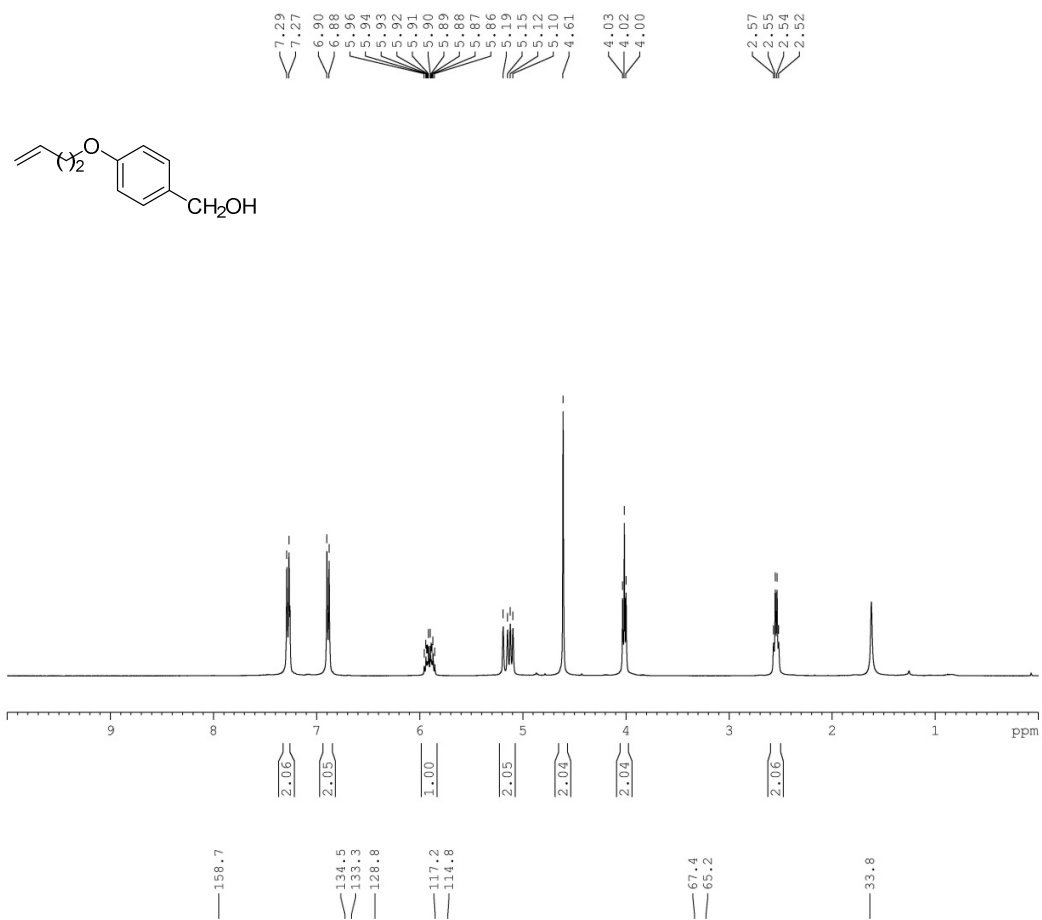


Figure S11: Analysis report for compound 10

Compound 11:

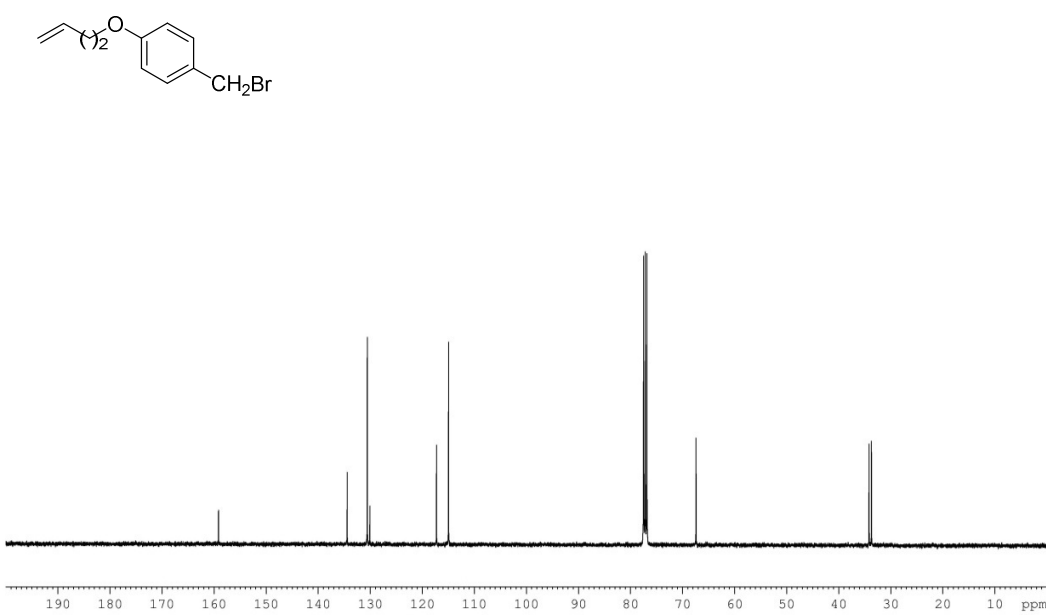
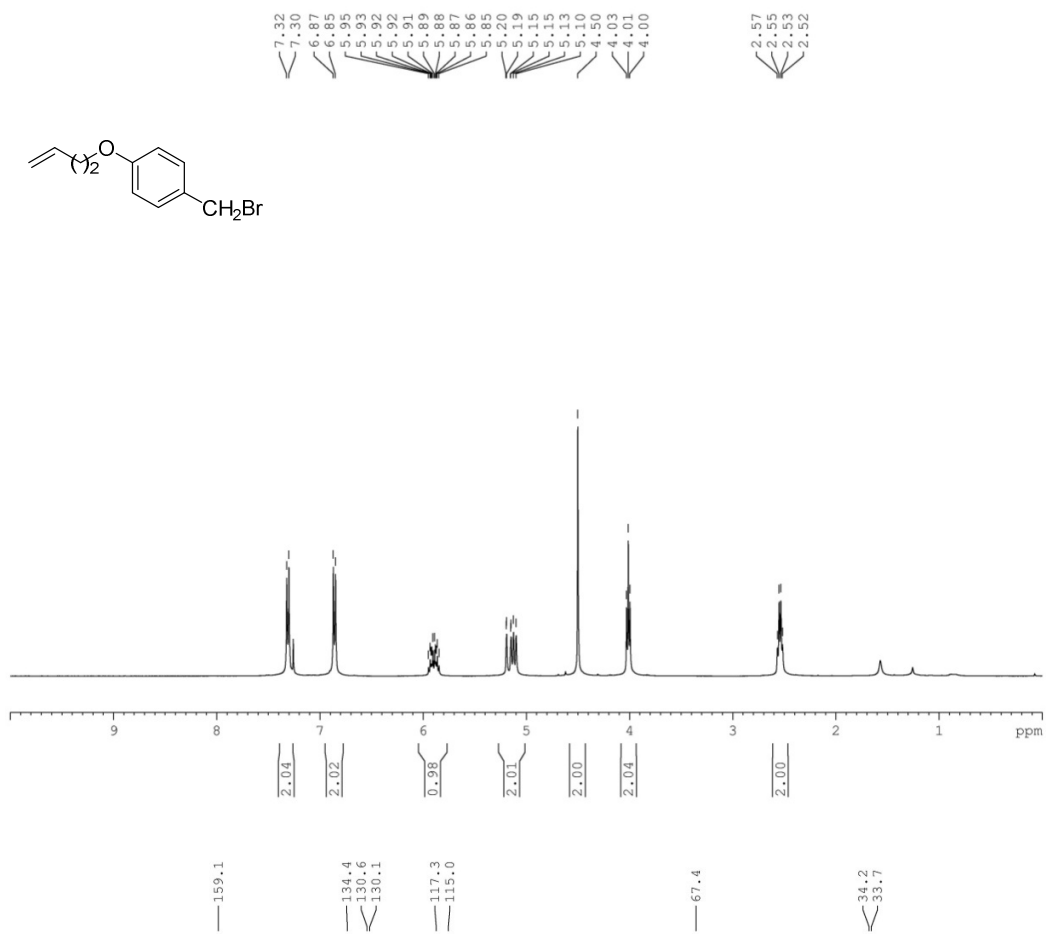


Figure S12: Analysis report for compound 11

Compound 12:

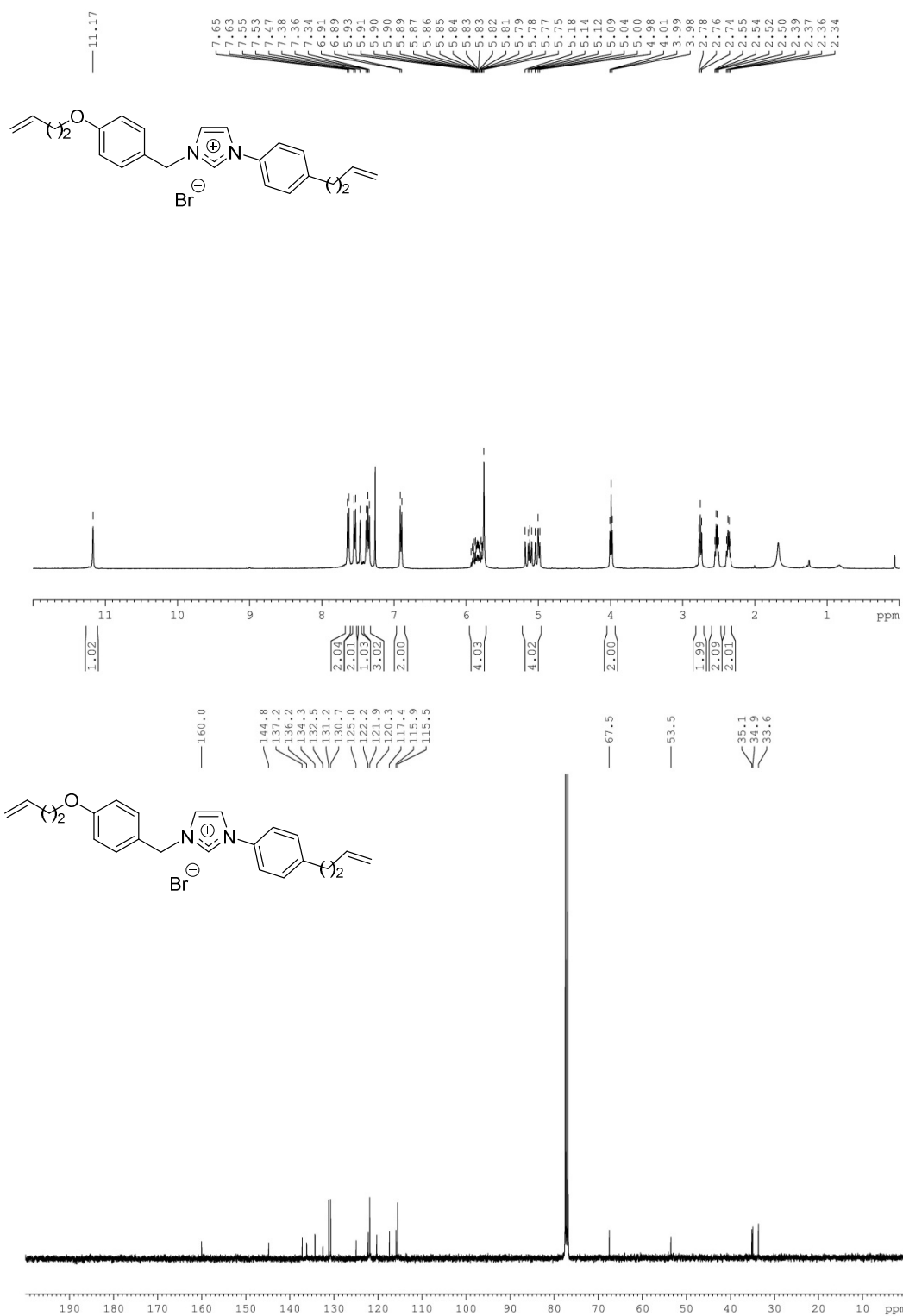
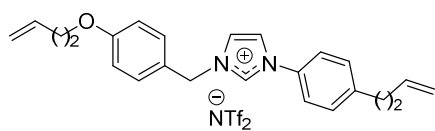
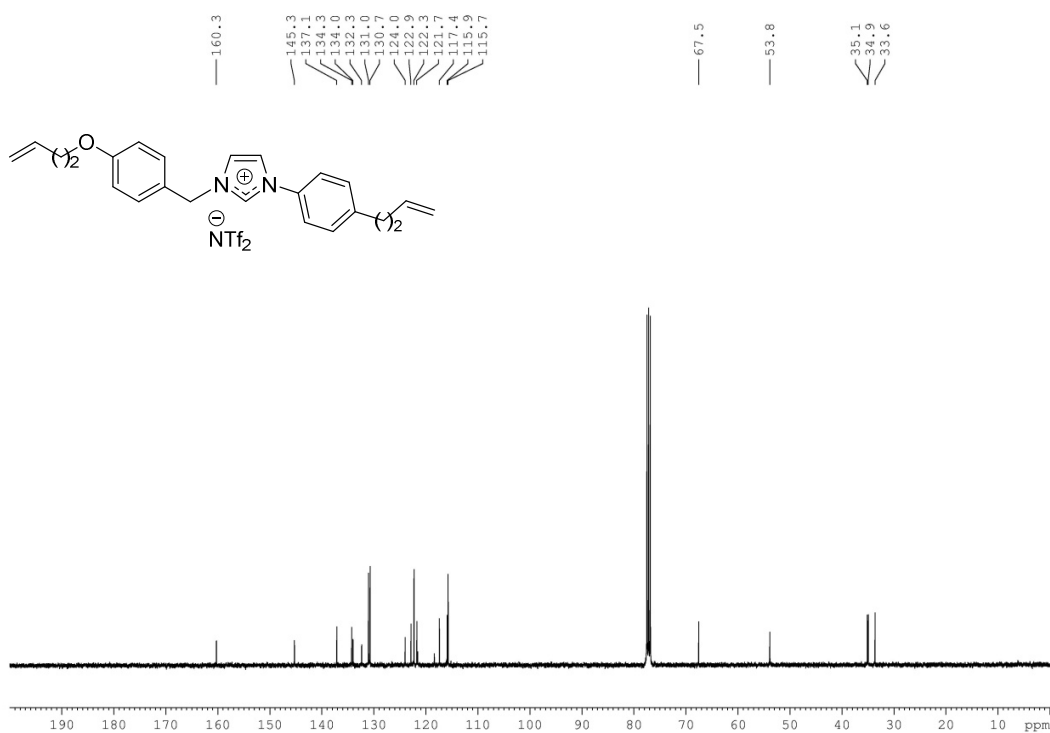
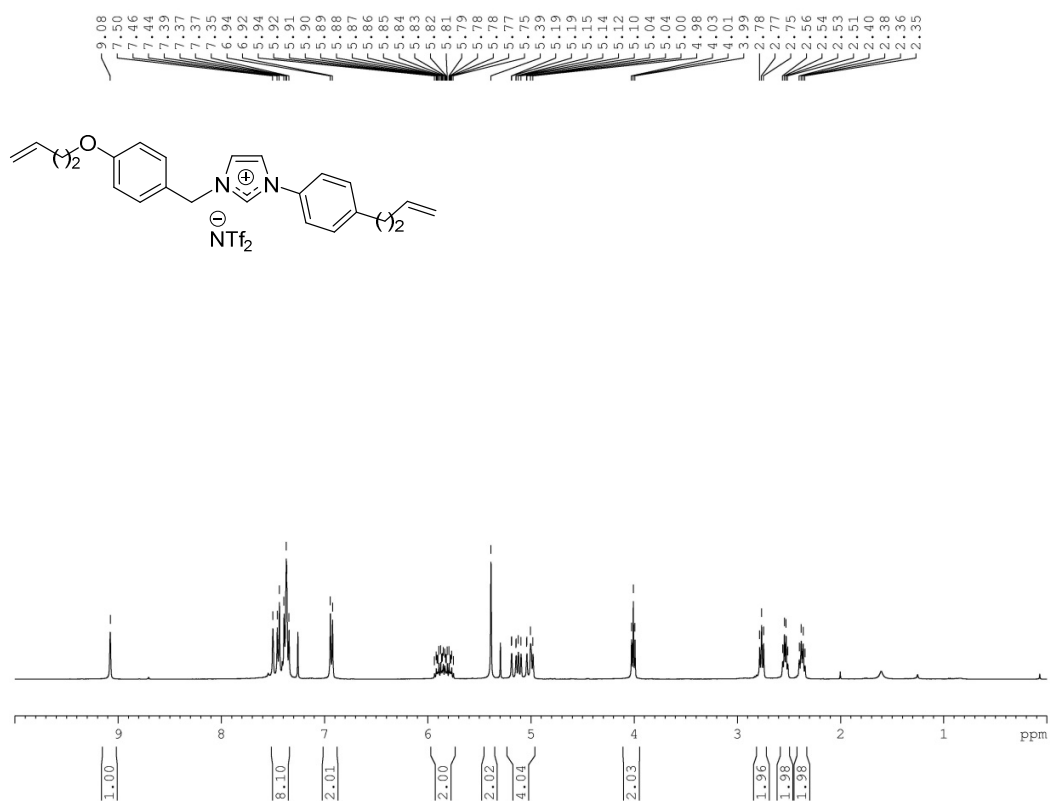


Figure S13: Analysis report for compound 12

Compound 13:



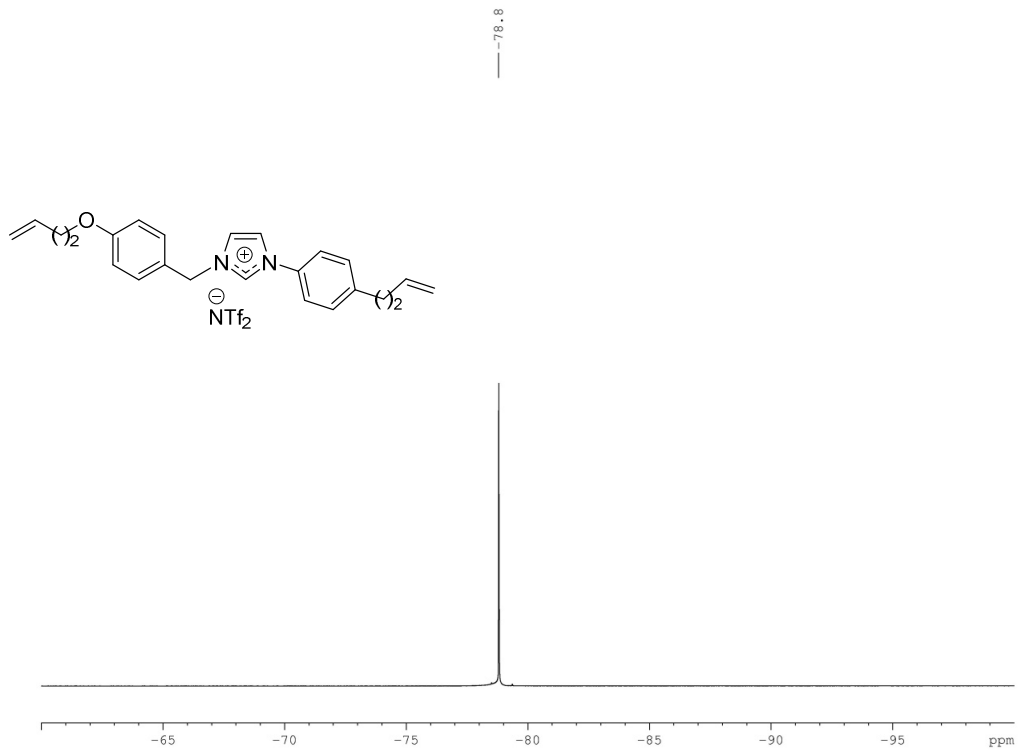
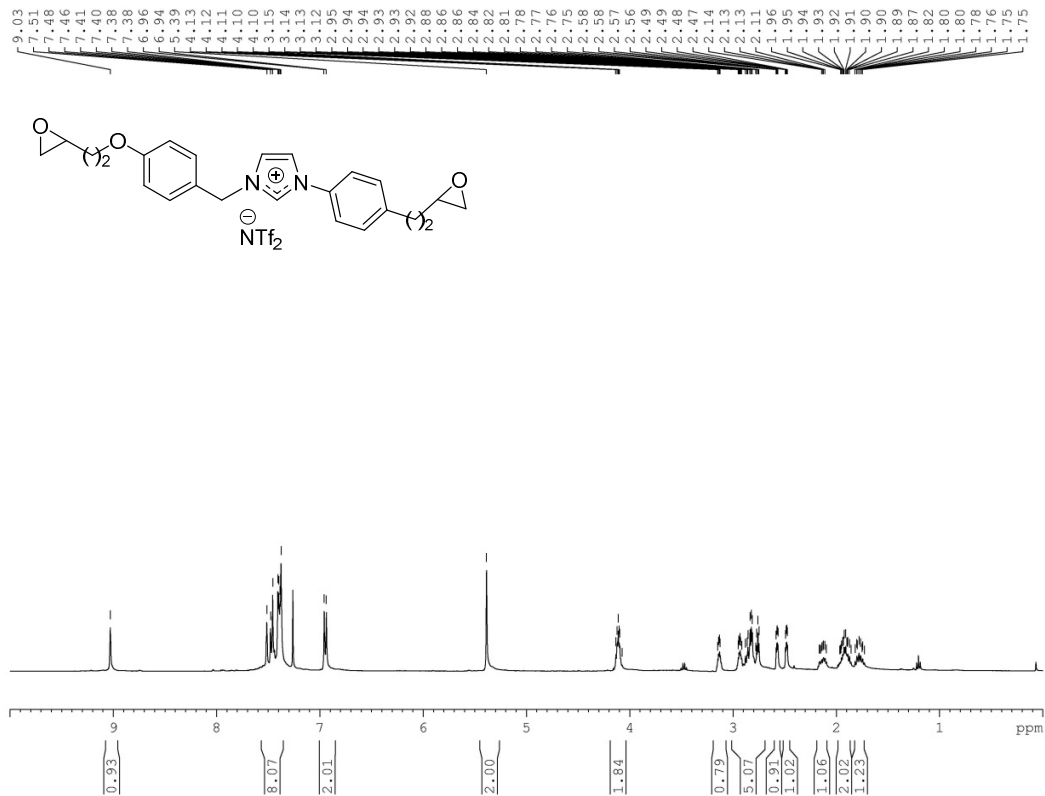


Figure S14: Analysis report for compound 13

Compound ILM-[NTf₂]-2:



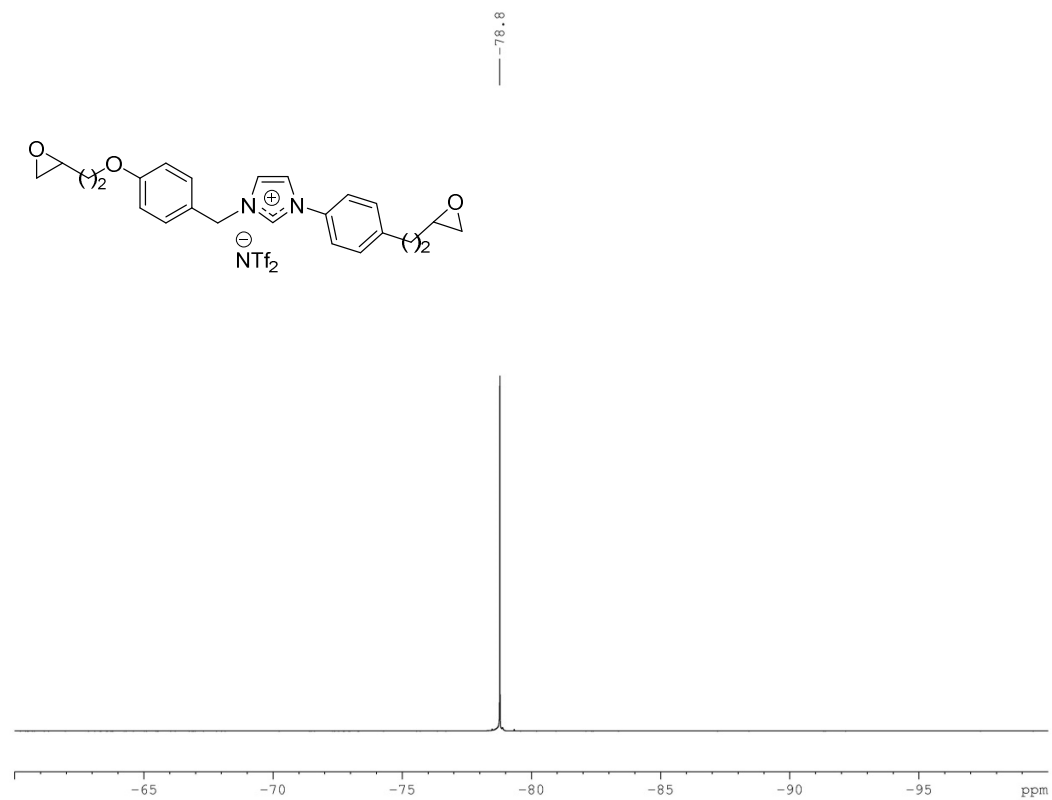
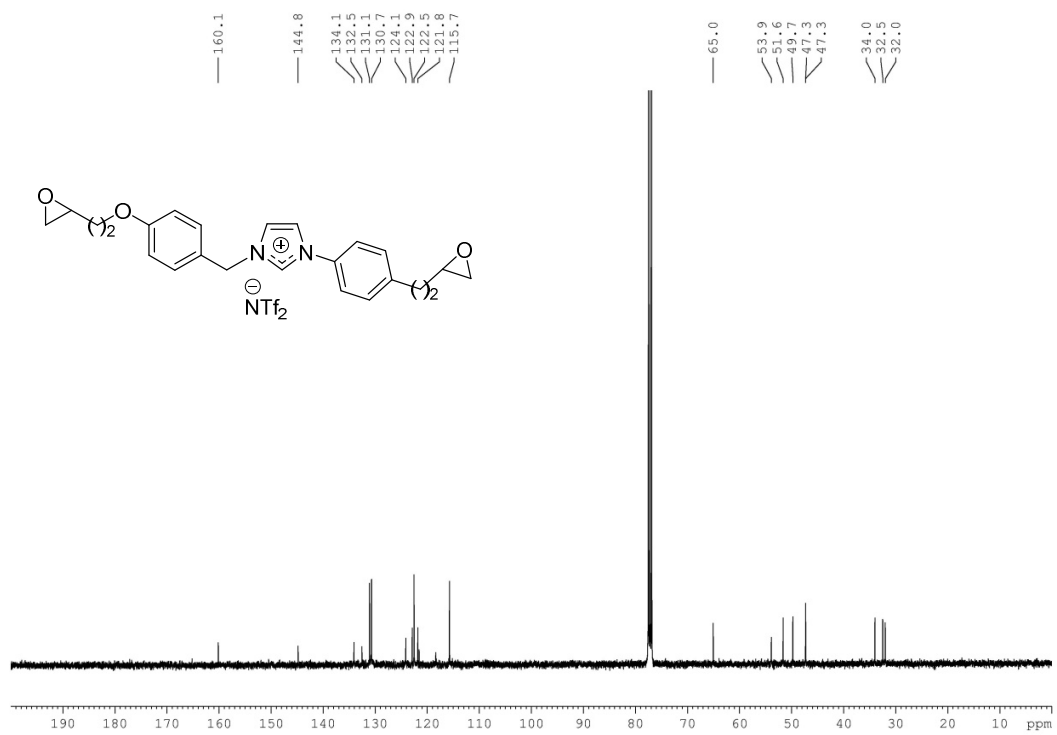


Figure S15: Analysis report for compound ILM-[NTf₂]-2

Compound 14:

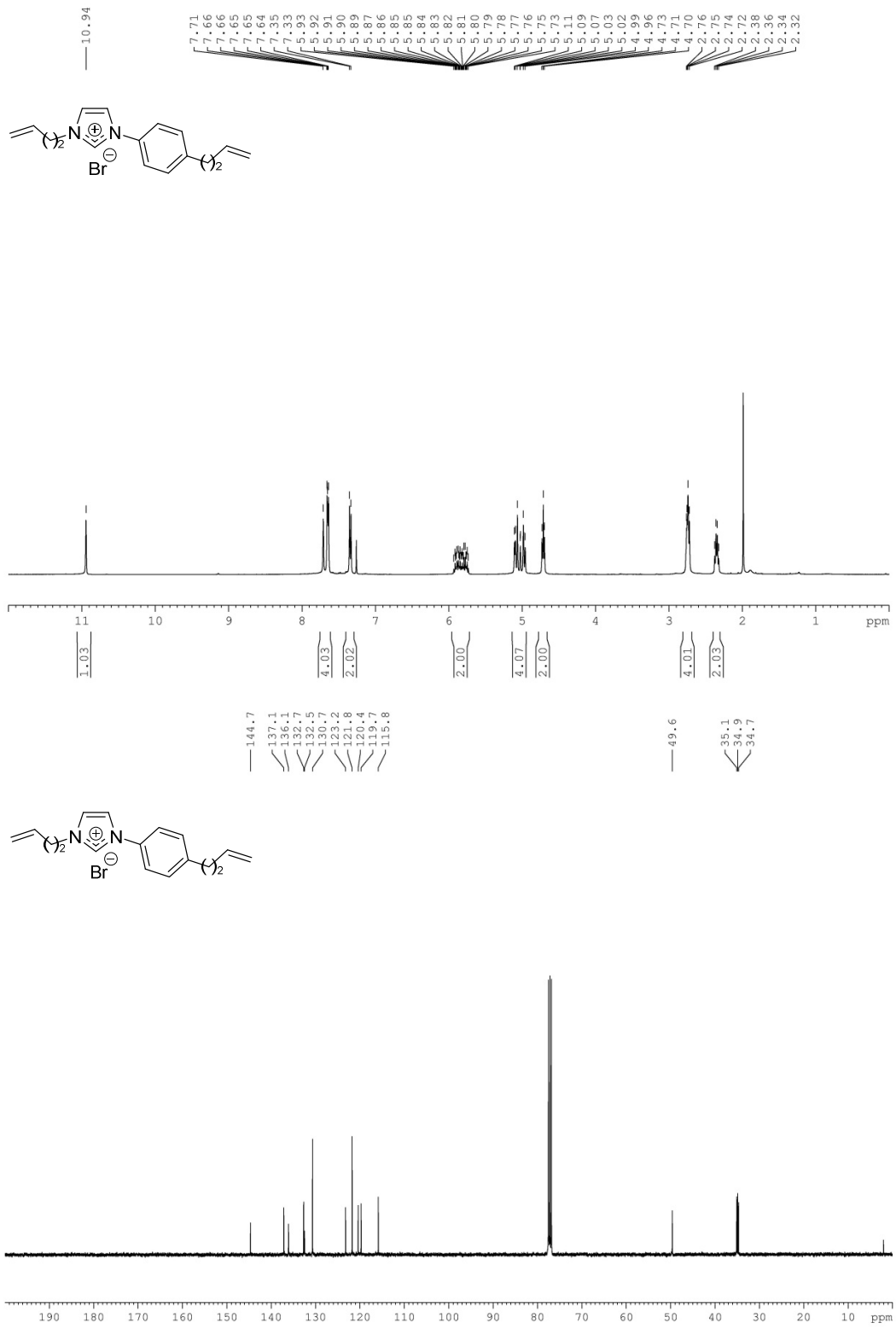
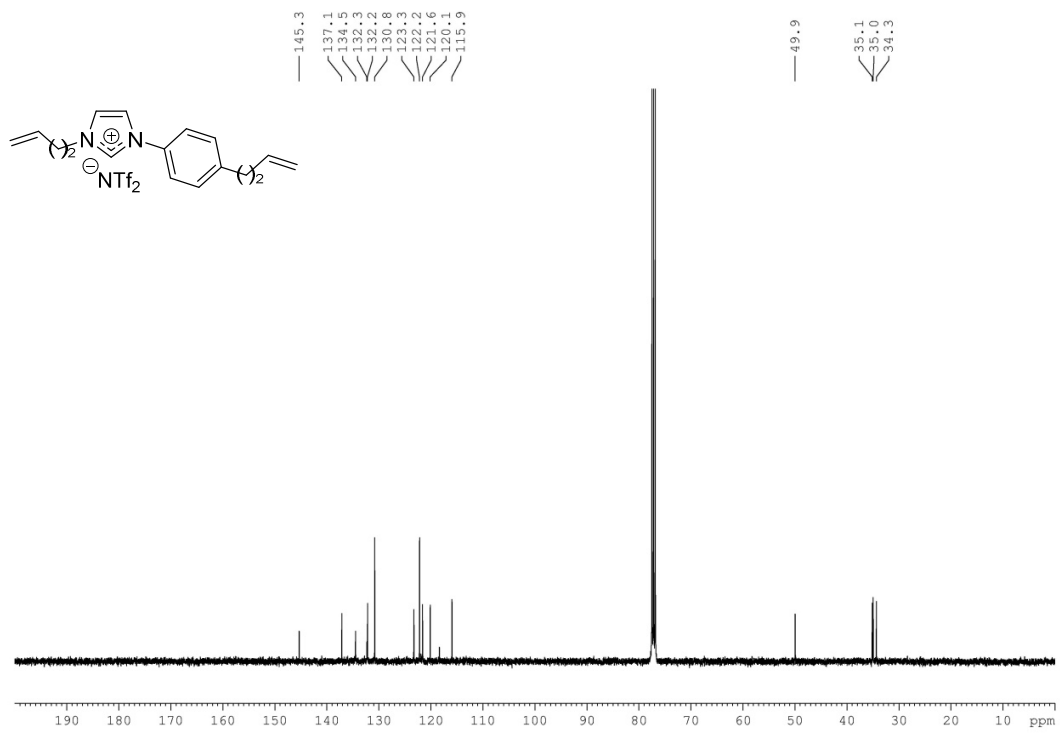
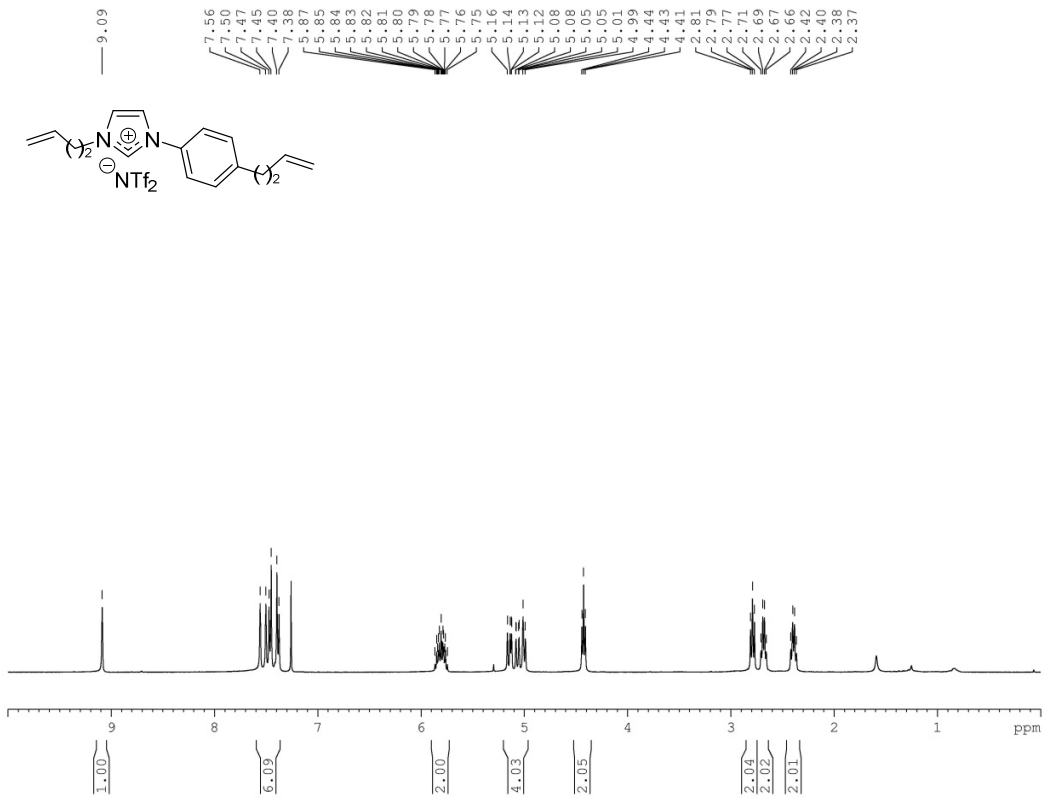


Figure S16: Analysis report for compound 14

Compound 15:



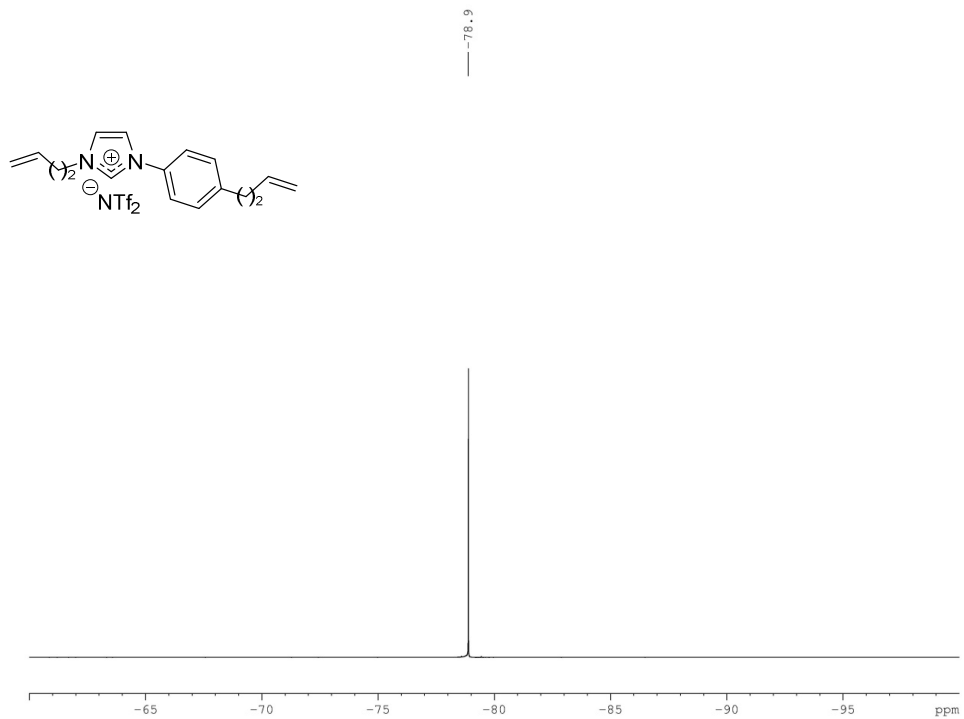
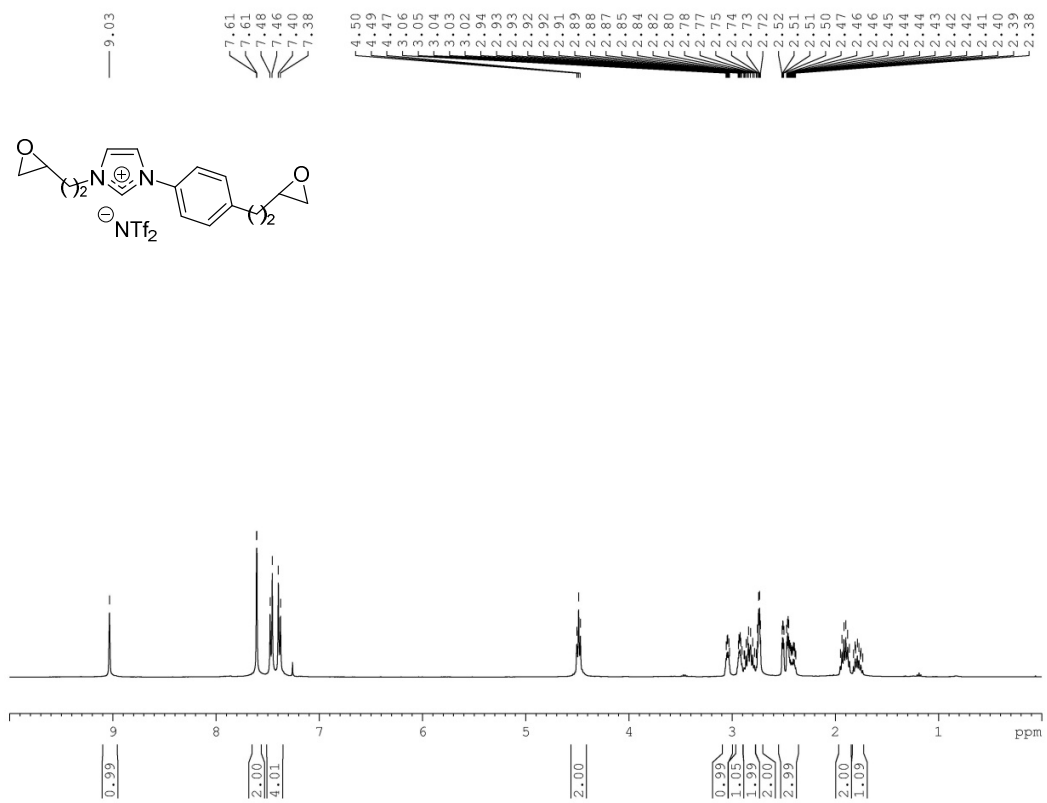


Figure S17: Analysis report for compound 15

Compound ILM-[NTf₂]-3:



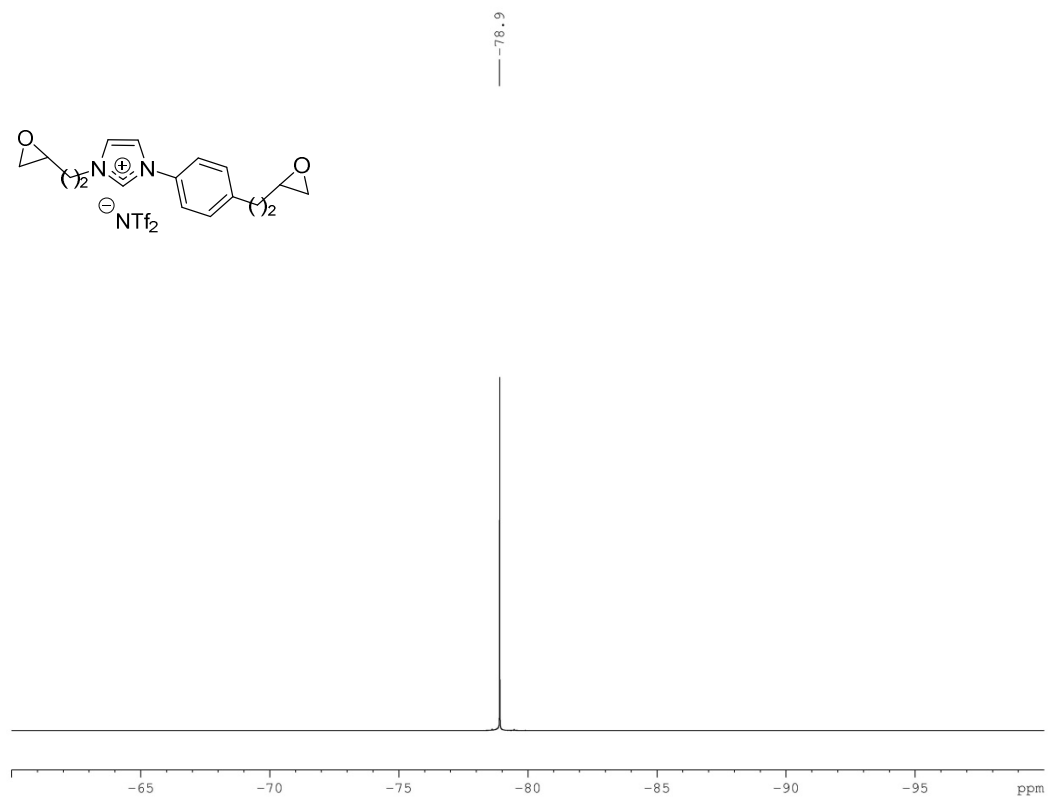
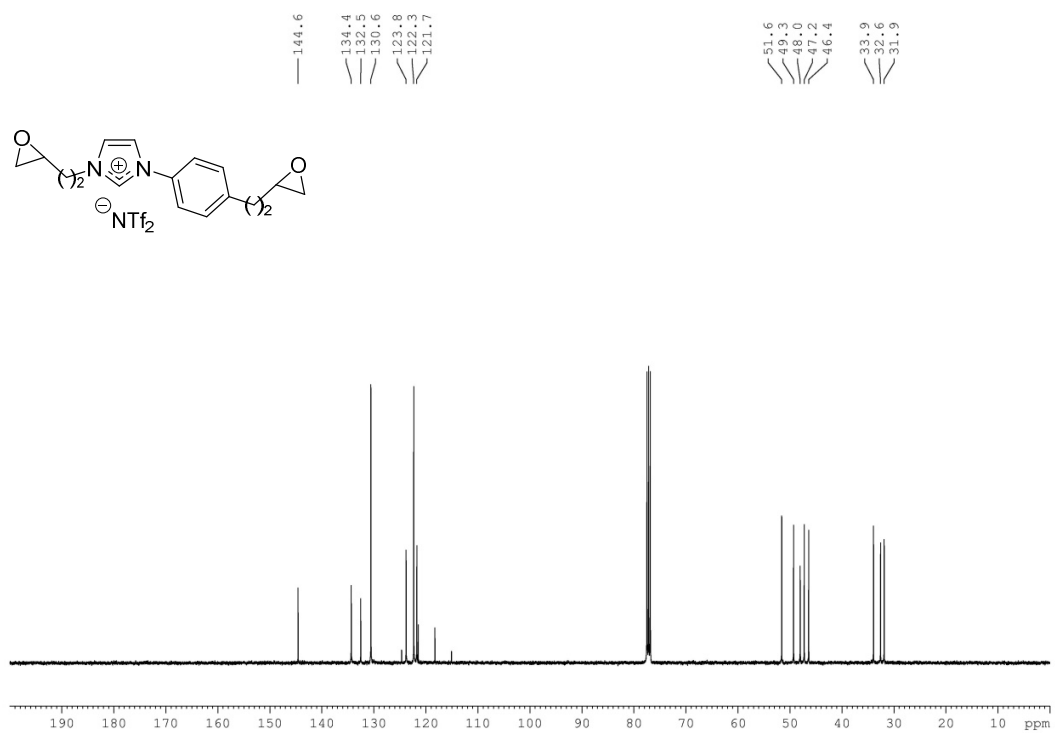


Figure S18: Analysis report for compound ILM-[NTf₂]-3

VI. FTIR spectra

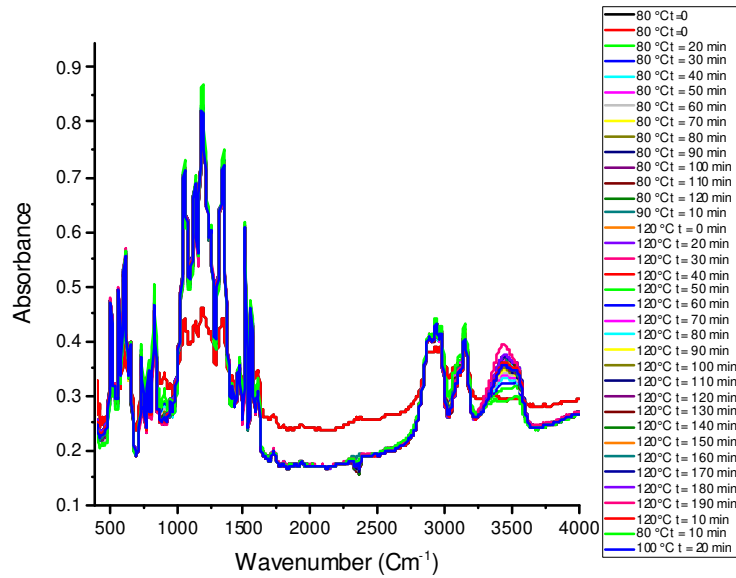


Figure S19: FTIR Spectrum of ILM-1 during curing process

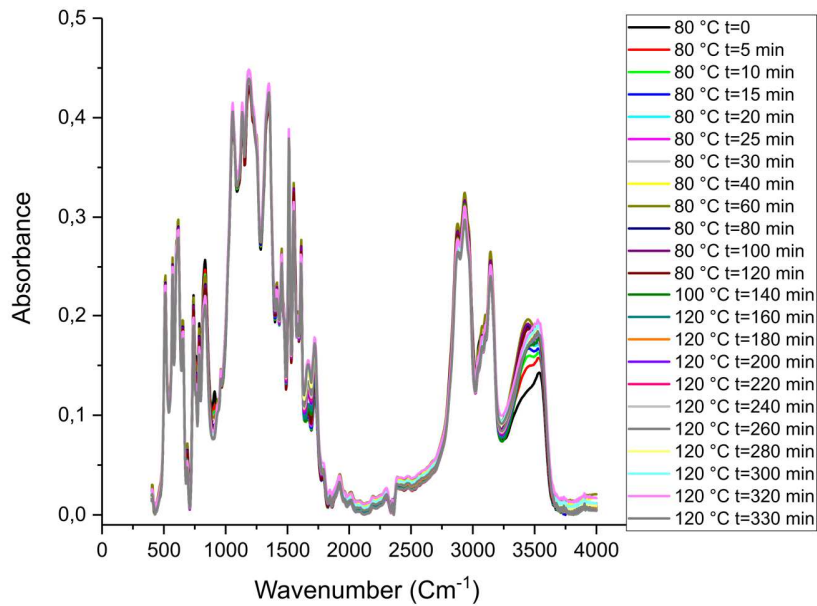


Figure S20: FTIR Spectrum of ILM-2 during curing process

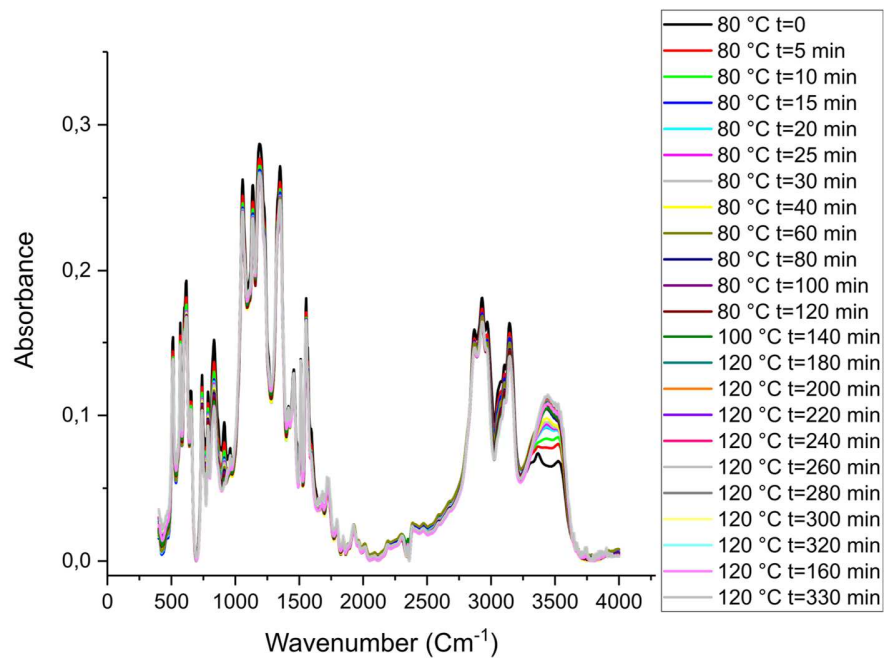


Figure S21: FTIR Spectrum of ILM-3 during curing process

VII. DSC analysis

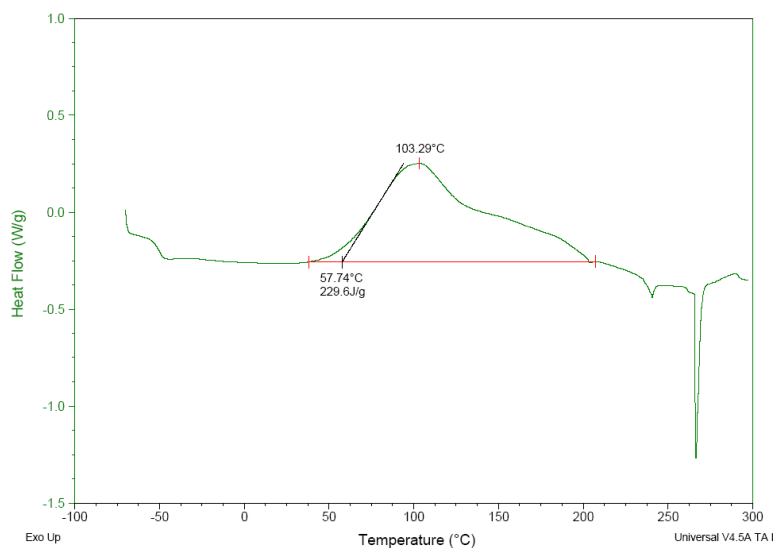


Figure S22: DSC thermogram of compound ILM-[NTf₂]-1

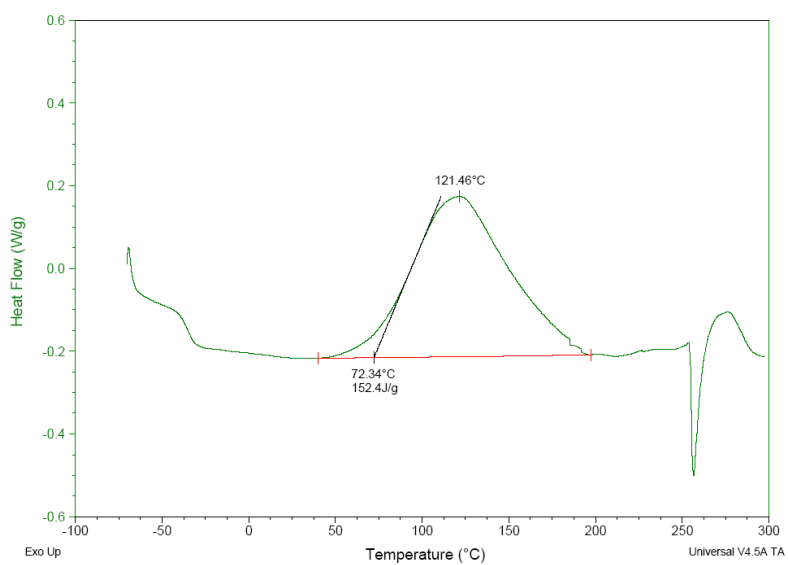


Figure S23: DSC thermogram of compound ILM-[NTf₂]-2

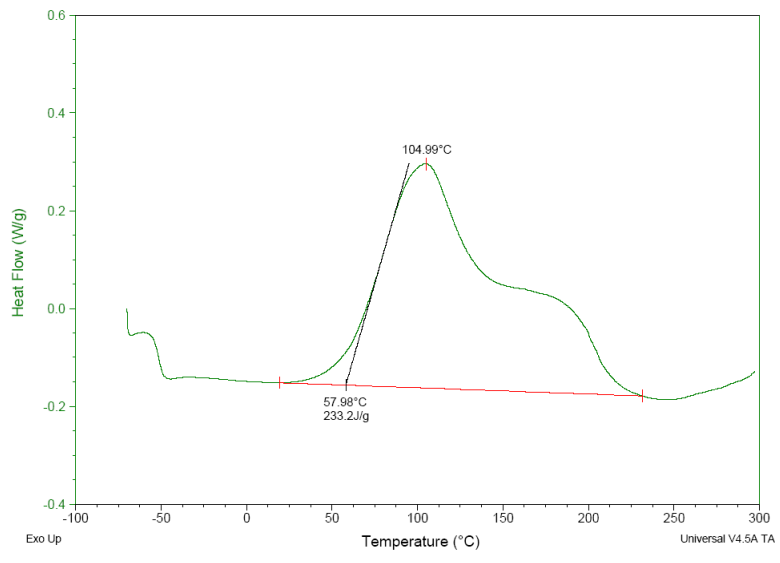
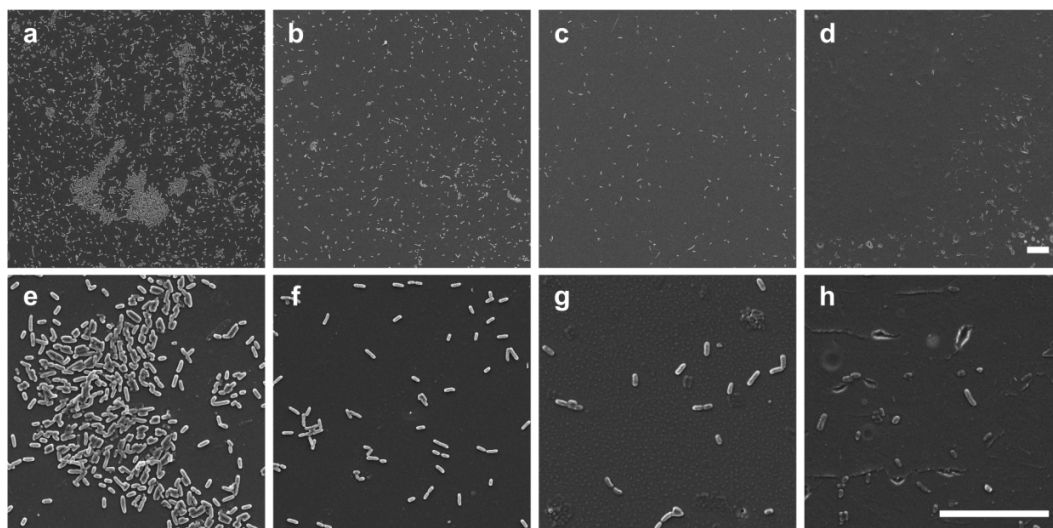


Figure S24: DSC thermogram of compound ILM-[NTf₂]-3

For Table of Contents Use Only



SEM micrographs of active surfaces against microorganisms such as *Escherichia coli* (*E. coli*) composed of conventional epoxy-amine (DGEBA/D230 (a,e)) and epoxy-amine networks based on Ionic Liquid Monomer (ILM) *i.e.* ILM-1 (b, f), ILM-2 (c, g) and ILM-3 (d, h)